國立臺灣大學醫學院藥理學研究所

碩士論文

Graduate Institute of Pharmacology

College of Medicine

National Taiwan University

Master Thesis

FcγRIIB 功能缺損導致生發中心反應異常

使低抗原親和性抗體增加之研究

A functionally impaired FcγRIIB variant contributes to

aberrant accumulation of low-affinity antibody-secreting

cells as a result of defective germinal center reaction

周峻霈

Jyun-Pei Jhou

指導教授：曾賢忠 博士

Advisor: Shiang-Jong Tzeng, M.D., Ph.D.

中華民國 104 年 7 月

July, 2015

國立臺灣大學（碩）博士學位論文
口試委員會審定書

FcγRIIB 功能缺損導致生發中心反應異常
使低抗原親和性抗體增加之研究

A functionally impaired FcγRIIB variant contributes to aberrant accumulation of low-affinity antibody-secreting cells as a result of defective germinal center reaction

本論文係 周峻霈 君（學號 R02443015）在國立臺灣大學藥理學研究所完成之碩士學位論文，於民國 104 年 7 月 17 日承下列考試委員審查通過及口試及格，特此證明

口試委員： _____曾賢忠_____（簽名）

（指導教授）

_____

_____

_____

系主任、所長 _____林琬琬___（簽名）

i

誌謝

　　兩年的碩士研究生涯，此刻算是告了一段落。兩年前，我從藥學系畢業進入了台大藥理所，大學時的我沒做過任何專題研究，對於研究所究竟都在"研究"些什麼？老實說我並不瞭解。對於科學研究的方法以及它的精神價值也都只是一知半解。就實驗操作技術而言，也僅僅是來自實驗課學到的雕蟲小技。至於那些訊息傳遞的分子，對於受以培育臨床專業教育的我，更是毫無概念。此刻回想起，兩年前這樣的我，兩年後卻能夠帶著"台大藥理所"這塊金字招牌走出去，還真著實不容易誒。當然，這要感謝一路上許多人的幫助。

　　最重要的莫過於感謝我的指導教授：曾賢忠老師，指導我做學問的態度與方法，培養我邏輯思考的能力，利用 seminar 的機會訓練我 present 的技巧，如何將一個複雜難懂的知識以淺顯易懂的語言讓每位聽眾都能理解。在實驗上，教導我秉持著實事求是的科學精神來從事研究，雖然研究之路不可能永遠順遂，難免會遇到失敗與挫折，但碰到問題時若選擇逃避，問題永遠存在，老師總是會提供意見如何 troubleshooting，這對於碰上實驗撞牆卡關的我，那可真是猶如在沙漠中看見綠洲。老師的每一個研究計畫方向都講求深度與廣度，力求創新，也藉此叮嚀我未來無論身在何崗位都應保持競爭力，尤以身為決策者更為重要，我想這就是所謂 T 型人才應具備的特質。

　　感謝口試委員江伯倫教授、林淑華教授以及陳基益教授的指正，使本論文能更臻盡善盡美。

　　感謝 TSJ 實驗室的每位夥伴，宜藍、宛諭、雨璇和琮智，一路上的相伴學習、互相鼓勵，在我被實驗轟炸時伸出援手，在我被實驗忙得無法抽身時幫我買午餐，讓我有體力繼續奮鬥。感謝藥理所所有的同學們，互相加油打氣，聊天說笑。另外，我要感謝動物中心的陳雪琴大姐在 IHC 技術上的協助，解決了困擾我許久的問題。

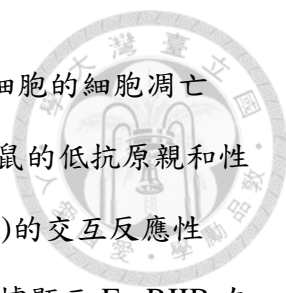　　最後，感謝我的父母總是尊重我的想法，支持我的決定，在教育上對我的極力栽培，讓我能夠無後顧之憂的全心全意投入在學業。

　　回想起當初選擇進入藥理所有種抱持著洗學歷的心態，想說帶著名校的光環未來在工作機會上能更有競爭力，如今走過了兩年的研究生活，我想我獲得的不僅僅是那張證書，更有價值的是從實驗中所學習到的邏輯批判思考與解決問題的能力，以及在面對每次的實驗失敗所培養出的抗壓性，我想或許這才是我此生受用無窮的收穫。我很慶幸我曾經來過台大藥理所，更慶幸能成為 TSJ lab 的一員！

周峻霈　謹誌於
國立台灣大學　藥理學研究所
中華民國一百零四年七月

中文摘要

後天免疫系統包含體液性和細胞性兩種，主要由淋巴球負責。體液性免疫最重要的目的在產生具抗原專一性的高親和性抗體。而抗體的製造則必須透過脾臟和淋巴結的生發中心(germinal center)對 B 細胞進行挑選和使之分化成漿細胞，專司抗體分泌的漿細胞則經由血流定居骨髓。在疫苗反應時，生發中心 B 細胞須經歷體細胞高突變(somatic hypermutation)、親和力成熟(affinity maturation)和免疫球蛋白轉換(class switching)。B 細胞抗原受器(B-cell antigen receptor, BCR)在體細胞高突變反應後，使生發中心 B 細胞對抗原具有各式不同親和力，接著抗原針對這些 B 細胞進行抗原親和力成熟反應，最重要的作用是去除低抗原親和性的生發中心 B 細胞，以確保產生高效價的高抗原親和性抗體。FcγRIIB 是 B 細胞上抑制 BCR 最重要的受器，負責調節體內抗體製造量。此外，它也能夠單獨活化使 B 細胞凋亡。由於研究指出生發中心 B 細胞的 FcγRIIB 表現在疫苗反應會上升，而 FcγRIIB 基因剔除鼠脾臟的生發中心會自發性地增加和變大，導致自體免疫抗體產生，終致紅斑性狼瘡。因此，我們推論 FcγRIIB 在生發中心進行親和力成熟反應時，可能扮演促使低抗原親和性生發中心 B 細胞凋亡的角色。我們採用功能低下的人類 FcγRIIB^{T232} 基因多型性突變鼠來研究這個問題。FcγRIIB^{I232T} 突變是 FcγRIIB 的第 232 個胺基酸位置由蘇胺酸(threonine)取代原本的異白胺酸(isoleucine)，這種多型性變異在亞洲人紅斑性狼瘡佔高比例。我們採用 4-hydroxy-3-nitrophenylacetyl (NP) hapten-chicken gamma globulin (CGG)做為疫苗原來探討 FcγRIIB^{T232} 突變鼠是否比正常鼠殘留較多的低抗原親和性生發中心 B 細胞？結果顯示在單次疫苗接種時，FcγRIIB^{T232} 突變鼠血液中的低抗原親和性 B 細胞和漿細胞的數量均增加和伴隨著血清中低抗原親和性抗體的增加。當再次疫苗接種，FcγRIIB^{T232} 突變鼠脾臟和骨髓中分泌低抗原親和性 IgG 的 B 細胞和低抗原親和性抗體均顯著增加。脾臟生發中心在 FcγRIIB^{T232} 突變鼠也是變大和 B 細胞數量增加，尤以位在執行親和力成熟的亮區(light zone)最顯著。此外，我們更發現 FcγRIIB^{T232} 突變鼠的低抗原親和性 B

細胞和抗體的增加確實是因為亮區的低抗原親和性生發中心 B 細胞的細胞凋亡 (apoptosis)減少，未能被清除所致。有趣的是，$FcγRIIB^{T232}$ 突變鼠的低抗原親和性抗體對於同源類似抗原 NIP (4-hydroxy-3-iodo-5-nitrophenylacetyl)的交互反應性 (cross-reactivity)亦比正常鼠增加。總結來說，本研究提供多項證據顯示 FcγRIIB 在生發中心進行親和力成熟反應時，扮演積極去除低抗原親和性 B 細胞的關鍵角色。在臨床應用上，則建議在疫苗接種時，應可藉由調控 FcγRIIB 的表達使產生的抗體對同源相近的病原菌具有交叉中和的保護效果。
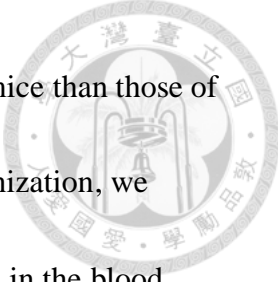
關鍵詞：

FcγRIIB、基因多型性、生發中心 、低親和性抗體、親和力成熟、疫苗接種

ABSTRACT

Germinal center (GC) reaction, which undergoes somatic hypermutation, affinity maturation and class switching, is the hallmark of humoral immunity. One important function of it is to eliminate GC B cells that secrete low-affinity antibody (Ab) to the antigen (Ag) to ensure successful generation of effective neutralizing Abs through affinity maturation. FcγRIIB, a critical inhibitory Fcγ receptor (FcγR) that can mediate apoptosis in B cells, has been found to up-regulate on the GC B cells. Interestingly FcγRIIB-deficient mice spontaneously develop lupus accompanied by retention of somatic mutated BCRs as well as increased number and increased size of GCs in the spleen, indicative of a failure in negative selection of GC B cells. Moreover, people carrying a functionally impaired variant of FcγRIIB, of which isoleucine at position 232 was replaced by threonine, are susceptible to lupus particularly in Asians. Here, we generated FcγRIIB^{T232} mutant mice to investigate the functional role of FcγRIIB in GC reaction. We hypothesized that to some extent the GC phenotype of FcγRIIB^{T232} mice should recapitulate that of FcγRIIB knockout mice after immunization. To address this, we immunized FcγRIIB^{I232} (wild-type) and FcγRIIB^{T232} mice respectively with 4-hydroxy-3-nitrophenylacetyl (NP) hapten-chicken gamma globulin (CGG), a model Ag that allows distinction of low vs. high affinity Ag-specific B cells. Indeed, we found an increase of low-affinity NP-specific IgG-expressing B cells and plasma cells in

circulation and a concomitant increase of serum Abs in $FcγRIIB^{T232}$ mice than those of $FcγRIIB^{I232}$ mice after primary immunization. After secondary immunization, we detected a significant increase of NP-specific B cells and plasma cells in the blood, spleen and bone marrow of $FcγRIIB^{T232}$ mice compared to that of $FcγRIIB^{I232}$ mice, accompanying an accumulation of low-affinity NP-specific IgG-secreting B cells in the spleen and bone marrow of $FcγRIIB^{T232}$ mice. Furthermore, $FcγRIIB^{T232}$ mice increased the formation of low-affinity NP-specific IgG in the circulation. Consistent with these findings, the spleen of $FcγRIIB^{T232}$ mice displayed an increased size of the GC of lymphoid follicles and had a concomitant increase of the number of GC B cells, especially the light zone GC B cells. Moreover, a decrease of apoptosis of GC B cells in the light zone of $FcγRIIB^{T232}$ mice correlated with their increased levels of low-affinity NP-specific B cells and Abs, supporting an active and essential role of FcγRIIB in GC reaction. Finally, we also found that the increased low-affinity antibodies in $FcγRIIB^{T232}$ mice resulted in the increase of cross-reactive antibodies. Taken together, these results support the notion that FcγRIIB plays an important role in negative selection of GC B cells. In addition, FcγRIIB may be considered as an ideal target for immunomodulation if the expression level of FcγRIIB on GC B cells holds the key to determine the stringency of Ab affinity as well as Ab repertoire to be generated during vaccination.

Key words: FcγRIIB, $FcγRIIB^{I232T}$ polymorphism, germinal center, low-affinity antibody, affinity maturation, immunization

CONTENTS

LIST of FIGURES

LIST of TABLES

LIST of ABBREVIATIONS

AEC	3-amino-9-ethylcarbazole
Ags	Antigens
ASCs	Antibody-secreting cells
Bcl-2	B-cell lymphoma 2
BCR	B cell receptor
Bim	Bcl-2-interacting mediator of cell death
BLC	B lymphocyte chemoattractant
BM	Bone marrow
BSA	Bovine serum albumin
BTK	Bruton's tyrosine kinase
CGG	Chicken gamma globulin
CXCL12	C-X-C motif chemokine 12
CXCL13	C-X-C motif chemokine 13
CXCR4	C-X-C chemokine receptor type 4
CXCR5	C-X-C chemokine receptor type 5
DZ	Dark zone
ELISA	Enzyme-linked immunosorbent assay
ELISPOT	Enzyme-linked immunosorbent spot assay
FACS	Fluorescence-activated cell sorting
FcγRIIB	Fc gamma receptor IIB
GC	Germinal center
GL7	T- and B-cell activation antigen
ICs	Immune complexes
IgG	Immunoglobulin G
IgM	Immunoglobulin M
Igs	Immunoglobulins
ITIM	Immunoreceptor tyrosine-based inhibitory motif
JNK1	c-Jun N-terminal kinase 1
LZ	Light zone
MHCII	Major histocompatibility complex class II
NIP	4-hydroxy-3-iodo-5-nitrophenylacetyl
NP	4-hydroxy-3-nitrophenylacetyl
PLCγ	phospholipase Cγ
SDF-1	Stromal cell-derived factor 1
SHIP	Src homology 2 domain-containing inositol-5-phosphatase

LIST of ABBREVIATIONS (continued)

SHM	Somatic hypermutation
SLE	Systemic lupus erythematosus
SNPs	Single nucleotide polymorphisms
T_{FH} cells	T follicular helper cells
TMB	Tetramethylbenzidine
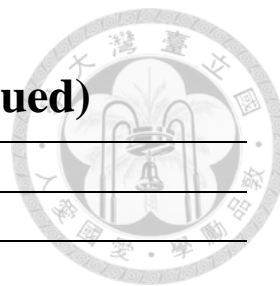
Chapter 1
Introduction

Chapter 1 Introduction

1.1 Fcγ receptors

Fcγ receptors are the receptors for the Fc region of immunoglobulin G (IgG). Up to now, three different classes and their respective subclasses of Fcγ receptors have been recognized in humans, known as FcγRI, FcγRII (including FcγRIIA, FcγRIIB and FcγRIIC), FcγRIII (including FcγRIIIA and FcγRIIIB) **(Table 1.1.1)**. In mice, a fourth class of Fcγ receptor, known as FcγRIV, has been identified **(Table 1.1.2)** (Nimmerjahn and Ravetch, 2008). Most Fcγ receptors are activating receptors, including FcγRI, FcγRIIA, FcγRIIC, FcγRIIIA and FcγRIIIB in humans, and FcγRI, FcγRIII and FcγRIV in mice. In contrast, FcγRIIB is the only inhibitory receptor in families of human and mouse Fcγ receptors. Among the Fcγ receptors, FcγRI is the sole high-affinity receptor, which comprises three immunoglobulin (Ig)-like domains in the extracellular region that can bind both monomeric IgG and immune-complexed IgG, whereas FcγRII, FcγRIII and FcγRIV are low- to medium-affinity receptors, each of which comprises two Ig-like domains in the extracellular portion that can bind only immune-complexed IgG (Ravetch and Kinet, 1991).

Table 1.1.1 The family of human Fcγ receptors (FcγRs)

Human FcγRs	Activating FcγRs					Inhibitory FcγRs
Structure	Immunoglobulin domain / Common γ chain / ITAM				GPI anchor	ITIM
Name	**FcγRI**	**FcγRIIA**	**FcγRIIC**	**FcγRIIIA**	**FcγRIIIB**	**FcγRIIB**
Receptor affinity	High affinity	Low to medium affinity				
Signaling motif	ITAM	ITAM	ITAM	ITAM	ITAM	ITIM
IgG binding affinity	IgG3>IgG1> IgG4>>IgG2	Variant H131 IgG3>IgG1> IgG2>>IgG4 Variant R131 IgG3>IgG1>> IgG2 and IgG4	IgG3>IgG1 and IgG4 does not bind IgG2	Variant V158 IgG3>IgG1>>> IgG2 and IgG4 Variant F158 IgG3>>>IgG1 does not bind IgG2 and IgG4	IgG3>>IgG1 does not bind IgG2 and IgG4	IgG3>IgG1 and IgG4 does not bind IgG2
Expression	Monocyte Dendritic cell Macrophage Neutrophil Eosinophil	Monocyte Dendritic cell Platelet Macrophage Neutrophil	NK cell	NK cell Monocyte Dendritic cell Macrophage	Neutrophil Mast cell Eosinophil	B cell Plasma cell Monocyte Dendritic cell Macrophage Neutrophil Basophil Mast cell

ITAM, immunoreceptor tyrosine-based activating motif

ITIM, immunoreceptor tyrosine-based inhibitory motif

GPI, glycosylphosphatidylinositol

(Nimmerjahn and Ravetch, 2008; Smith and Clatworthy, 2010)
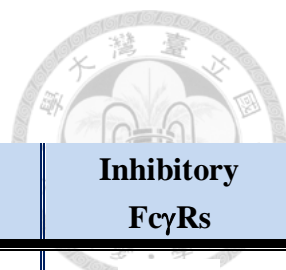
Table 1.1.2 The family of mouse Fcγ receptors (FcγRs)

Mouse FcγRs	Activating FcγRs			Inhibitory FcγRs
Structure				
Name	FcγRI	FcγRIII	FcγRIV	FcγRIIB
Receptor affinity	High affinity	Low to medium affinity		
Signaling motif	ITAM	ITAM	ITAM	ITIM
IgG binding affinity	IgG2a and IgG3>>>IgG1 and IgG2b	IgG3>IgG2a> IgG2b>>IgG1	IgG2a and IgG2b>>>IgG1 and IgG3	IgG2a and IgG2b>IgG1
Expression	Monocyte Macrophage Dendritic cell	NK cell Monocyte Macrophage Neutrophil Dendritic cell	Monocyte Macrophage Neutrophil	B cell Plasma cell Monocyte Macrophage Neutrophil Dendritic cell

ITAM, immunoreceptor tyrosine-based activating motif

ITIM, immunoreceptor tyrosine-based inhibitory motif

(Dijstelbloem*, et al.*, 2001; Nimmerjahn*, et al.*, 2005; Nimmerjahn and Ravetch, 2008; Smith and Clatworthy, 2010)
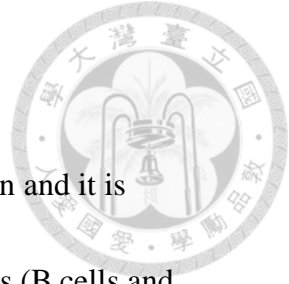
1.2 Fcγ receptor IIB (FcγRIIB)

FcγRIIB is the only Fcγ receptor that has inhibitory function and it is ubiquitously expressed by immune cells, including lymphoid cells (B cells and plasma cells), myeloid cells (macrophages, monocytes and dendritic cells), and granulocytes (neutrophils, basophils and mast cells), with the exception of NK cells and T cells (Ravetch and Kinet, 1991). FcγRIIB has distinct functions when expressed by different types of immune cells. When expressed on B cells, FcγRIIB increases activation threshold, and therefore inhibits B cell activation. By same token, when expressed on myeloid cells and granulocytes, FcγRIIB inhibits the functions of activating Fcγ receptors, such as phagocytosis and release of pro-inflammatory cytokines. In contrast, when expressed on follicular dendritic cells, FcγRIIB does not transduce inhibitory signals but plays an important role in trapping the antigen-containing immune complexes (ICs) and mediating the generation of GC reaction (Qin, *et al.*, 2000).

Three isoforms of FcγRIIB, referred to as FcγRIIB-1, FcγRIIB-2 and FcγRIIB-3, have been identified in humans and mice (Brooks, *et al.*, 1989; Hogarth, *et al.*, 1991; Ravetch, *et al.*, 1986; Stuart, *et al.*, 1989). Both FcγRIIB-1 and FcγRIIB-2 are membrane proteins that contain an immunoreceptor tyrosine-based inhibitory motif (ITIM) within the cytoplasmic domain, whereas FcγRIIB-3 is a

soluble receptor that lacks the transmembrane and first cytoplasmic domains

(Tartour, *et al.*, 1993). FcγRIIB-1 and FcγRIIB-2 are differentially expressed in

hematopoietic cells. FcγRIIB-1 is predominantly expressed by B cells, while

FcγRIIB-2 is mainly expressed by myeloid cells (Joshi, *et al.*, 2006). Although

FcγRIIB-1 and FcγRIIB-2 are encoded by the same gene, FcγRIIB-2 has a deletion

of exon 6, which contains 47 amino acids and resides in the cytoplasmic domain,

due to alternative mRNA splicing and this prevents FcγRIIB-1, but not FcγRIIB-2,

from localization into clathrin-coated pits for endocytosis (Miettinen, *et al.*, 1992).

In spite of the difference of membrane trafficking between FcγRIIB-1 and

FcγRIIB-2, both B1 and B2 isoforms of FcγRIIB are functional inhibitory receptors

in the phagocytic process (Joshi, *et al.*, 2006).

1.3   FcγRIIB triggers inhibitory signaling pathways to block B-cell function

FcγRIIB has been shown to play an important role in regulating the humoral

immunity. FcγRIIB exerts inhibitory function mainly through co-ligation of FcγRIIB

with activating Fcγ receptors in myeloid cells or with the B-cell antigen receptor

(BCR) by cognate ICs in B lymphocytes. The co-engagement of BCR and FcγRIIB

leads to phosphorylation of the ITIM in the cytoplasmic domain by the Src family

kinase Lyn (Malbec, *et al.*, 1998), followed by the recruitment of SHIP (Src

homology 2 domain-containing inositol-5-phosphatase) that hydrolyzes

phosphatidylinositol-3,4,5-trisphosphate (PtdIns(3,4,5)P$_3$) into

phosphatidylinositol-3,4-bisphosphate (PtdIns(3,4)P$_2$) (Ono, *et al.*, 1996; Ono, *et al.*,

1997). This results in prevention of the subsequent recruitment of pleckstrin

homology-domain-containing kinases, such as BTK (Bruton's tyrosine kinase) or

PLCγ (phospholipase Cγ) to the cell membrane, thereby inhibiting downstream

activating signaling cascade (Bolland and Ravetch, 1999).

In addition to co-ligation of FcγRIIB with activating Fcγ receptors or with

BCR, cross-linking of FcγRIIB itself has recently been shown functional. Clustered

FcγRIIB in the absence of BCR ligation on B cells can induce apoptosis through

BTK and JNK1 (c-Jun N-terminal kinase 1) as well as c-Abl tyrosine kinase in

chicken and mouse B cells, respectively (Pearse, *et al.*, 1999; Tzeng, *et al.*, 2005),

and this is independent of ITIM- and SHIP-mediated signaling pathways (Tzeng, *et al.*, 2005). The cross-linking of FcγRIIB by itself to trigger B cell apoptosis has been

proposed to be involved in the regulation of B-cell responses and the maintenance of

self-tolerance by the deletion of low-affinity B cells during the GC reaction and by

elimination of self-reactive B cells in lymphoid organs. This idea mainly bases on

the affinity and specificity of Ag to BCR in the IC. When B cells encounter ICs the

BCR with Ag specificity can co-engage both BCR and FcγRIIB, whereas BCR with

low affinity or no specificity for the Ag will predominantly receive signals from FcγRIIB only and lack survival signaling provided by the BCR, thereby allowing low-affinity B cells to be deleted by apoptosis.

Terminally differentiated plasma cells in the bone marrow do not express BCR and merely express little receptors elsewhere, but they express higher level of FcγRIIB than that of mature B cells or less-differentiated plasma cells (Xiang, *et al.*, 2007). Studies have also shown that cross-linking FcγRIIB itself on plasma cells can induce apoptosis through Bim (Bcl-2-interacting mediator of cell death), a Bcl-2 (B-cell lymphoma 2) family member (Xiang, *et al.*, 2007). Consistent with this notion, plasma cells from SLE-prone mouse strains, which do not express FcγRIIB or have strongly reduced expression of FcγRIIB, are resistant to induction of apoptosis (Xiang, *et al.*, 2007).

1.4 Functions of FcγRIIB in innate immunity

In dendritic cells (DCs), engagement of activating FcγRs by ICs in the absence of coligation of FcγRIIB enhances the maturation of DCs (Kalergis and Ravetch, 2002). Blockade of FcγRIIB enables DCs to produce inflammatory cytokine, such as interleukin-12 (IL-12) and type 1 interferon (IFN) and enhances DCs to generate the immunity of tumor-reactive T cells (Dhodapkar, *et al.*, 2007; Dhodapkar, *et al.*, 2005). In macrophages, FcγRIIB negatively regulates
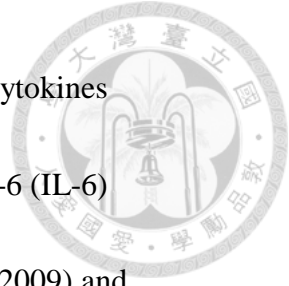
antibody-dependent phagocytosis and reduces proinflammatory cytokines

production, such as tumor necrosis factor α (TNF-α), interleukin-6 (IL-6)

(Clatworthy and Smith, 2004; Clynes, *et al.*, 1999; Zhang, *et al.*, 2009) and

interleukin-1α (IL-1α) (Yuasa, *et al.*, 1999) through FcγRIIB-dependent PGE$_2$

production (Zhang, *et al.*, 2009). In mast cells and basophils, costimulation of

high-affinity IgE receptor FcϵRI and FcγRIIB by DNP-Ova and anti-DNP IgG

inhibits FcϵRI-mediated histamine and serotonin release and interleukin-4 (IL-4)

production (Daeron, *et al.*, 1995; Kepley, *et al.*, 2000).

1.5   FcγRIIB and autoimmunity

Since FcγRIIB is a key negative regulator of B-cell activation, it is not

surprising that FcγRIIB is involved in the pathogenesis of autoimmune diseases.

Studies have shown that FcγRIIB-deficient mice spontaneously develop high levels

of serum anti-nuclear autoantibodies and autoimmune glomerulonephritis

resembling systemic lupus erythematosus (SLE) (Bolland and Ravetch, 2000).

Moreover, loss of FcγRIIB increases serum collagen-specific antibodies and

exacerbates disease severity in a mouse model of type II collagen-induced arthritis

(CIA) (Yuasa, *et al.*, 1999). Similarly, in multiple sclerosis deficiency of FcγRIIB

exacerbates the disease severity of experimental autoimmune encephalomyelitis

(EAE) and enhances the activation of myelin-specific T cells (Iruretagoyena, *et al.*,

2008). One important caveat is that FcγRIIB-deficient mice gradually develop an increase of self-reactive GC B cells and plasma cells (Tiller, *et al.*, 2010). Likewise, GC B cells and activated B cells display reduced levels of FcγRIIB in mice that develop spontaneous autoimmune diseases (Jiang, *et al.*, 1999; Pritchard, *et al.*, 2000; Xiu, *et al.*, 2002). In humans, FcγRIIB expression is also decreased on memory B cells in SLE patients (Mackay, *et al.*, 2006). Cross-linking the surface dsDNA-specific Ig and FcγRIIB by a chimeric antibody, which was constructed by coupling the dsDNA-mimicking DWEYSVWLSN peptide to an anti-mouse FcγRIIB monoclonal antibody, selectively suppresses dsDNA-specific auto-reactive B cells and alleviates the SLE symptoms as well as decreases the level of anti-dsDNA IgG autoantibodies in MRL/*lpr* mice (Tchorbanov, *et al.*, 2007).

Restoration of FcγRIIB expression levels on B cells in lupus-prone mouse strains alleviates the symptoms of SLE and prevents autoimmunity (McGaha, *et al.*, 2005). Transgenic mice overexpressing FcγRIIB on B cells exhibit reduced disease severity of CIA and SLE as well as reduced collagen-specific and anti-dsDNA autoantibodies. However, overexpressing FcγRIIB on macrophages does not have these effects but increase mortality after *Streptococcus pneumoniae* infection due to impaired phagocytosis of bacteria (Brownlie, *et al.*, 2008).

1.6 Polymorphisms of *FCGR2B*

1.6.1 Mouse *fcgr2b* polymorphisms

In mice, *fcgr2b* polymorphisms include three haplotypes that are distributed within the region of promoter and intron 3 regions, and two *Ly17* polymorphisms in the coding regions.

1.6.1.1 Polymorphisms in the promoter and intron

In the promoter and intron of *fcgr2b* gene, three haplotypes have been identified. These haplotypes result from the deletion in different regions within the promoter (region 1 and region 2) and intron 3 (region 3 and region 4). Inbred mouse strains with the group 1 haplotype (NZB, BXSB, MRL, NOD and 129 mice) share three deletion sites in region 1, region 2 and region 3 and are prone to autoimmune diseases. Inbred mouse strains with the group 2 haplotype (NZW, SJL and SWR mice) do not have deletions in promoter but in the two regions within intron 3. Mice with group 2 haplotype are not prone to autoimmune diseases, but appear to have the potential to accelerate the autoimmune diseases. Inbred mouse strains with the group 3 (BALB/c, C57BL/6 and DBA mice) haplotype do not have deletions in the region 1 to 4 and are normal healthy mouse strains (Jiang*, et al.*, 2000; Pritchard*, et al.*, 2000).

1.6.1.2 Polymorphisms in the coding region

In the coding regions of *fcgr2b* gene, there are two variants of *Ly17*, termed *Ly17.1* and *Ly17.2* (Hibbs, *et al.*, 1985). The *Ly17* polymorphisms include four single nucleotide polymorphisms (SNPs), three are (Pro116, Gln161, and Thr166 in Ly17.1 protein; Leu116, Leu161, and Pro166 in Ly17.2 protein) in the exon 6 and one (Ile258 in Ly17.1 protein; Ser258 in Ly17.2 protein) in the exon 8. Although these SNPs lead to the change of amino acids, whether they have effects on the inhibitory function of FcγRIIB is still not clear.

1.6.2 Human *FCGR2B* polymorphisms

In humans, several SNPs have been identified within the promoter and coding regions of *FCGR2B* gene.

1.6.2.1 Polymorphisms in the promoter

In the promoter of *FCGR2B* gene, two haplotypes have been described, namely the more common −386G-120T variant and the less common −386C-120A variant (Su, *et al.*, 2004b). Previous studies have shown that the −386C-120A haplotype increases the binding capacity for the transcription factors GATA-binding protein 4 (GATA4) and Yin-Yang 1 (YY1), leading to higher promoter activities of *FCGR2B* gene. As a result, people with the −386C-120A haplotype express more FcγRIIB on B cells and monocytes than those with the −386G-120T haplotype (Su,
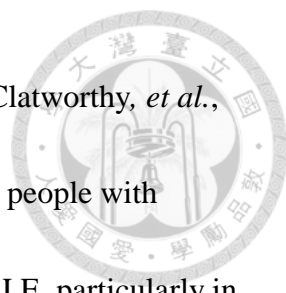
et al., 2004a). Decreased transcription of the human *FCGR2B* gene mediated by the

-343 G/C promoter polymorphism associates with systemic lupus erythematosus

(Blank*, et al.*, 2005).

1.6.2.2 Polymorphisms in the coding region

In the coding region of *FCGR2B* gene, there are seven non-synonymous SNPs,

i.e. T43I, Q83P, T118I, H153R, Y205F, I232T and L282P. Among them, only I232T

polymorphism occurs at noteworthy frequency and has been studied in detail. This

I232T polymorphism originates from the T-to-C transition in exon 5 of the *FCGR2B*

gene, which results in a single amino acid substitution of a threonine (T) for

isoleucine (I) at position 232 within the transmembrane domain of FcγRIIB (known

as the FcγRIIB^{T232} allele). The inhibitory function of FcγRIIB^{T232} polymorphism is

remarkably impaired for B cells with FcγRIIB^{T232} variant exhibit decreased

inhibition on BCR-triggered proliferation in that unlike wild-type FcγRIIB it is

excluded from sphingolipid rafts where BCR transduces signals. On the other hand,

macrophages with FcγRIIB^{T232} variant display enhanced phagocytic capacity,

indicating that FcγRIIB^{T232} polymorphism is unable to inhibit activating receptors

(Floto*, et al.*, 2005; Kono*, et al.*, 2005).
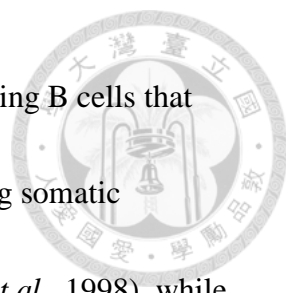
The prevalence of FcγRIIB^{T232} polymorphism has greater association with

ethnic variation. There is a higher frequency in Africans (8~11%) and Southeast

Asians (5~7%), whereas a lower incidence in Caucasians (1%) (Clatworthy, *et al.*, 2007; Kyogoku, *et al.*, 2002; Siriboonrit, *et al.*, 2003). Moreover, people with FcγRIIB[T232] polymorphism have an increase of susceptibility to SLE, particularly in Asians. In Taiwan, 35% of SLE patients are heterozygous FcγRIIB[T232] variants (232I/T) and 11% are homozygous FcγRIIB[T232] variants (232T/T) (Chen, *et al.*, 2006). Similarly, in Japanese SLE patients 34.2% individuals are of 232I/T and 10.9% are of 232T/T genotypes (Kyogoku, *et al.*, 2002). In Thai SLE patients, 36.7% individuals are 232I/T heterozygous and 15.2% are 232T/T homozygous genotypes (Siriboonrit, *et al.*, 2003).

1.7 Germinal centers (GCs)

The essential feature of humoral immunity is the progressive generation of somatically mutated high-affinity B cells and plasma cells over time, eventually production of high-affinity antibodies that can provide effective protection against invading pathogens. This process takes place in the germinal centers (GCs), which are temporary structures that form in the peripheral lymphoid organs in response to T cell-dependent Ags after immunization or infection (MacLennan, 1994). The structure of GCs is comprised of two zones, the dark zone and the light zone, which were named on the basis of the histological appearance of the B cell density. The dark zone is the more densely packed area while the light zone is the less densely

assembled region. The dark zone is abundant in rapidly proliferating B cells that

adapt their BCRs to the immunizing Ags through the process of Ig somatic

hypermutation (Jacob, *et al.*, 1991; Rajewsky, 1996; Takahashi, *et al.*, 1998), while

the light zone is the compartment where B cells are selected on the basis of their

affinity of the BCRs for the Ags. B cells with the higher-affinity Ag receptors will be

positively selected and proceed to divide or to differentiate into plasma cells or

memory B cells (Meyer-Hermann, *et al.*, 2012). On the contrary, B cells with the

lower-affinity antigen receptors or B cells that can no longer make a functional BCR

(not Ag-specific) will be eliminated by apoptosis because they cannot compete with

the higher-affinity B cells that bind Ags more strongly.

The organization of GC dark and light zones requires expression of the

chemokine receptors CXCR4 and CXCR5 by GC B cells (Allen, *et al.*, 2004). This

is supported by the findings that CXCR4-deficient mice result in GC disorganization

(Allen, *et al.*, 2004). Rapidly proliferating B cells in the dark zone, called

centroblasts, highly express CXCR4 and CXCR5. CXCL12 (also known as SDF-1,

stromal cell-derived factor 1), a ligand for CXCR4, was more abundant in the dark

zone than in the light zone of GCs, rendering centroblasts to localize to the dark

zone (Allen, *et al.*, 2004; Bannard, *et al.*, 2013). As time goes on, some centroblasts

reduce the rate of cell division and down-regulate the expression of CXCR4 but

begin to produce high levels of surface Ig. These B cells are called centrocytes.

CXCL13 (also known as BLC, B lymphocyte chemoattractant), a ligand for CXCR5, has an opposite distribution to CXCL12 in the GC, being more abundant in the GC light zone than in the GC dark zone. Therefore, the reduced expression of CXCR4 and increased expression of CXCR5 facilitates centrocytes to migrate to the light zone.

T follicular helper (T_{FH}) cells are required for the development and function of GCs and for the regulation of differentiation of GC B cells into memory B cells and plasma cells. It has been known that interleukin-21 (IL-21) produced by T_{FH} cells is important for the formation of GCs as absence of IL-21 signaling in IL-21-deficient or IL-21R-deficient mice decrease the generation of plasma cells in the spleen and bone marrow, and also remarkably reduce the number of GC B cells and their affinity maturation (Linterman, *et al.*, 2010; Zotos, *et al.*, 2010). Furthermore, the development of GCs is impaired in CD28-knockout mice, presumably because of a lack of T_{FH} cells when co-stimulation is absent (Ferguson, *et al.*, 1996).

1.7.1 Somatic hypermutation (SHM)

Somatic hypermutation (SHM) primarily occurs in rapidly proliferating centroblasts. SHM is an event of point mutations that occurs in the Ig variable region genes to result in changes of a single or a few amino acids, leading to a

16
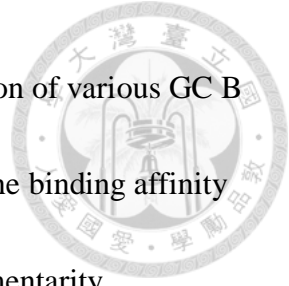
diversified BCR repertoire. The outcome of SHM is the production of various GC B

cells with different affinities. Most SHM has negative effect on the binding affinity

of BCR to antigen because these point mutations render complementarity

determining regions (CDRs) of Ig unable to recognize Ag. In contrast, only a small

number of SHM variants can increase the affinity of BCR to Ag.

1.7.2 Affinity maturation
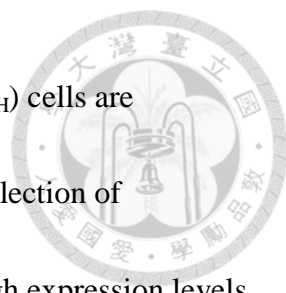
The hallmark of GC reaction is to preferentially select high-affinity B-cell

clones that bind Ags more strongly. GC selection involves the process of survival,

clonal selection and cell differentiation. As the result of somatic hypermutation in

the dark zone, GC reaction produces a variety of BCR mutant clones with various

Ag affinities. B cells carrying these distinct BCRs then move to the light zone and

compete for Ags where affinity selection occurs. Higher affinity B-cell clones will

be positively selected and expanded, whereas lower affinity B-cell clones will be

eliminated by apoptosis because of deprivation of survival signals from Ag to ligate

BCR. In the condition of absence of Ag competition, both higher- and lower-affinity

B cells have the same intrinsic capacity to produce GC responses to Ag and also

have the similar GC numbers (Shih, *et al.*, 2002). However, lower-affinity B cells

are unable to form GCs in the presence of higher-affinity B cells using B1-8[high] and

B1-8[low] NP-specific transgenic mice (Dal Porto, 2002; Shih, *et al.*, 2002).

17
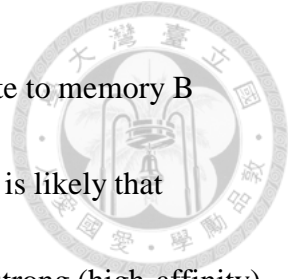
Interestingly, lower-affinity B cells can form GCs and differentiate to memory B cells when higher-affinity B cells is reduced (Dal Porto, 2002). It is likely that low-affinity B cells are able to capture Ag as a result of reduced strong (high-affinity) competitors.

Affinity-based selection occurs when GC B cells move to the light zone where the Ags also localize. In addition to centrocytes, GC light zone is abundant in follicular dendritic cells (FDCs) that can capture antibody-antigen ICs on the surface through the FcγRIIB (Allen and Cyster, 2008; Mandel, *et al.*, 1980; Qin, *et al.*, 2000; Tew, *et al.*, 1980). Consistently, lymphotoxin β receptor (LTβR)-deficient mice are absent of FDCs and exhibit impaired affinity maturation of the antibody response, suggesting that FDCs have a crucial role in the selection of high-affinity GC B cells (Futterer, *et al.*, 1998). On the contrary, a report has shown that GC formation and affinity selection appear normal in the absence of ICs on FDCs, suggesting that other non-IC sources of Ag to drive the GC response may also be important (Hannum, *et al.*, 2000). It seems that whether ICs retention on FDCs is required for GC development is still a controversial issue (Haberman and Shlomchik, 2003; Kosco-Vilbois, 2003).

Recently, studies have shown that competition for T-cell help is also an important factor in the selection of high-affinity B-cell mutants (Victora and

Nussenzweig, 2012; Victora, *et al.*, 2010). T follicular helper (T_{FH}) cells are considered to be a dominant player in the T-cell help-mediated selection of high-affinity B cells in the GC (Victora, *et al.*, 2010), because high expression levels of CXCR5 allow T_{FH} cells to migrate into CXCL13-rich B cell follicles, particularly the light zone of GC (Breitfeld, *et al.*, 2000; Kim, *et al.*, 2001; Schaerli, *et al.*, 2000). In addition to providing survival signals, BCR is also an endocytic receptor. When GC B cells capture Ags via the BCR, Ags will be internalized to intracellular major histocompatibility complex class II (MHCII)-containing compartments to process, then these processed Ags will be presented on MHCII complexes to T_{FH} cells (Lanzavecchia, 1985). B cells with higher-affinity BCR capture more antigens than those with lower-affinity BCR resulting in presenting higher density of peptide-MHC complexes on the surface of B cells (Victora, *et al.*, 2010). Increasing the amount of Ags presented by higher-affinity GC B cells to T_{FH} cells will increase the help of T_{FH} cells, leading to proportional and selective expansion of higher-affinity GC B cells (Gitlin, *et al.*, 2014). Furthermore, increased Ag capture and presentation result in increased rates of cell proliferation of high-affinity GC B cells (Gitlin, *et al.*, 2014).

1.8 Motivation

FcγRIIB is a key negative regulator in mediating the B-cell activity and plays

a crucial role in regulating the humoral immunity. Interestingly, FcγRIIB-deficient

mice spontaneously develop systemic lupus erythematosus (Bolland and Ravetch,

2000), which is accompanied by a decrease of apoptosis of autoreactive GC B cells

as well as an increased number and increased size of GCs in the spleen (McGaha, *et*

al., 2008; Tiller, *et al.*, 2010). A functionally impaired I232T polymorphism of

FcγRIIB, of which isoleucine at position 232 is replaced by threonine, has higher

incidence rate in Asia populations. In Asian SLE patients, about 34-37% patients are

heterozygous FcγRIIB^{T232} variants (232I/T) and 11-15% are homozygous

FcγRIIB^{T232} variants (232T/T) (Chen, *et al.*, 2006; Kyogoku, *et al.*, 2002;

Siriboonrit, *et al.*, 2003). Taken together, these findings indicate that FcγRIIB plays

an important role in the B-cell tolerance and in the prevention of the development of

autoantibodies and autoimmunity.
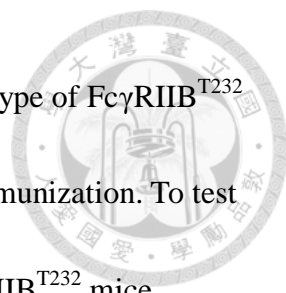
B cells carrying the somatic mutated BCRs that possess the ability to

recognize self-antigens can be deleted through negative selection during the GC

reaction (Pulendran, *et al.*, 1995; Shokat and Goodnow, 1995); however, this

process appears to be defective in autoimmune diseases, resulting in retention of the

self-reactive B cells (Davidson, *et al.*, 1987). Consistently, a decreased exclusion of

auto-reactive B cells also has been found in FcγRIIB-deficient mice (Paul, *et al.*, 2007), implying that loss of FcγRIIB or functionally impaired FcγRIIB can result in a failure in negative selection of GC B cells.

Autoantibodies to some degree can be regarded as low-affinity antibodies when they first arise. Deletion of low-affinity B cells during the GC reaction is an important physiologic process for ensuring the production of effective neutralizing antibodies. So far the elimination of low-affinity GC B cells is considered mainly through the competition mechanism of BCR for Ags. B cells with low-affinity BCR will die because they cannot acquire the survival signaling from the BCR in the absence of Ag engagement. In addition, co-ligation of FcγRIIB by itself on B cells induces the apoptosis of B cells. It was hypothesized that this event might occur when low-affinity BCRs cannot capture Ags during the GC reaction, suggesting an important role of FcγRIIB in negative selection of GC B cells (Pearse, *et al*., 1999). The findings that FcγRIIB-deficient mice develop increased number of self-reactive GC B cells and increased size of GCs (McGaha, *et al.*, 2008; Tiller, *et al.*, 2010) indicate a failure to delete self-reactive (low-affinity) GC B cells.

Based on these results, we reasoned that FcγRIIB might play a decisive role in the negative selection of low-affinity GC B cells. To address this question, we generated FcγRIIB^{T232} mutant mice to investigate the functional role of FcγRIIB in

GC reaction. We hypothesized that to some extent the GC phenotype of FcγRIIB^{T232}

mice should recapitulate that of FcγRIIB knockout mice after immunization. To test

our hypothesis, we immunized FcγRIIB^{I232} (wild-type) and FcγRIIB^{T232} mice

respectively with 4-hydroxy-3-nitrophenylacetyl (NP) hapten-chicken gamma

globulin (CGG), a model antigen that allows discrimination between low- and high-

affinity Ag-specific B cells. In order to produce more IgG, which is a ligand of

FcγRIIB, we primarily immunized mice on day 1 and delivered a booster 28 days

later. Subsets of B cells in the blood, spleen and bone marrow were compared

between FcγRIIB^{I232} and FcγRIIB^{T232} mice by flow cytometry. ELISPOT

(Enzyme-linked immunosorbent spot) assay was used to determine the number of

total and Ag-specific antibody-secreting cells (ASCs) of high vs. low affinities in the

spleen and bone marrow of FcγRIIB^{I232} and FcγRIIB^{T232} mice. The amount and

affinity of serum Ag-specific IgG antibodies were measured by ELISA assay. To

further determine whether the GCs of FcγRIIB^{T232} mice displayed a failure in the

deletion of low-affinity Ag-specific B cells during the GC reaction, we analyzed the

GC B cells of dark and light zones of these mice using flow cytometry and

immunohistochemistry. Our prediction was that an impaired signaling through

FcγRIIB^{T232} for apoptosis at GCs should result in an accumulation of low-affinity

Ag-specific B cells. Finally, to investigate whether the Ag-specific low-affinity

antibodies might be more cross-reactive with the analogue Ags in FcγRIIB^{T232} mice, we performed ELISA assays for measurement of serum cross-reactive antibodies to NIP (4-hydroxy-3-iodo-5-nitrophenylacetyl) hapten.

Through these approaches, we should be able to determine whether FcγRIIB can be an ideal target for immunomodulation on the level of FcγRIIB on GC B cells so that the desired stringency of antibody affinity as well as antibody repertoire to be generated may be pre-determined during vaccination.

This Page Intentionally Left Blank

Chapter 2
Materials and Methods

Chapter 2 Materials and Methods

2.1 Mice

In collaboration with the transgenic core at the Laboratory Animal Center of

National Taiwan University the point mutant mice of $Fc\gamma RIIB^{I232T}$ were generated

by replacement of wild-type allele with the I232T mutant allele. The sequences of

isoleucine at position 232 of $Fc\gamma RIIB$ gene are conserved in humans, mice and other

mammals. The targeting vector contained floxP and FRT sites that flank the

neomycin selection marker and mutated exon 5 of $Fc\gamma RIIB$ gene, respectively.

Standard procedures of electroporation and gene targeting by homologous

recombination were used to select correct embryonic stem (ES) cell clones.

$Fc\gamma RIIB^{T232}$ (232T/T) mutant mice were bred by mating one heterozygous (232I/T)

male mouse with two heterozygous (232I/T) female mice. Of the same littermates

the $Fc\gamma RIIB^{T232}$ (232T/T) mutant mice were compared with the wild-type

$Fc\gamma RIIB^{I232}$ (232I/I) control mice in most experiments. The genotype of

$Fc\gamma RIIB^{I232T}$ mutant mice was determined by genomic polymerase chain reaction

(PCR) with the following primers: Cu, FD and Neo3', which were either adjacent or

within the neo cassette. The detailed sequences of primers were listed in **Table 2**.

Mice were maintained in specific pathogen-free (SPF) conditions at the Center for

Laboratory Animals of College of Medicine of National Taiwan University. The

animal use protocols were reviewed and approved by the Institutional Animal Care

and Use Committee (IACUC) of College of Medicine of National Taiwan

University.

2.2 Immunization

2.2.1 Primary Immunization

$Fc\gamma RIIB^{I232}$ (232I/I) and $Fc\gamma RIIB^{T232}$ (232T/T) mice of six to eight weeks old

were injected intraperitoneally with 50 μg nitrophenyl-chicken gamma globulin

(NP-CGG; conjugation ratio 27; 1 mg/ml, Bioresearch Technologies) emulsified

with equal volume of Alum (Imject Alum®, Thermo Scientific). Blood drawing was

performed one day (day 0) before primary immunization. Mice were immunized on

day 1 and were sacrificed and analyzed 13 days (day 13) after immunization.

2.2.2 Secondary Immunization

Six- to eight-week-old $Fc\gamma RIIB^{I232}$ (232I/I) and $Fc\gamma RIIB^{T232}$ (232T/T) mice

were injected intraperitoneally with 50 μg nitrophenyl-chicken gammaglobulin

(NP-CGG; conjugation ratio 21; 1 mg/ml, Bioresearch Technologies) emulsified

with equal volume of Alum (Imject Alum®, Thermo Scientific). Blood drawing was

performed one day before primary immunization. Mice were first immunized on day

1, followed by a second booster with the same amount of Ags after 28 days (day 28).

Fourteen days after primary immunization, blood drawing was performed. Mice

were sacrificed and analyzed one week (day 35) after the secondary immunization.
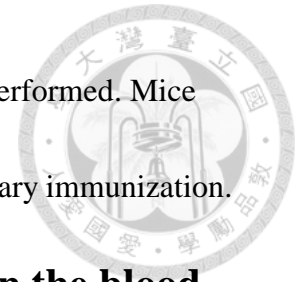
2.3 Flow cytometry to analyze cell populations in the blood, spleen, and bone marrow

2.3.1 Blood

Mouse blood was drawn by puncturing the submandibular vein using blood

lancets (Goldenrod Animal Lancet, MEDIpoint, Inc.) and collected into

K_2EDTA-coated tubes (BD Microcontainer® tubes with K_2EDTA, BD Biosciences).

For secondary immunization, blood drawing was performed 14 days (day 14) after

primary immunization (day 1) and 7 days (day 35) after secondary immunization

(day 28). Red blood cells (RBC) were removed from blood samples by adding RBC

lysis buffer for 5 min at ambient temperature. Cells were centrifuged at 350×g

(2,200 rpm) for 5 min and re-suspended in 100 µl staining buffer (0.5% BSA and 2

mM EDTA in PBS). Peripheral blood cells were then pre-stained with

FITC-conjugated anti-CD16/32 antibody (clone 2.4G2, BD Biosciences) for 10 min

at 4 °C, followed by staining for 20 min with the following antibodies:

CD138-BV421 (clone 281-2, BD Biosciences), CD19-PE-Cy7 (clone 1D3,

eBioscience), and NP-PE (Bioresearch Technologies). After washes and

centrifugation, cells were re-suspended in PBS and analyzed using BD LSRFortessa

(BD Biosciences). Analysis of staining results of cell subsets was performed using

FlowJo software version X (Tree star Inc.).

2.3.2 Spleen

Mouse spleen was dissected out 7 days (day 35) after secondary immunization

(day 28). Mouse splenocytes were collected by gently crushing the spleen placed in

between the coarse surface of two glass slides, followed by passing through a 40-μm

cell strainer before into the 15 mL centrifuge tube. All pre-treatment (removal of

RBC) and staining procedures of splenocytes were performed virtually the same as

described in **Section 2.3.1** except for staining with different antibody cocktails.

Splenocytes were pre-stained with CD16/32-FITC antibody (clone 2.4G2, BD

Biosciences) for 10 min at 4 $^{\circ}$C, followed by staining for 20 min with an antibody

cocktail containing CD19-PE-Cy7 (clone 1D3, eBioscience), CD138-BV421 (clone

281-2, BD Biosciences), CD11b-PerCP-Cy5.5 (clone M1/70, BD Biosciences),

CD11c-AlexaFluor$^{®}$700 (clone HL3, BD Biosciences), GL7-AlexaFluor$^{®}$647 (clone

GL7, BD Biosciences), and NP-PE (Bioresearch Technologies).

To distinguish light zone from dark zone B cells of GCs, splenocytes were

pre-stained with FITC-conjugated anti-CD16/32 antibody (clone 2.4G2, BD

Biosciences) for 10 min at 4 $^{\circ}$C, followed by staining for 20 min with an antibody

cocktail containing B220-APC-Cy7 (clone RA3-6B2), CD86-BV605 (clone GL1),

GL7-AlexaFluor®647 (clone GL7), CXCR4-BV421 (clone 2B11), and

CD95-PE-Cy7 (clone Jo2), all of which were purchased from BD Biosciences. The

NP-PE to stain Ag-specific B cells was obtained from Bioresearch Technologies.
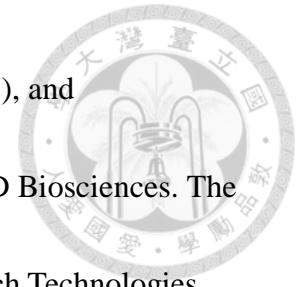
To identify and quantify the T follicular helper (T$_{FH}$) cells, splenocytes were

Fc blocked with anti-CD16/32 antibody (clone 2.4G2, BD Biosciences) for 10 min

at 4 °C before staining with the following antibodies: B220-APC-Cy7 (clone

RA3-6B2, BD Biosciences), CD4-AlexaFluor®647 (clone RM4-5, BD Biosciences),

PD-1-BV421 (clone J43, BD Biosciences), CXCR5-PE (clone 2G8, BD

Biosciences), ICOS-FITC (clone 7E.17G9, eBioscience), and CD69-BV605 (clone

H1.2F3, BioLegend) for 20 min.

2.3.3 Bone marrow

Mouse bone marrow was collected at 7 days (day 35) after secondary

immunization (day 28). Bone marrow cells in femurs were flushed out using

syringes to rinse the bone cavities and transferred to a 15 mL centrifuge tube after

passing through a 40-μm cell strainer. RBC lysis and antibody staining of bone

marrow cells were performed as described in **Section 2.3.2** except for leaving out

the GL7-AlexaFluor®647 (clone GL7, BD Biosciences).

2.4 ELISPOT assay (Enzyme-linked immunosorbent spot)

ELISPOT assays were performed to detect and quantify total and Ag-specific antibody-secreting cells (ASCs). Membranes of PVDF-based ELISPOT plates (MultiScreen$_{HTS}$ IP Filter Plate, Merck Millipore) were pre-treated with 15 µl of 35% ethanol for 1 min, immediately followed by two washes of ddH$_2$O and then one wash of PBS. For detection of total IgG- and IgM-secreting cells, membranes were coated with 5 µg/mL (in 100 µL) of either AffiniPure F(ab')$_2$ fragment specific goat anti-mouse IgG (Jackson ImmunoResearch) or µ chain specific AffiniPure goat anti-mouse IgM (Jackson ImmunoResearch) at 4 ^{o}C overnight. For detection of Ag-specific ASCs, membranes in 96-well plates were coated with 100 µL (10 µg/mL) of either NP7-BSA or NP30-BSA (Biosearch Technologies) at 4 ^{o}C overnight. Following coating, plates were washed once with PBS and then blocked with BlockPRO^{TM} blocking buffer (Visual Protein) for 2 hr at room temperature. To assay and quantify the number of total IgG- or IgM-secreting cells in spleen and bone marrow of day 35 samples from secondary immunization, splenocytes and bone marrow cells were seeded with 6.0×10^4 cells per well and 1.5×10^5 cells per well, respectively. Similarly, splenocytes and bone marrow cells were seeded with 2.4×10^5 cells/well and 3.0×10^5 cells/well, respectively for detection of Ag-specific ASCs. Cells were cultured in 100 µl/well of RPMI 1640 medium

31

supplemented with 10% FCS (fetal calf serum) in a 5% CO_2 incubator at 37 ^{o}C for

16 hr. Following incubation, plates were aspirated and washed twice with ddH_2O,

followed by three washes with PBS-T (0.05% Tween-20 in PBS). Plates were

allowed to soak for 5 min at each wash step. Detection antibodies of horseradish

peroxidase (HRP)-conjugated Fcγ fragment specific AffiniPure rabbit anti-mouse

IgG (Jackson ImmunoResearch) and HRP-conjugated μ chain specific AffiniPure

goat anti-mouse IgM (Jackson ImmunoResearch) were diluted in PBS-T and 100 μl

of them were added into corresponding wells for incubation for 1 hr at room

temperature. Plates were then washed four times with PBS-T and three additional

washes with PBS. During each wash plates were allowed to soak for 2 min. Spots in

each well were developed by addition of 50 μl per well of 3-amino-9-ethylcarbazole

(AEC substrate, BD Biosciences) for ~20 to 30 min. Due to variation in antibody

secretion the time needed for developing visible spots was adjusted accordingly in

some experiments. To stop the substrate reaction, plates were washed vigorously

with ddH_2O. Spots in ELISPOT plates were then enumerated using ImmunoSpot

5.0.2 software (C.T.L.).

2.5 Detection of serum total and antigen-specific antibodies by ELISA

2.5.1 Blood collection and serum separation

Mouse blood was drawn from the submandibular vein using blood lancets (Goldenrod Animal Lancet, MEDIpoint, Inc.) and collected into eppendorf tubes. Blood specimens were left standing upright for 30 min at room temperature until coagulation. Serum was separated from blood clot by centrifugation at 5,500 rpm for 20 min at 4 ^{o}C, and the supernatant was transferred to a new eppendorf tube. Sera were stored at −80 ^{o}C until analysis.

2.5.2 Detection of serum total or antigen-specific IgG and IgM

To detect serum total IgG or IgM, 96-well plates were coated with 5 μg/mL (in 100 μL) of either AffiniPure F(ab')$_2$ fragment specific goat anti-mouse IgG (Jackson ImmunoResearch) or μ chain specific AffiniPure goat anti-mouse IgM (Jackson ImmunoResearch) antibodies at 4 ^{o}C overnight. To detect serum Ag-specific IgG or IgM, plates were pre-coated with 10 μg/mL of either NP7-BSA or NP30-BSA (Bioresearch Technologies) at 4 ^{o}C overnight. Following coating, plates were washed three times with PBS-T and then blocked with BlockPRO^{TM} blocking buffer (Visual Protein) for 2 hr at room temperature, followed by two washes with PBS-T. Mouse serum samples were diluted 20,000-folds in PBS-T and

incubated in pre-coated plates at 4 $^{\circ}$C overnight. To quantify the amount of

antibodies, standard curves were generated using mouse IgG (mouse gamma

globulin, Jackson ImmunoResearch) or IgM (mouse IgM isotype control,

SouthernBiotech). Plates were washed five times with PBS-T and incubated with

diluted horseradish peroxidase (HRP)-conjugated AffiniPure rabbit anti-mouse IgG,

Fcγ fragment specific (Jackson ImmunoResearch) or AffiniPure μ chain specific

goat anti-mouse IgM (Jackson ImmunoResearch) antibodies for 1 hr at room

temperature. Plates were then washed four times with PBS-T followed by three

washes with PBS and then developed with tetramethylbenzidine (TMB) substrate

(BD Biosciences). To quench the reaction, 2N H_2SO_4 was added. Plates were read at

$OD_{450 \text{ nm}}$ and $OD_{570 \text{ nm}}$ using ELISA reader (BioTek). The OD_{450} minus OD_{570} was

calculated to calibrate the background of each well.

2.6 Detection of the cross-reactivity of low-affinity antigen-specific antibodies by sequential ELISA

Mouse serum was drawn as described in **Section 2.5.1**. The 96-well plates

were coated with 100 μL (10 μg/mL) per well of NP7-BSA, NP30-BSA, NIP7-BSA,

or NIP26-BSA (Biosearch Technologies) at 4 $^{\circ}$C overnight. Following coating

antigens, plates were washed three times with PBS-T and blocked with 200 μL/well

BlockPRO^{TM} blocking buffer (Visual Protein) for 2 hr at room temperature. Plates

were then washed twice with PBS-T. Mouse serum samples were diluted

20,000-folds in PBS-T and then added into the NP7-BSA or NIP7-BSA coated wells

of the plate #1 to incubate for 12 hr at 4 $^{\circ}$C. Meanwhile, the standard curve for

quantification was generated using various amounts of mouse IgG (mouse gamma

globulin, Jackson ImmunoResearch). Before washes, the mouse sera in the plate #1

were transferred into NP30-BSA, NIP26-BSA or NIP7-BSA coated wells (for the

group pre-incubated with NP7-BSA coated wells) or NIP26-BSA, NP30-BSA or

NP7-BSA coated wells (for the group pre-incubated with NIP7-BSA coated wells),

both of which were designated as the plate #2 and incubated for 12 hr at 4 $^{\circ}$C **(as

shown in Figure 2.6.1**). After serum transferred to plate #2, the plate #1 was

washed five times with PBS-T and incubated with diluted HRP-conjugated

AffiniPure Fcγ fragment specific rabbit anti-mouse IgG (Jackson ImmunoResearch)

for 1 hr at room temperature. Plates #1 were washed four times with PBS-T,

followed by three washes with PBS and then developed with TMB substrate (BD

Biosciences) until 2N H_2SO_4 was added to stop the reaction. Plates were read at

$OD_{450\,nm}$ and $OD_{570\,nm}$ using ELISA reader (BioTek). The value of OD_{450} minus

OD_{570} was calculated to calibrate the background of each well. After finish of serum

incubation, plates #2 were treated and analyzed as plates #1 for OD reading. A

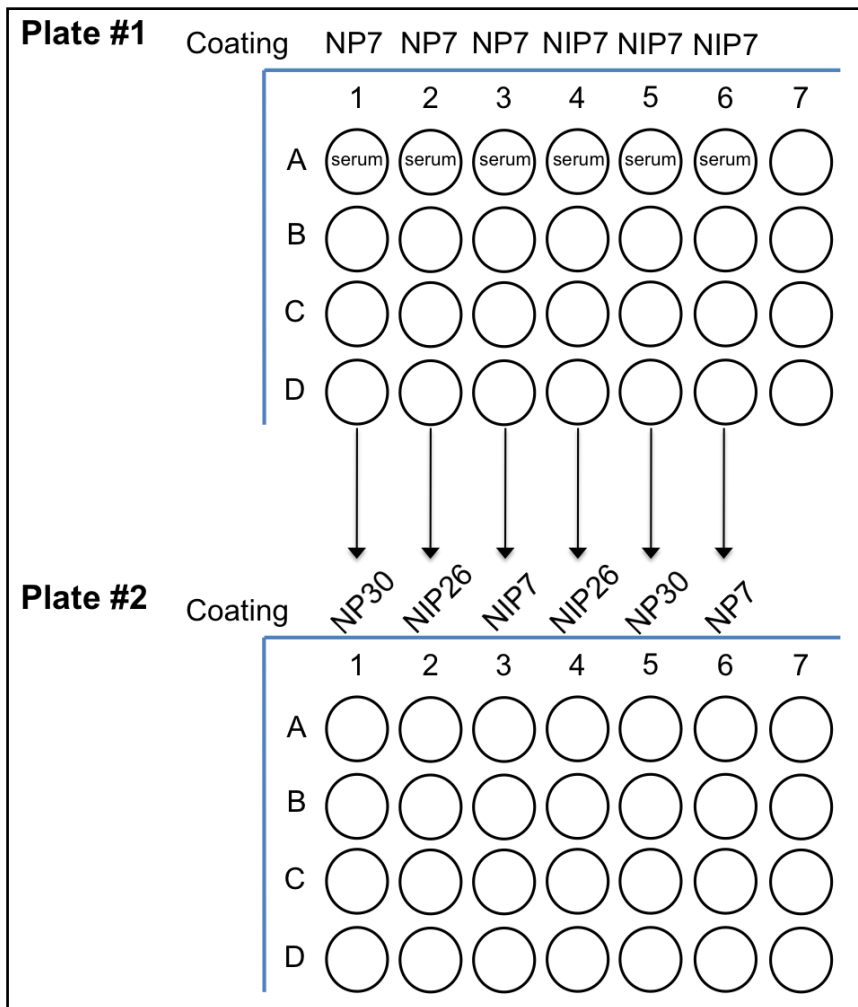schematic of detailed procedures was illustrated in **Figure 2.6.2**.
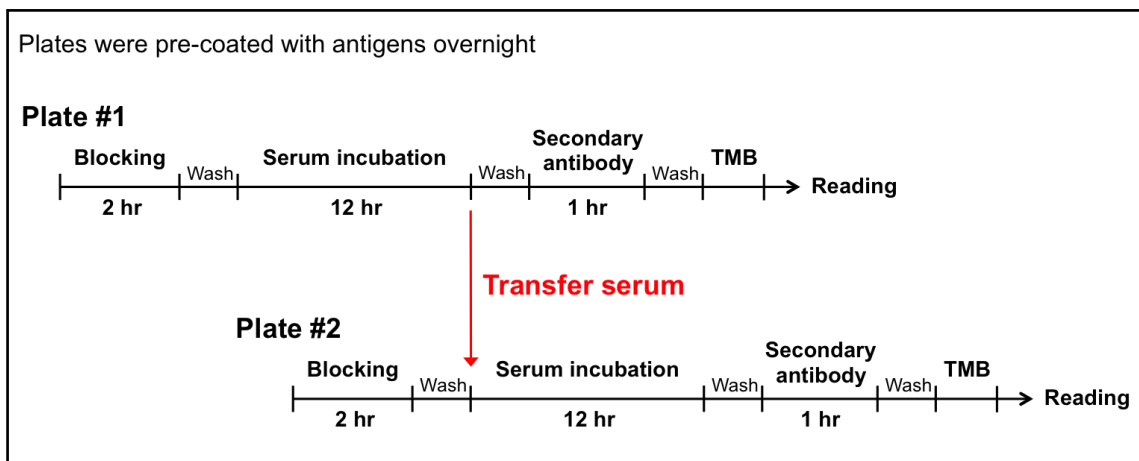
Figure 2.6.1 A schematic of sequential ELISA.

Figure 2.6.2 A schematic of the procedures of sequential ELISA.

2.7 Tissue preparation

2.7.1 Tissue fixation and paraffin block trimming
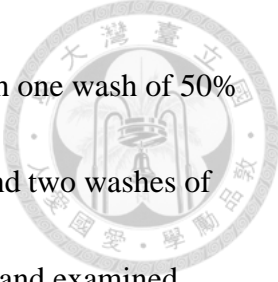
Mouse spleen was dissected and fixed overnight in 10% neutral buffered

formalin (Fisher Scientific) at 4 ^{o}C. Fixed tissues were first dehydrated sequentially

by each wash of 50% ethanol, 70% ethanol, 80% ethanol and 95% ethanol, followed

by two washes of 100% ethanol, and xylene wash for one hr for three times.

Dehydrated tissues were infiltrated in liquid wax for two hr and then embedded in

paraffin. Paraffin block was cut into 4-μm thick sections using rotary microtome

(Leica RM2125 RTS).

2.7.2 Dewaxing and rehydration

Tissue sections were incubated at 60 ^{o}C incubator for 15 min before

deparaffinization with three washes of xylene for 5 min each. Rehydration with two

washes of 100% ethanol followed by two washes of 95% ethanol, one wash of 75%

ethanol, one wash of 50% ethanol, and two washes of ddH$_2$O for 5 min each time in

a sequential manner.

2.7.3 H&E staining

After dewaxing and rehydration, tissue sections were stained with

hematoxylin for 10 min followed by three washes of ddH$_2$O for 2 min each time.

Tissues were then stained with eosin for 1 min followed by three washes of ddH$_2$O

for 2 min each time. Dehydrating was performed sequentially with one wash of 50%

ethanol, one wash of 75% ethanol, two washes of 95% ethanol, and two washes of
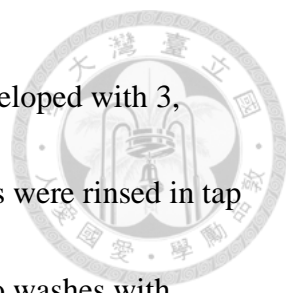
100% ethanol for 3 min each time. Tissue sections were mounted and examined

using a light microscope (Axioplan 2, Zeiss).

2.7.4 Immunohistochemistry (IHC)

After completion of deparaffinization, sections were immersed in boiling

buffer of 10 mM sodium citrate (pH 6.0) and 0.05% Tween-20 for Ag retrieval.

Slides were pressure boiled at 120 $^{\circ}$C for 10 min, and then cooled off for 10 min at

room temperature. Slides were washed twice with ddH$_2$O for 5 min each time,

followed by incubation in 3% H$_2$O$_2$ for 10 min before two washes of ddH$_2$O for 5

min each time. Slides were blocked with PBS containing 5% BSA for one hr at

room temperature. Primary antibodies were diluted in PBS containing 1% BSA

before applying to the sections for incubation at 4 $^{\circ}$C overnight. Slides were washed

twice with PBS-T for 5 min each. Diluted biotinylated goat anti-rabbit IgG

secondary antibodies (VECTASTAIN$^{®}$ ABC Kit (Rabbit IgG), Vector Laboratories)

were added and incubated for 1 hr at room temperature. After two washes with

PBS-T for 5 min each time, slides were incubated with VECTASTAIN$^{®}$ ABC

reagent (Avidin/Biotinylated Horseradish Peroxidase Complex) (VECTASTAIN$^{®}$

ABC Kit (Rabbit IgG), Vector Laboratories) for 40 min at room temperature. Slides

were washed twice with PBS-T for 5 min each time and then developed with 3,

3'-diaminobenzidine (DAB) substrate (Thermo Scientific). Slides were rinsed in tap

water and then counterstained with hematoxylin, followed by two washes with

PBS-T for 5 min each time. Mounted sections were examined with a light

microscope (Axioplan 2, Zeiss).

2.8 Statistics

Statistical analysis was performed using GraphPad Prism 6.0 (GraphPad

Software, Inc.). All data were analyzed by two-tailed unpaired Student's t-test. The

t-test was modified by Welch's correction in case of unequal variance. All results

were showed mean ± SEM. $P < 0.05$ were considered as statistical significance
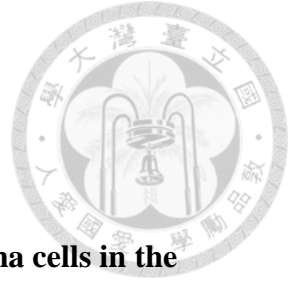
between two groups.

This Page Intentionally Left Blank

Chapter 3
Results

Chapter 3 Results

3.1 FcγRIIB^{T232} mice exhibit more Ag-specific B cells and plasma cells in the spleen and bone marrow during GC reaction

To determine the role of FcγRIIB in the germinal center (GC) reaction, we generated functionally impaired FcγRIIB^{T232} mutant mice, which carried a threonine in substitution for isoleucine at position 232 within the transmembrane domain of FcγRIIB (**Figure 1**). To test our hypothesis that FcγRIIB might involve in the negative selection of GC B cells that have low affinity to Ag, we immunized FcγRIIB^{I232} (wild-type) and FcγRIIB^{T232} mice, respectively with 4-hydroxy-3-nitrophenylacetyl (NP) hapten-chicken gamma globulin (CGG), which enables distinction between low- and high-affinity NP-specific B cells. As illustrated in **Figure 2**, 6- to 8-week old FcγRIIB^{I232} (wild-type) or FcγRIIB^{T232} mice were first immunized (primary immunization) with NP-CGG in alum, followed by a booster (secondary immunization) 28 days later (Day 28). The timing of secondary immunization does not interfere with prior GC reaction, which generally dissolves after about 21 days after Ag administration (Victora, 2014). In circulation we found that FcγRIIB^{T232} mice exhibited more NP-specific B cells and plasma cells than those of FcγRIIB^{I232} mice at two weeks after the primary immunization (**Figure 3, C and E**) as well as one week after the secondary
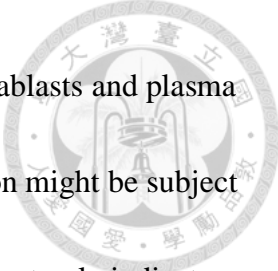
immunization **(Figure 4, C and E)**. Likewise, at one week after the booster when GC

reaction is actively ongoing, we found that both the frequency and cell number of

NP-specific B cells and plasma cells in the spleen of $Fc\gamma RIIB^{T232}$ mice were increased

than those of $Fc\gamma RIIB^{I232}$ mice **(Figure 5, C and E)**. Interestingly, the total (NP-specific

and -non-specific) number of splenic B cells and plasma cells were not significantly

different between these two genotypes of mice **(Figure 5, B and D)**. A greater increase

of the NP-specific B cells and plasma cells was observed in $Fc\gamma RIIB^{T232}$ mice in the

bone marrow **(Figure 6, C and E)**. Of note the NP-specific B cells of $Fc\gamma RIIB^{T232}$ mice

was 27% (i.e. $(5.52\% - 4.35\%)/4.35\%$) higher than that of $Fc\gamma RIIB^{I232}$ mice in the

spleen, but the degree of such difference increased up to 49% (i.e. $(2.78\% - 1.87\%)/$

1.87%) than that of $Fc\gamma RIIB^{I232}$ mice in the bone marrow **(Figures 5C and 6C)**.

Whether there is a survival advantage of NP-specific B cells and plasma cells generated

from the GCs of $Fc\gamma RIIB^{T232}$ mice or an additional selection process in circulation and

in the bone marrow is an interesting open question for $Fc\gamma RIIB^{T232}$ is less inhibitory.

Similarly, the frequency of NP-specific plasma cells of $Fc\gamma RIIB^{T232}$ mice was 19% (i.e.

$(25.6\% - 21.5\%)/21.5\%$) and 48% (i.e. $(9.3\% - 6.3\%)/6.3\%$) more than those of

$Fc\gamma RIIB^{I232}$ mice in the spleen and bone marrow, respectively **(Figures 5E and 6E)**. It is

well known that plasma cells express the highest level of $Fc\gamma RIIB$ in subsets of B cells.
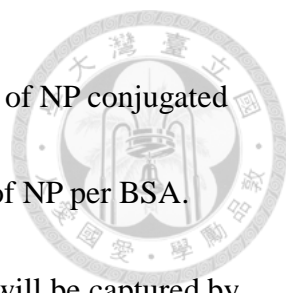
Given the fact that crosslinking $Fc\gamma RIIB$ induces apoptosis of plasma cells in the bone

marrow (Xiang*, et al.*, 2007), it is likely that the extrafollicular plasmablasts and plasma cells in circulation where ICs are readily accessible after immunization might be subject to apoptosis triggered through FcγRIIB. Taken together, these results not only indicate a defect in the negative selection of NP-specific B cells and plasma cells carrying FcγRIIB^{T232} in the spleen but suggest an extended negative regulation of FcγRIIB in circulation and bone marrow. From the standpoint of homeostasis, FcγRIIB may play an unappreciated role in the control of total B-cell number outside the GCs.

3.2 FcγRIIB^{T232} mice produce more low-affinity Ag-specific IgG-secreting cells in the spleen and bone marrow during GC reaction

As shown in **Figures 3-6**, the functionally impaired FcγRIIB^{T232} resulted in retention of more Ag-specific B cells and plasma cells during GC reaction. We next examined the antibody affinity secreted by these increased Ag-specific plasma cells, i.e. NP-specific antibody-secreting cells (ASCs) in the spleen and bone marrow in particular from FcγRIIB^{T232} mice by enzyme-linked immunosorbent spot (ELISPOT). Since our phenotypic data by flow cytometry suggest a defect in the deletion of low-affinity NP-specific B cells **(Figures 3-6)**, we measured the low- vs. high-affinities of NP-specific ASCs in the spleen and bone marrow from FcγRIIB^{I232} and FcγRIIB^{T232} mice after secondary immunization. To do so, we coated ELISPOT plates with either NP7-BSA or NP30-BSA, both of which contain different numbers of NP molecules

44

conjugated to one BSA. For instance, NP7-BSA harbors 7 molecules of NP conjugated to each BSA while NP30-BSA contains an average of 30 molecules of NP per BSA. With these in hands, ASCs that secrete high-affinity NP-specific Igs will be captured by both NP7-BSA and NP30-BSA, whereas ASCs that secrete low-affinity Igs will be captured predominantly by NP30-BSA only owing to a disadvantage in binding to an NP Ag of low valency number. Consistently, we observed a significant increase of total IgG-secreting B cells in the spleen of FcγRIIB^{T232} mice compared to those of FcγRIIB^{I232} mice (**Figure 7A**). Moreover, the NP30-specific IgG-secreting cells in the spleen of FcγRIIB^{T232} mice were also markedly increased than those of FcγRIIB^{I232} mice (**Figure 7C**). Interestingly, however, the NP7-specific IgG-secreting cells were not significantly different (**Figure 7B**). When the absolute numbers of NP30-specific and NP7-specific IgG-secreting cells were compared, we found that the increase of NP-specific IgG-secreting cells in FcγRIIB^{T232} mice were predominantly of low-affinity, indicating a failure of GC reaction to eliminate these cells (**Figure 7D**). In contrast, total IgM ASCs in the spleen of FcγRIIB^{T232} mice were not increased (**Figure 7F**), and both NP7-specific and NP30-specific IgM ASCs were not significantly different in groups of FcγRIIB^{T232} and FcγRIIB^{I232} mice after secondary immunization (**Figure 7, G and H**). Consistent with the notion that IgG, but not IgM, is a ligand of FcγRIIB, the generation of IgG ASCs, but not IgM ASCs, are affected during the GC reaction. In addition, we

detected more total and Ag-specific (both NP7- and NP30-specific) IgG ASCs in the

bone marrow of FcγRIIB^{T232} mice after boosting **(Figure 8, A-C)**, in particular the

increase of low-affinity NP-specific ASCs **(Figure 8D)**. Taken together, these data

indicate a strong causal relationship of a functionally impaired FcγRIIB and the

retention of low-affinity Ag-specific B cells as a result of defective negative selection

during the GC reaction. This defect is likely a consequence of defective function of

FcγRIIB^{T232} during the process of affinity maturation that normally can enable stringent

negative selection of low-affinity Ag-specific B cells to ensure the production of high

affinity neutralizing antibodies through GC reaction.

3.3   FcγRIIB^{T232} mice increase the generation of low-affinity Ag-specific IgG in the circulation during GC reaction

To assess whether the increased low-affinity NP-specific IgG-secreting cells in

FcγRIIB^{T232} mice caused a concomitant increase of low-affinity NP-specific antibodies

in the circulation, we performed an ELISA assay for antibody quantification. We found

that the level of total IgG in the sera of FcγRIIB^{T232} mice was significantly increased

than that of FcγRIIB^{I232} mice after primary and secondary immunizations **(Figure 9A)**.

Furthermore, the serum levels of both NP7-specific and NP30-specific IgG in

FcγRIIB^{T232} mice were significantly elevated than those of FcγRIIB^{I232} mice after

primary and secondary immunizations **(Figure 9B)**. Using the ratio of NP7/NP30 to

determine the affinity stringency of the NP-specific IgG, we found a lower ratio of

serum IgG of $Fc\gamma RIIB^{T232}$ mice than that of $Fc\gamma RIIB^{I232}$ mice after both primary and

secondary immunizations (**Figure 9C**). Taken together, these data suggest that the

impaired function of $Fc\gamma RIIB$ leads to an increase of predominant low-affinity

Ag-specific IgG and to a lesser degree of high-affinity IgG after secondary

immunization.

3.4 A functionally impaired FcγRIIB increases the number of GC B cells with a concomitant increase of the size of GCs

As described above, immunized $Fc\gamma RIIB^{T232}$ mice tended to reserve more

low-affinity Ag-specific ASCs in the spleen and bone marrow in comparison with those

of $Fc\gamma RIIB^{I232}$ mice. We went on to examine the morphology of GCs, which can be

divided into dark and light zones by their structural density and respective functions.

While somatic hypermutation occurs in the dark zone, the affinity maturation and

selection operate in the light zone in the GC response. The purpose of affinity-based

selection is to ensure the high-affinity GC B cell mutants are positively selected for

development, while the low-affinity BCR mutant GC B cells to be eliminated through

apoptosis. If there is a failure to delete the low-affinity mutants, the size and number of

GCs are likely increased as a result of accumulation of these GC B cells. Furthermore,

the negative selection during affinity maturation is thought to occur in the light zone of

GCs; therefore, an expansion of GC B cells (centrocytes) in the light zone will confirm our notion. To address this issue we analyzed the cell composition within the GCs of FcγRIIB^{T232} and FcγRIIB^{I232} mice after secondary immunization. The results showed an increase in not only the proportion but the number of GC B cells in the spleen of FcγRIIB^{T232} mice compared to FcγRIIB^{I232} mice **(Figure 10B)**. When the B cells in the dark zone and light zone were analyzed by surface staining of CXCR4 and CD86, we found the percentage and number of light zone B cells (CD86^{hi}CXCR4^{low}) but not those of dark zone (CD86^{low}CXCR4^{hi}) B cells in FcγRIIB^{T232} mice were significantly increased **(Figure 10, C and D)**. In addition, we also investigated the morphology of the GC within lymphoid follicles using H&E staining. Consistent with an increased number of GC B cells, the spleen of FcγRIIB^{T232} mice displayed an increased size of the GC within lymphoid follicles **(Figure 11)**. These data further support the crucial role of FcγRIIB in the negative selection of low-affinity B cells during GC reaction for the functionally impaired FcγRIIB^{T232} mice manifest with a remarkable increase of the low-affinity Ag-specific B cells in the spleen. In addition, since the ability to exert inhibitory function is the only difference between wild-type FcγRIIB^{I232} and FcγRIIB^{T232} mice, we argue that the central theory of poor Ag competition for survival of low-affinity Ag-specific B cells, which eventually develop into low-affinity Ag-specific ASCs, to prevent their retention might not be fully accountable.
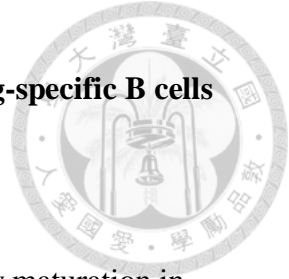
3.5 T$_{FH}$ cells do not contribute to the increase of low-affinity Ag-specific B cells and antibodies in FcγRIIB^{T232} mice

As T$_{FH}$ cells are known to be essential in the process of affinity maturation in addition to class switching (Schwickert*, et al.*, 2011, Victora*, et al.*, 2010), we next investigated whether the increase of low-affinity B cells in FcγRIIB^{T232} mice might in part result from the defect of T$_{FH}$ cells although FcγRIIB is not known to influence the interaction between T$_{FH}$ cells and GC B cells at the light zone. As expected, we found the number of T$_{FH}$ cells in FcγRIIB^{T232} mice were roughly the same as that in FcγRIIB^{I232} mice **(Figure 12A)**. Since the T$_{FH}$ cells are associated with class switch of immunoglobulin, we examined whether FcγRIIB might have an impact on Ig isotypes. In mice T$_H$1 cells predominantly produce interferon-γ (IFN-γ) and T$_H$2 cells predominantly produce interleukin-4 (IL-4). IL-4 induces the class switching to IgG1 production, while IFN-γ switches Ig synthesis to IgG2a by B cells (Abbas*, et al.*, 1990). We investigated the isotype of total IgG and NP-specific IgG in FcγRIIB^{I232} and FcγRIIB^{T232} mice and found that not only total but Ag-specific (NP7- and NP30-specific) IgG isotypes (IgG1, IgG2a, IgG2b and IgG3) in FcγRIIB^{T232} mice had a similar pattern to that of FcγRIIB^{I232} mice **(Figure 12, B and C)**, indicating that FcγRIIB^{T232} mice appeared not affect the production of Ag-specific IgG isotypes during immunization. Taken together, these data suggest that the impaired function of FcγRIIB on GC B cells

is unlikely to influence the T_{FH} cells to contribute to the increase of low-affinity

Ag-specific B cells and their secreted antibody isotypes.

3.6 The increased low-affinity Ag-specific B cells and antibodies in FcγRIIB[T232] mice are caused by a decrease of apoptosis of GC B cells
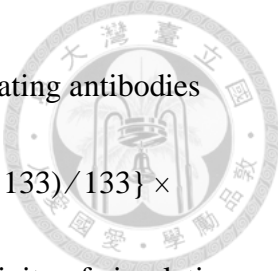
The GC B cells carrying low-affinity BCR are eliminated through apoptosis. To

determine whether the increased level of low-affinity Ag-specific B cells and antibodies

in FcγRIIB[T232] mice might result from a decrease of apoptosis of low-affinity GC B cells,

we performed flow cytometry to determine the percentage of dead cells of GC B cells in

FcγRIIB[I232] and FcγRIIB[T232] mice. We found that FcγRIIB[T232] mice had lower

percentage of dead cells in GC B cells compared to that of FcγRIIB[I232] mice (**Figure

13A**). As caspase-3 is one of the key executioners of apoptosis, and previously study has

shown that cross-linking of FcγRIIB induces the apoptosis through caspase-9

and-3-mediated pathways (Tzeng, *et al.*, 2005). We then assessed the levels of activated

caspase-3 in the GCs of FcγRIIB[I232] and FcγRIIB[T232] mice by performing an

immunohistochemistry (IHC) assay. The IHC analysis revealed that the FcγRIIB[T232]

mice possessed less activated caspase-3-expressed GC B cells that undergoing apoptosis

in the light zone than FcγRIIB[I232] mice (**Figure 13B**). Taken together, these data suggest

that the functionally impaired FcγRIIB indeed results in decreased apoptosis of GC B

cells during GC reaction. This is consistent with a crucial role of FcγRIIB in the

negative selection of GC B cells.

3.7 The increased low-affinity Ag-specific antibodies in FcγRIIB^{T232} mice have an

increased cross-reactivity to homologous antigen

As illustrated in **Figure 9, B and C**, FcγRIIB^{T232} could result in an increased

production of serum low-affinity Ag-specific antibodies. We then determined whether

these low-affinity antibodies in FcγRIIB^{T232} mice possessed cross-reactivity to Ag

homologues. To examine our hypothesis, we performed a sequential ELISA assay to

measure the potential cross-reactivity of NP-specific antibodies to the NIP

(4-hydroxy-3-iodo-5-nitrophenylacetyl) hapten, which is a homolog of NP hapten. We

started by incubating the serum of FcγRIIB^{I232} mice and FcγRIIB^{T232} mice separately in

NP7-BSA pre-coated plates to capture and remove high-affinity NP-specific antibodies

in the mouse sera. When the incubation period was finished we transferred the

remaining sera into another plate containing NP30-BSA, NIP26-BSA or NIP7-BSA

pre-coated wells separately for a second incubation to detect the potential

cross-reactivity to NIP from the low-affinity NP-specific antibodies. Our results showed

that circulating antibodies with cross-reactivity to NIP26 and to a lesser degree to NIP7

in FcγRIIB^{T232} mice were higher than those of FcγRIIB^{I232} mice, suggesting that the

impaired function of FcγRIIB can lead to an increase of cross-reactive antibodies to

homologous Ags **(Figure 14A)**. Remarkably, we found that the circulating antibodies cross-reactive to NIP26 in $Fc\gamma RIIB^{T232}$ mice were 123% (i.e. $\{(296 - 133)/133\} \times 100\%$) higher than those of $Fc\gamma RIIB^{I232}$ mice, whereas the cross-reactivity of circulating antibodies to NIP7 in $Fc\gamma RIIB^{T232}$ mice was even greater with a 183% (i.e. $\{(147 - 52)/52\} \times 100\%$) higher than those of $Fc\gamma RIIB^{I232}$ mice. This finding suggests that the circulating low-affinity Ag-specific antibodies in $Fc\gamma RIIB^{T232}$ mice have stronger cross-reactivity to homologous Ags compared to $Fc\gamma RIIB^{I232}$ mice.

Consistent with the results shown in **Figure 9B**, we found that the level of low-affinity (NP30-specific) Ag-specific antibodies in $Fc\gamma RIIB^{T232}$ mice were indeed higher than that in $Fc\gamma RIIB^{I232}$ mice when the high-affinity (NP7-specific) Ag-specific antibodies had been removed in prior incubation **(Figure 14A)**. Interestingly, as shown in **Figure 14A** the high-affinity (NP7-specific) antibodies in $Fc\gamma RIIB^{T232}$ mice was 117% (i.e. $\{(1085 - 499)/499\} \times 100\%$) higher than that in $Fc\gamma RIIB^{I232}$ mice, whereas the low-affinity (NP30-specific, after removal of NP7-specific) antibodies in $Fc\gamma RIIB^{T232}$ mice was even higher with 178% (i.e. $\{(203 - 73)/73\} \times 100\%$) compared to that in $Fc\gamma RIIB^{I232}$ mice. On the other hand, if we first removed the cross-reactive antibodies by incubating the mouse sera with pre-coated NIP7-BSA, the level of both high-affinity and low-affinity NP-specific antibodies of $Fc\gamma RIIB^{T232}$ mice remained higher than that in $Fc\gamma RIIB^{I232}$ mice **(Figure 14B)**. These results provide additional

evidence of the increase of low affinity NP-specific antibodies in FcγRIIB^{T232} mice

under no interference of cross-reactive antibodies. On the other hand, these data also

suggest that the signaling dysfunction of ligation of FcγRIIB^{T232} itself may be more

severe than that of co-ligation of FcγRIIB^{T232} and BCR, which is not known to influence

the outcome of affinity maturation. In addition, due to the presence of cross-reactive

antibodies in the pool of low-affinity Ag-specific antibodies this phenomenon cannot be

simply explained by an increase in proliferation of GC B cells in FcγRIIB^{T232} mice.

Namely, the increased level of low-affinity Ag-specific antibodies in FcγRIIB^{T232} mice

supports a defect of apoptosis caused by signaling dysfunction of ligation of

FcγRIIB^{T232} itself by ICs. Since co-ligation of FcγRIIB^{T232} and BCR has a defect in

inhibitory signaling, this can contribute to an increased number of naïve B cells in the

follicle, leading to an increased input of GC B cells in the GC response, but the

increased number of Ag-specific GC B cells is not expected to be biased to low-affinity

Ag-specific B cells under affinity maturation and selection. On the other hand, a defect

in FcγRIIB-mediated apoptosis of B cells is expected to favor the existence of

low-affinity Ag-specific GC B cells even though they are widely thought to be less

competitive for Ag capture for survival. Taken together, our data have provided a great

deal of evidence to demonstrate that the apoptotic response of FcγRIIB is essential for

elimination of low-affinity GC B cells during GC reaction and a failure of this process

results in the emergence of low-affinity Ag-specific antibodies, which possess

cross-reactivity to homologous Ags.

Chapter 4

Discussion

Chapter 4 Discussion

4.1 Using FcγRIIB^{T232} mice as a model to investigate the role of FcγRIIB in the negative selection during GC reaction

In this study, we generated a transgenic mouse line carrying a functionally impaired FcγRIIB^{T232} to study immune dysfunction of B cells. The FcγRIIB^{I232T} mutant mice contained a *neo* cassette in the recombinant allele and it has not been deleted by *Cre* recombinase. Despite of this, the neomycin-resistant gene in the cassette did not appear to affect the development of B cells in FcγRIIB^{T232} mice. Likewise, the FcγRIIB-deficient mice (B6.129S4-*Fcgr2b*^{tm1Ttk}), which were generated by Jeffrey V. Ravetch, also retain the *neo* cassette. Similarly, the development of myeloid and lymphoid cells of these mice were not affected (Takai, *et al.*, 1996).

Although FcγRIIB^{T232} is an SLE susceptible allele, these mice do not exhibit spontaneous lupus up to 40 weeks old. Studies have shown that the expression level of FcγRIIB on B cells up-regulates during GC reaction. In contrast, down-regulation of FcγRIIB on B cells is often found in autoimmune prone mice, leading to increased number and size of GCs (Jiang, *et al.*, 2000; Jiang, *et al.*, 1999; McGaha, *et al.*, 2008; Paul, *et al.*, 2007; Pritchard, *et al.*, 2000; Tiller, *et al.*, 2010; Xiu, *et al.*, 2002). Furthermore, the lack of FcγRIIB eventually results in lupus-like disease, manifested by

an expansion of ASCs in the spleen (Bolland and Ravetch, 2000). Based on these

findings, we proposed that FcγRIIB might play a crucial role in GC reaction. To test our

hypothesis, we immunized wild-type FcγRIIB[I232] and mutant FcγRIIB[T232] mice with

NP-CGG, which allows for detection and discrimination of low- and high-affinity

Ag-specific B cells as well as their secreted antibodies to determine whether a failure in

the negative selection of low-affinity cells during GC reaction occurs. Our results

showed that FcγRIIB[T232] mice displayed an increased number of low-affinity

NP-specific IgG ASCs in the spleen and in the bone marrow as well as an increased

serum level of low-affinity NP-specific IgG antibodies (**Figures 7C, 8C and 9, B and

C**). Moreover, an increase in the size of GCs pointed to the pathological origin of these

low-affinity NP-specific ASCs and antibodies. Since every GC B cell carries a mutated

BCR with various degree of affinity for Ag, we should be able to obtain genetic

evidence by sequencing and analyzing the repertoire of somatic hypermutants of the

BCR's V_H186.2 gene, which is specific for NP. An increase in the repertoire and

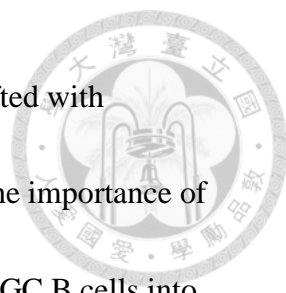frequency of VH186.2 gene mutation is expected in GC B cells of FcγRIIB[T232] mice.

It is not surprising that to some degree the phenotype of FcγRIIB[T232] mice may

resemble that of FcγRIIB knockout mice in GC reaction in that both FcγRIIB[T232] mice

(**Figures 10B and 11**) and FcγRIIB-deficient mice (McGaha, *et al.*, 2008; Tiller, *et al.*,

2010) develop increased number of GC B cells and increased size of GCs. Since

FcγRIIB-deficient mice spontaneously develop massive autoantibodies and undergo

continuous GC reaction, these mice are not suitable for studying GC response to

immunization. In addition, partial restoration of FcγRIIB's expression by retroviral

transfection of B cells can ameliorate lupus syndrome (McGaha, *et al.*, 2005). This

report is consistent with our preliminary findings that FcγRIIB^{T232} mice do not

spontaneously develop lupus up to 40-week-old, suggesting that FcγRIIB^{T232}, despite its

lower inhibitory ability, may still be competent for maintenance of tolerance for a while.

The use of FcγRIIB^{T232} mice to study the role of FcγRIIB in negative selection of

low-affinity GC B cells has unique advantages over FcγRIIB knockout mice. For

example, since the inhibitory function of FcγRIIB^{T232} is not entirely lost and the

mutated amino acid of FcγRIIB^{T232} is of clinical relevance, manipulation of FcγRIIB^{T232}

for treating autoimmune diseases is of superior feasibility to that of FcγRIIB-deficient

mice. Specifically we can try to up-regulate the expression of FcγRIIB^{T232} by

pharmacological agents to ameliorate disease activity of patients. Whether up-regulation

of FcγRIIB^{T232} on the GC B cells can enhance the inhibitory role of FcγRIIB^{T232} and

reverse the GC phenotype during immunization is an important question to answer in

the future. Obviously this question cannot be addressed in the setting of FcγRIIB

knockout mice.

The current dogma attributes the deletion of low-affinity Ag-specific GC B cells

to a lack of survival signal from BCR due to its low affinity for Ag. However, our data

revealed that without a change of the BCR itself along with the process of Ag-driven

somatic hypermutation, a lower inhibitory function of $Fc\gamma RIIB^{T232}$ can evidently result

in retention of low-affinity Ag-specific B cells during the GC reaction. The conventional

paradigm exclusively weighs on the affinity of Ag for BCR to determine cell fate with

the assumption that Ag is essential for GC B cells both in proliferation and in

differentiation during GC response. However, an engineered membrane BCR transgenic

line, which lacks antibody (secreted form of BCR) secretion, also presents an

enlargement of GCs in immunization argues against the central dogma of Ag as the

major, if not the sole, determinant in negative selection of low-affinity Ag-specific B

cells (Hannum, *et al.*, 2000). Together with our data from $Fc\gamma RIIB^{T232}$ mice, we are

inclined to place emphasis on $Fc\gamma RIIB$ as an active player in the induction of apoptosis

of low-affinity Ag-specific GC B cells during the process of affinity maturation. Since

$Fc\gamma RIIB$ is widely expressed on immune cells except for T cells and NK cells, a bone

marrow chimera experiment with transfer of $Fc\gamma RIIB^{T232}$ bone marrow into irradiated

$Fc\gamma RIIB^{I232}$ mice and vice versa will provide further insights into whether the defective

GC response is intrinsic and autonomous to $Fc\gamma RIIB^{T232}$ in GC B cells. Specifically, the

GC response of $Fc\gamma RIIB^{I232}$ mice that receive $Fc\gamma RIIB^{T232}$ GC B cells is expected to

resemble that of FcγRIIB^{T232} mice, whereas FcγRIIB^{T232} mice engrafted with

FcγRIIB^{I232} GC B cells will behave like wild-type mice. In spite of the importance of

T$_{FH}$ cells in class switch of antibody isotype and in differentiation of GC B cells into

plasmablasts during GC reaction, T cells do not express FcγRIIB and our data indicate

no involvement of T$_{FH}$ cells **(Figure 12, A-C)**. Therefore, the results from bone marrow

chimera experiments are likely to support an intrinsic defect of FcγRIIB^{T232} GC B cells.

Another feasible way to provide evidence for FcγRIIB to be in charge of negative

selection of GC B cells is to use an inducible knockout system to induce deletion of

FcγRIIB gene prior to immunization. However, current commonly used inducible

systems are based on doxycycline and tamoxifen for induction. The potential problem is

whether doxycycline or tamoxifen might have adverse effects on B cells and perhaps

other immune cells. The inducible FcγRIIB knockout system obviously has the

advantage to delineate the requirement of FcγRIIB at different stages of the GC reaction,

which last for about 21 days, by switching on and off the gene deletion (De Silva and

Klein, 2015). Typically subcutaneous immunization with hapten-carrier emulsified in

alum adjuvant, the affinity selection occurs at days 8 to 21 after injection (Victora,

2014). Under this circumstance, if FcγRIIB is deleted when affinity maturation is

ongoing, more low-affinity Ag-specific GC B cells are expected to accumulate, thereby

reminiscent of the phenotype of FcγRIIB^{T232}. In practical sense pharmacological

modulation to regulate the expression level of FcγRIIB at different stages of the GC

reaction is easier to translate into clinical use. Future direction will aim to screen and

analyze the modulators of FcγRIIB for this purpose.

4.2 Does FcγRIIB^{T232} have a haploinsufficient effect or a dominant-negative role in the negative regulation of GC B cells?

Haploinsufficiency occurs when only one copy of a wild-type gene is not enough

to provide wild-type function, whereas dominant-negative effect occurs when the

mutant allele directly inhibits the function of wild-type gene or inhibits other genes that

are required for the function of wild-type gene. To determine whether FcγRIIB has such

effects, analysis of FcγRIIB$^{+/-}$ heterozygous mice should be able to answer this question.
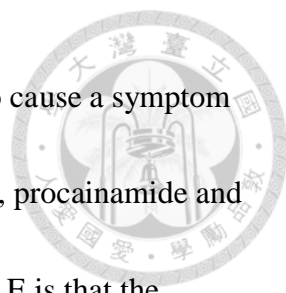
FcγRIIB$^{+/-}$ heterozygous mice that are partially deficient in FcγRIIB exhibit an

increased production of rheumatoid factors (RF) and anti-DNA autoantibodies in the

presence of the Y-linked autoimmune acceleration (*Yaa*) locus, which harbors a

duplicate copy of TLR-7 (Pisitkun*, et al.*, 2006). This result supports the possibility of

FcγRIIB haploinsufficiency for a dysfunction in the elimination of auto-reactive B cells

(Moll*, et al.*, 2004). To investigate whether FcγRIIB^{I232T} mutation has a

dominant-negative effect on the inhibition of B cell activation and proliferation, we took

advantage of the availability of FcγRIIB^{I232T} heterozygous (232I/T) mice. As a matter of

fact, we were surprised to find that more FcγRIIB^{I232T} heterozygous mice exhibited a

phenotype reminiscent of FcγRIIB^{232T} homozygous (232T/T) than wild-type mice in

GC response. This finding thereby suggests that FcγRIIB^{232T} allele is dominant-negative

to the wild-type FcγRIIB^{232I} allele (**Supplementary Figure 1**). Future works are

underway to address this issue.

4.3 Potential strategies to induce SLE in FcγRIIB^{T232} mice

Our initiative to generate FcγRIIB^{T232} mice was to use it as a model to study the

pathogenesis of the human I232T polymorphism of FcγRIIB with SLE in particular in

Asian populations. Previous studies have shown that when the peripheral blood

mononuclear cells of FcγRIIB^{T232} donors were transplanted into immunodeficient mice,

spontaneous elevation of autoantibodies can be observed overtime but whether this

eventually will lead to full blown lupus-like disease remains to be determined

(Baerenwaldt, *et al.*, 2011). The availability of FcγRIIB^{T232} mice provides us an unique

opportunity to interrogate not only the pathogenesis of human SLE but the efficacy of

therapeutic intervention. However, we could not observe any lupus symptoms of female

FcγRIIB^{T232} mice up to 40 weeks old. Since human SLE is considered as a

multi-factorial disease, a relevant trigger or an additional gene abnormality is likely

required to induce lupus or autoimmune disease in the FcγRIIB^{T232} mice. Two potential

strategies can be used to induce lupus in FcγRIIB^{T232} mice. One way is to induce by

drugs, while the other means is to introduce additional gene aberration. In terms of

induction of lupus by drugs, a number of drugs have been reported to cause a symptom that resembles SLE. The most common agents in use are hydralazine, procainamide and quinidine (Rubin, 1992). A major drawback of these drug-induced SLE is that the symptom of SLE is only transient and it will restore to normal within a few days to months once withdrawal of the drugs. In addition to drugs, several studies have shown that estrogen promotes development of SLE (Holmdahl, 1989). It is known that use of estrogen-contraceptive therapy exacerbates SLE disease in humans (Jungers, *et al.*, 1982), and in NZB/NZW F_1 mice that receive prepubertal castration in combination with estrogen treatment results in a significant increase in mortality both in male and female mice (Roubinian, *et al.*, 1978). These findings suggest that estrogen seems to be a suitable choice to induce lupus in the FcγRIIB^{T232} mice. As for induction of SLE through gene manipulation, it will be preferred to select genes related to signaling and differentiation of B cells to concentrate on further determination of the contribution of FcγRIIB in the disease onset, course and severity of SLE. Several genes in the B-cell signaling pathways have been reported to be susceptible to SLE (Mohan and Putterman, 2015; Vaughn, *et al.*, 2012); for instance, LYN (Lu, *et al.*, 2009), BLK (B lymphoid tyrosine kinase) (Hom, *et al.*, 2008; Ito, *et al.*, 2009; Wu, *et al.*, 2015; Yang, *et al.*, 2009), BANK1 (B-cell scaffold protein with ankyrin repeats 1) (Chang, *et al.*, 2009; Guo, *et al.*, 2009; Kozyrev, *et al.*, 2008), and so on. The genetic modeling of a disease is usually

compelling and more definitive, but it is time-consuming, labor-intensive and costly. In addition, epigenetic regulators and modifiers also contribute to the pathogenesis and disease activity of SLE. For the same reason, we will prioritize these regulators related to B-cell signaling, in particular those susceptible genes from linkage studies and genome-wide gene analyses.

4.4 Potential strategies to treat SLE carrying FcγRIIB-I232T polymorphism

To treat and to cure disease is the ultimate goal for us to study SLE. Current main treatment for SLE is still corticosteroids, cytotoxic drugs and immunosuppressants, e.g. cyclophosphamide. Given the fact that FcγRIIB is an essential inhibitory molecule in B cells and the functional status of FcγRIIB closely correlates with the prevention of antibody-mediated autoimmunity, our central idea to use drugs to target FcγRIIB for patients with SLE and for restoration of normal GC response in FcγRIIB^{T232} mice represents a new strategy for translational research. Such notion is further supported by a previous study that plasma cells from FcγRIIB-deficient mice as well as lupus-prone mice are protected from apoptosis and this may contribute to the production of autoantibodies (Xiang, *et al.*, 2007). This result suggests that up-regulation of FcγRIIB might compensate for the impaired function of FcγRIIB^{T232} polymorphism, supporting our strategy for the treatment of SLE. Alternatively, we should be able to enhance the downstream signaling of FcγRIIB to achieve the same goal as boosting the expression

64

of FcγRIIB. Studies indicate that the polymorphic FcγRIIB[T232] is unable to inhibit activating receptor because it is excluded from sphingolipid rafts, resulting in the susceptibility to SLE for B-cell activation is less inhibited (Floto, *et al.*, 2005; Kono, *et al.*, 2005). However, whether FcγRIIB[T232]-mediated apoptosis of B cells is more important than its inhibition on BCR in GCs is not easily reconciled for the signaling transduction of the former is not yet fully understood and it is difficult to completely tweeze out these two distinct pathways *in vivo* though our data support the apoptotic response mediated by FcγRIIB is likely more critical in GC response *in vivo*. In this regard, utilization of drugs that can enhance B-cell apoptosis through FcγRIIB is potentially a better strategy for the treatment of SLE.

4.5 Peritoneal B-1a cells express high level of FcγRIIB and are highly associated with autoimmune diseases

It has been found that B-1a cells are associated with autoimmunity. B-1a cells are distinguished from conventional B-2 cells by their functions and high expression of CD5, a pan T-cell surface glycoprotein (Stall, *et al.*, 1996). B-1a cells are mainly located in peritoneal and pleural cavities and play an important role in response to thymus-independent antigens and invading microbial pathogens. B-1a cells are primary source of the production of natural IgM, which are polyreactive low-affinity antibodies providing an innate immunity of defense against pathogens (Murakami and Honjo,

1995). The characteristics of polyreactivity and low affinity enable these IgM antibodies

recognize a broad range of antigens; however, on the flip side these antibodies also can

lead to the cross-reactivity with autoantigens (Baumgarth, *et al.*, 2005). Studies show

that the number of B-1a cells is elevated in patients with Sjoren's syndrome (Dauphinee,

et al., 1988) and rheumatoid arthritis (Youinou, *et al.*, 1990). In addition, lupus-prone

NZB and NZB/NZW F1 mice exhibit increased number of B-1a cells (Hayakawa, *et al.*,

1983).
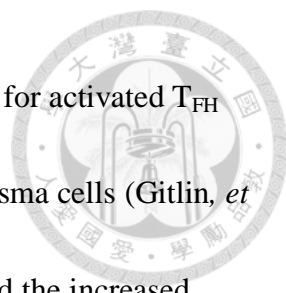
Peritoneal B-1 cells express significantly higher level of FcγRIIB than other B

cell subsets (splenic B-1, B-2, and marginal zone B cells and peritoneal B-2 cells)

(Amezcua Vesely, *et al.*, 2012). FcγRIIB-deficient mice dramatically increase the

number of peritoneal B-1 cells because of protection from FcγRIIB-mediated apoptosis.

Furthermore, FcγRIIB-deficient mice exhibit increased serum levels of

anti-phosphatidylcholine (PtC) IgM and IgG antibodies (Amezcua Vesely, *et al.*, 2012),

which are the most widely expressed natural antibodies (Mercolino, *et al.*, 1988).

However, whether FcγRIIB[T232] mice also exhibit increased number of peritoneal B-1

cells remains to be determined. It is likely that FcγRIIB[T232] mice might delay the

appearance of autoreactive B-1 cells as seen in FcγRIIB knockout mice. Since

autoimmune diseases often display an increase of B-1a cells, which highly express

FcγRIIB, and conversely FcγRIIB-deficient mice spontaneously develop autoimmune

diseases (Bolland and Ravetch, 2000; Iruretagoyena, *et al.*, 2008; Tiller, *et al.*, 2010; Yuasa, *et al.*, 1999), it is important to investigate the likelihood of FcγRIIB[T232] on B-1a cells to break tolerance, leading to aberrant homeostasis of B-1 cells overtime.

4.6 T$_{FH}$ cells involve in the affinity maturation of GC B cells

T follicular helper (T$_{FH}$) cells are essential for GC formation and development (Johnston, *et al.*, 2009; Linterman, *et al.*, 2010; Nurieva, *et al.*, 2009; Yu, *et al.*, 2009). Interleukin-21 (IL-21) produced by T$_{FH}$ cells is critical for promotion of survival, differentiation and proliferation of GC B cells as IL-21R-deficient mice or IL-21-deficient mice reduce plasma cells formation and proliferation in spleen and bone marrow as well as reduce the differentiation of memory B cells into plasma cells (Zotos, *et al.*, 2010). Furthermore, T$_{FH}$ cells are important for affinity maturation (Schwickert, *et al.*, 2011; Victora, *et al.*, 2010) and IL-21R-deficient mice decrease the number of high-affinity plasma cells (Zotos, *et al.*, 2010). To the best of our knowledge, there is no evidence of FcγRIIB on GC B cells to influence IL-21 production from T$_{FH}$ cells when both cells interact in the light zone of GCs.

The interaction between GC B cells and T$_{FH}$ cells is important for the selection of high-affinity Ag-specific GC B cells. GC B cells with higher-affinity BCR will capture more antigens than those with lower-affinity BCR, and therefore will present higher density of peptide-MHC complexes on the surface of GC B cells to T$_{FH}$ cells, resulting

67

in proportional and selective expansion of higher-affinity GC B cells for activated T_{FH}

cells to release cytokines, e.g. IL-21 to promote differentiation of plasma cells (Gitlin, *et al.*, 2014; Lanzavecchia, 1985; Victora, *et al.*, 2010). We have showed the increased

low-affinity Ag-specific antibodies in $Fc\gamma RIIB^{T232}$ mice is totally associated with the

defect of $Fc\gamma RIIB$ on B cells, independent of T_{FH} cells **(Figure 12, A-C)**. However,

whether $Fc\gamma RIIB$ regulates the interaction between GC B cells and T_{FH} cells to control

the affinity maturation of high-affinity GC B cells has not been thoroughly examined.

Bone marrow chimera experiments described above will help address this issue.

4.7 $Fc\gamma RIIB^{T232}$ on FDCs seems to have no effect on the ICs trapping

$Fc\gamma RIIB$ expressed on follicular dendritic cells (FDCs) plays an important role in

trapping the Ag-containing ICs for presentation to GC B cells and mediating the

generation of GC reaction (Qin, *et al.*, 2000). On the contrary, the results from a

transgenic line carrying a genetically defined BCR showed that GC formation and

selection appear normal in the absence of ICs on FDCs, suggesting that other sources of

Ag to drive the GC reaction may also be important (Hannum, *et al.*, 2000). Whether ICs

trapped by $Fc\gamma RIIB$ on FDCs are required for GC development seems in doubt

(Haberman and Shlomchik; 2003; Kosco-Vilbois, 2003). In spite of this controversy,

whether $Fc\gamma RIIB^{T232}$ has an impaired ability to trap ICs is unclear. Our data suggest that

$Fc\gamma RIIB^{T232}$ seems not affect the ICs trapping since we have found no decrease but

increase in the number of B cells entering the GC for reaction in FcγRIIB^{T232} mice

(Figure 10).

4.8 The effect of co-ligation of FcγRIIB^{T232} and BCR on the increase of low-affinity Ag-specific antibodies
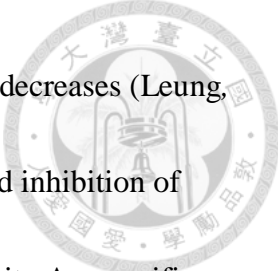
Cross-linking FcγRIIB itself in the absence of BCR ligation can induce apoptosis

of B cells, but not other cell types, through BTK, JNK1 and c-Abl in chicken and mouse

B cells (Pearse*, et al.*, 1999; Tzeng*, et al.*, 2005). The proximal signaling through

FcγRIIB is entirely independent of ITIM and SHIP, which are essential when FcγRIIB

inhibits co-ligated BCR (Tzeng*, et al.*, 2005). A failure of FcγRIIB aggregation to

trigger B-cell apoptosis can well account for the increase of low-affinity Ag-specific GC

B cells in FcγRIIB^{T232} mice for defective FcγRIIB signaling leads to reduced

elimination of low-affinity GC B cells during the GC reaction. On the other hand, the

increase of low-affinity Ag-specific GC B cells in FcγRIIB^{T232} mice may in part result

from an increased input of B cells that enter the GC since the impaired FcγRIIB^{T232}

mutant weakens the inhibitory signaling from FcγRIIB to block co-ligated BCR,

rendering B cells more activated and proliferative. So far, the defect of FcγRIIB^{T232}

co-ligation with BCR has been shown; however, the degree of functional impairment of

FcγRIIB^{T232} in the co-ligation with BCR versus by itself might be difficult to distinguish

and might vary *in vivo*. Although we cannot rule out the contribution of increased input

of B cells to the increased number of low-affinity Ag-specific B cells in FcγRIIB^{T232}

mice, the findings from gene knockout mice of SHIP, which is essential for co-ligated

BCR and FcγRIIB to transduce inhibitory signals, appear to support our argument in

that mice deficient in SHIP in B cells exhibit paradoxically decreased GC number and

reduced GC size after immunization (Leung, *et al.*, 2013). Taken together, it is

undoubtedly that FcγRIIB^{T232} contributes to the retention of low-affinity Ag-specific B

cells that normally would die during the GC reaction. In this regard, FcγRIIB-mediated

apoptosis of B cells is of more importance than inhibition by co-ligation with BCR in

the GC.

4.9 Additional genes or molecules that are related to morphological change of

GCs and involved in the affinity maturation

Several genes or molecules in B cells have been reported to affect affinity

maturation and/or the size of GCs. Transgenic mice that overexpress a suppressor of

apoptosis, Bcl-xL (B-cell lymphoma-extra large), a member of Bcl-2 family proteins, in

B cells have an increased retention of low-affinity B cells and an increased number of

splenic ASCs, but show no increase of the number or size of GCs (Takahashi, *et al.*,

1999). SHIP is recruited to the ITIM of FcγRIIB when BCR and FcγRIIB are co-ligated

by cognate ICs. Unexpectedly, B cells deficient in SHIP promote the survival of

low-affinity B cells by lowering the threshold for B-cell activation; however, the size of

GCs reduces and diversity of mutant BCR by somatic hypermutation decreases (Leung, *et al.*, 2013). These findings argue against the contribution of impaired inhibition of FcγRIIB[T232] on co-ligated BCR in promotion of retention of low-affinity Ag-specific GC B cells. Moreover, Igα (CD27a) and Igβ (CD79b) are the essential components of the BCR complex but both are down-regulated in part by IL-21 in GC B cells (centroblasts). Whether blunting the BCR signaling in GC B cells promotes FcγRIIB-mediated apoptosis is an interesting thought. In addition, the suppression of down-regulation of Igβ, whose decrease is more pronounced than Igα, by B cell-specific Igβ transgenic reduces the number of GC B cells and impairs the affinity maturation, leading to reduced antibody production. Moreover, when B cell-specific Igβ transgenic mice were backcrossed to BXSB-Yaa autoimmune mice, the lupus manifestation is ameliorated (Todo*, et al.*, 2015). These results imply that co-ligation of BCR and FcγRIIB that dampens the BCR functionality is somehow reminiscent of Igα/Igβ down-regulation and might actually affect merely positive selection during affinity maturation, but not the negative selection of GC B cells. In terms of epigenetic modulators of GCs, BRD4 (bromodomain-containing protein 4), a member of the BET (bromodomain and extra-terminal domain) family protein, is up-regulated on GC B cells and inhibition of BRD4 results in the suppression of GC formation and the reduction of both the number and size of GCs. The effects of BRD4 on GC B cells are mediated by

down-regulation of Bcl6 and block of NF-κB activation (Gao, *et al.*, 2015). Whether

BRD4 regulates the dichotomy of expression levels of Igα/Igβ and FcγRIIB of GC B

cells is worth investigation.
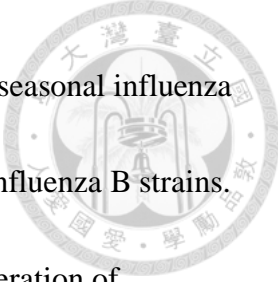
As shown in **Figure 13B**, caspase-3 is active in low-affinity Ag-specific GC B

cells undergoing apoptosis. Deletion of caspase 8 in GC B cells, however, leads to an

increased size but not the number of GCs, accompanied by a delay in affinity selection

of high-affinity B cells (Boulianne, *et al.*, 2013). Noxa, also known as

phorbol-12-myristate-13-acetate-induced protein 1 (Pmaip1), is a pro-apoptotic member

of the BH3-only proteins. Noxa-deficient mice develop increased size of GCs and

reduce the affinity of BCR, resulting in increased low-affinity antibodies (Wensveen, *et*

al., 2012). Protein phosphatase subunit G5PR, a catalytic subunit of the serine/threonine

protein phosphatase 2A, is up-regulated in GC B cells following Ag immunization.

Overexpression of G5PR enlarges the size of GCs and increases the number of GC B

cells, but the number of GCs is not changed. Furthermore, overexpression of G5PR also

impairs the affinity maturation, resulting in a significantly increase of low-affinity

antibody titers, whereas the level of high-affinity antibodies is unchanged (Kitabatake,

et al., 2012). Since G5PR inhibits JNK and Bim to promote BCR-mediated proliferation

(Xing, *et al.*, 2005) and FcγRIIB mediates B-cell apoptosis through JNK (Pearse, *et al.*,

1999), the up-regulation of both G5PR and FcγRIIB and their potential

inter-relationship during GC reaction needs to be delineated.

4.10 Reassessing the strategies to detect cross-reactivity of low-affinity Ag-specific

antibodies

The anti-NP antibodies produced after NP Ag immunization have 3 to10 times

higher affinity for NIP than NP (Imanishi and Makela, 1973). According to this, it

might be a better approach to determine the cross-reactivity of low-affinity antibodies

produced by FcγRIIB^{T232} mice by immunizing them with NIP Ag for measurement of

the cross-reactivity of anti-NIP antibodies with NP. In this study, we immunized mice

with NP Ags and were still able to detect cross-reactivity of low-affinity NP-specific

antibodies to NIP **(Figure 14)**. In order to provide firm evidence for whether the

increased level of low-affinity antibodies in FcγRIIB^{T232} mice contains more

cross-reactive antibodies than FcγRIIB^{I232} mice, we think the best way is to use a

clinical relevant vaccine immunogen, such as influenza H1, a hemagglutinin (HA)

subtype of influenza viruses, to immunize FcγRIIB^{I232} and FcγRIIB^{T232} mice. If the

low-affinity H1-specific IgG antibodies can cross-react to other HAs in the same group

or different group, e.g. H3 and H5, pharmacological modulation of FcγRIIB's

expression may be of great importance in the enhancement of vaccine efficacy. As a

matter of fact, it would be even better if we can directly analyze the serum antibodies or

memory B cells of the FcγRIIB^{T232} subjects with prior vaccination of seasonal influenza that contains immunogens from H1N1, H3N2 and either one or two influenza B strains. The FcγRIIB^{T232} subjects are expected to confer advantage in the generation of cross-protective antibodies against pathogen than FcγRIIB^{I232} subjects. In other words, it will be interesting to know whether subjects carrying FcγRIIB^{T232} will be prone to elicit broadly neutralizing antibodies against other subtypes of influenza A virus. If the cross-reactive antibodies can neutralize cross-reactive virus strain(s), the usefulness of FcγRIIB modulation in vaccination will be highly appreciated.

Figures

Figure 1
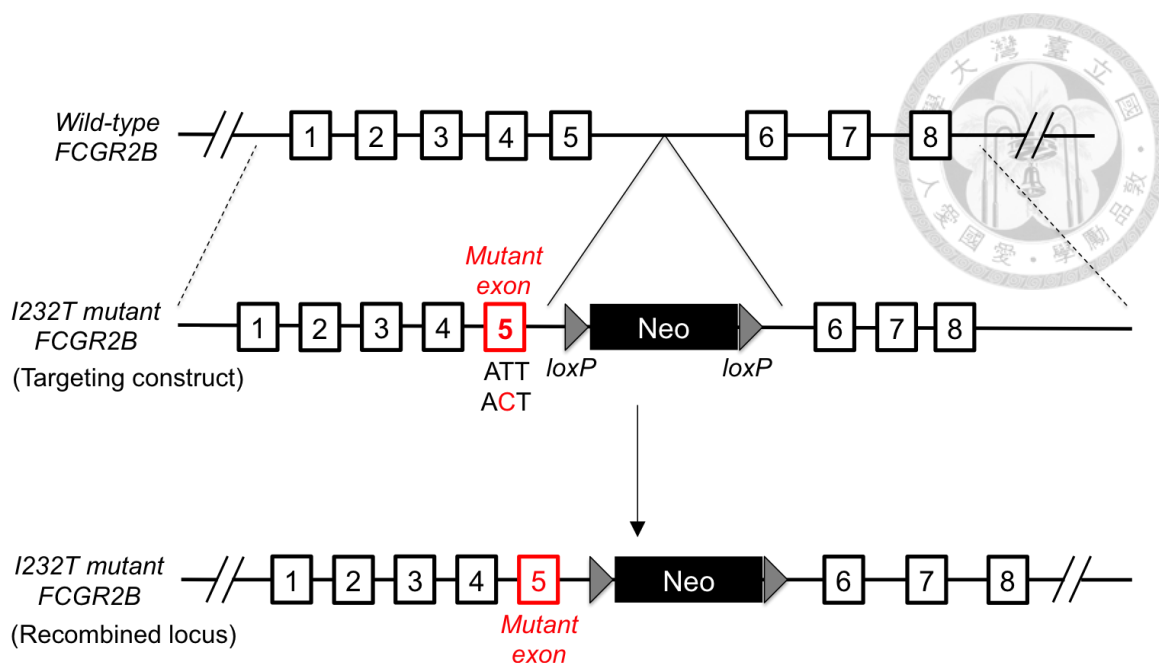
Figure 1. Strategy for generation of FcγRIIB^{I232T} mutant mice.

FcγRIIB^{I232T} mutant mice were generated via homologous recombination between the targeting construct that contains a point mutation in exon 5 and the wild-type (endogenous) *fcgr2b* gene in embryonic stem (ES) cells. The recombined ES cells were injected into blastocysts, and the blastocysts were then transferred into a foster female mouse. To breed FcγRIIB^{T232} mice, one heterozygous (FcγRIIB$^{232I/T}$) male mouse was mated with two heterozygous (FcγRIIB$^{232I/T}$) female mice. Neo, neomycin resistant gene.

Figure 2

(A)

Primary immunization
50 μg NP-CGG in Alum

Second booster
50 μg NP-CGG in Alum

Draw blood

Draw blood

Draw blood & Sacrifice

Day 0   **1**   14   **28**   35

(B)

Immunization
50 μg NP-CGG in Alum

Draw blood

Draw blood & Sacrifice

Day 0   **1**   13
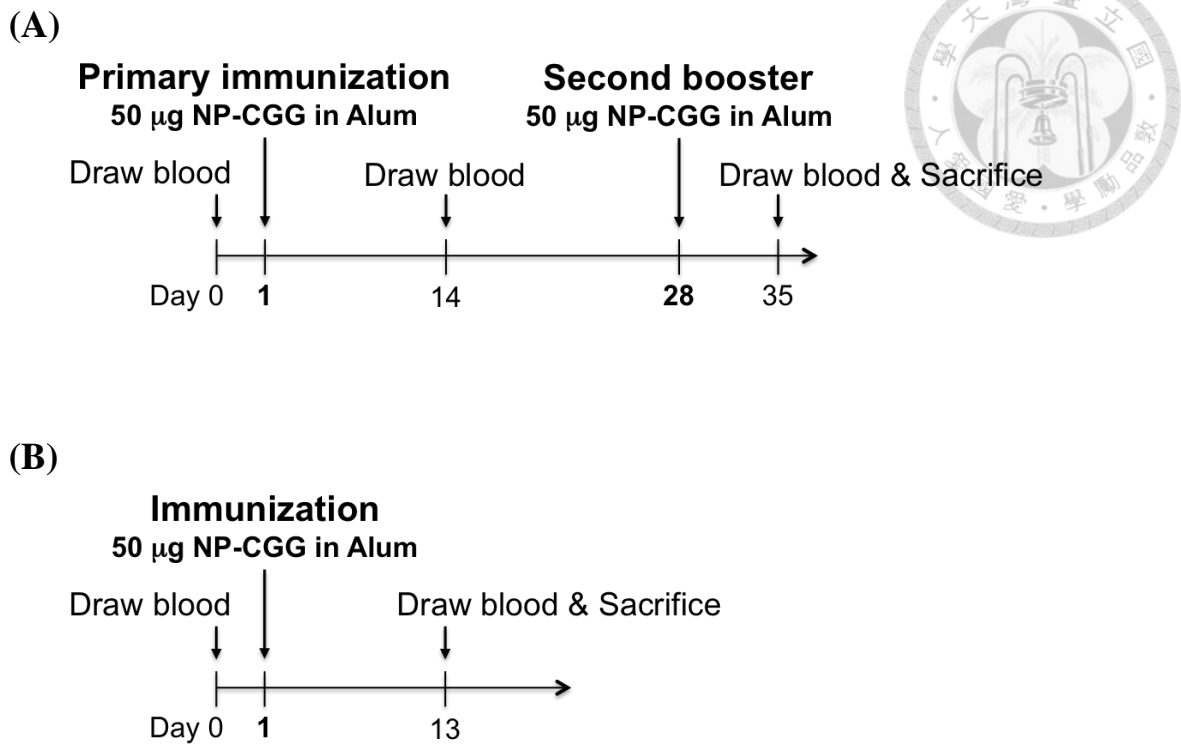
Figure 2. Schematic representation of the schedule of immunization.

(A) Schedule of two immunizations. The 6- to 8-week-old FcγRIIB^{I232} (232I/I) or

FcγRIIB^{T232} (232T/T) mice were primarily immunized with 50 μg of NP-CGG in

alum on day 1, followed by a booster with the same antigen and dose 28 days later

(Day 28). Mice were sacrificed and analyzed one week after secondary

immunization (Day 35).

(B) Schedule of one immunization. The 6- to 8-week-old FcγRIIB^{I232} or FcγRIIB^{T232}

mice were immunized with 50 μg of NP-CGG in alum on day 1. Mice were

sacrificed and analyzed 13 days after immunization (Day 13).

Figure 3

(A)
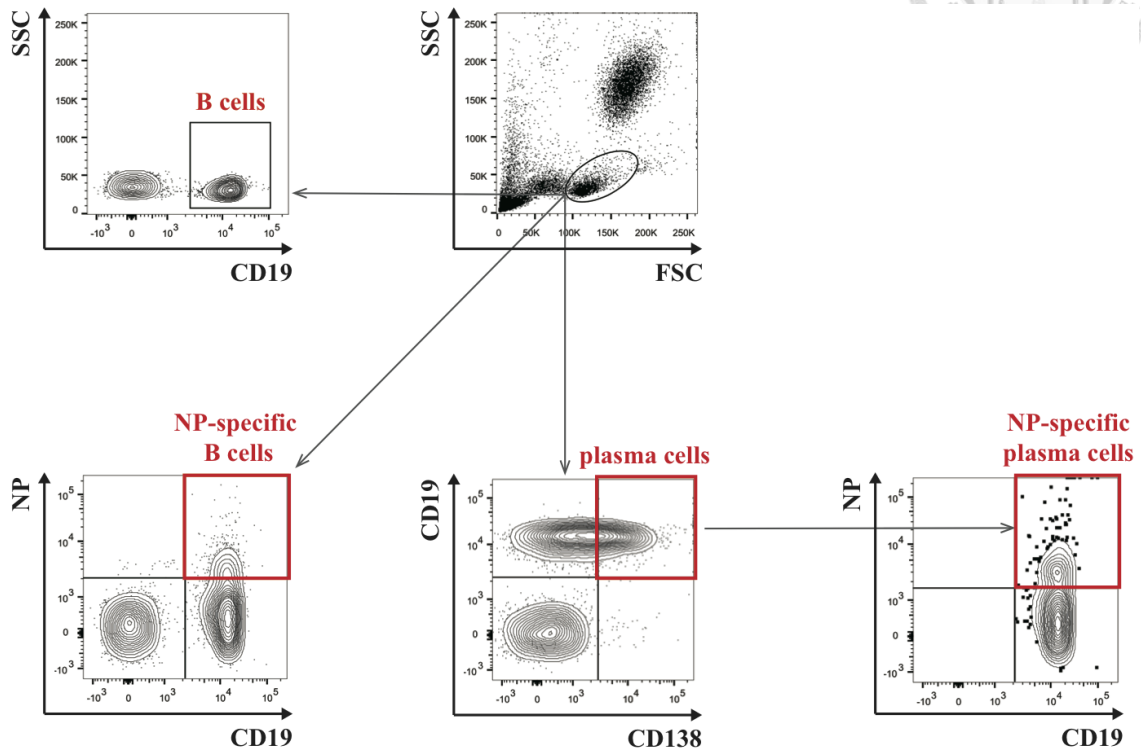
Figure 3

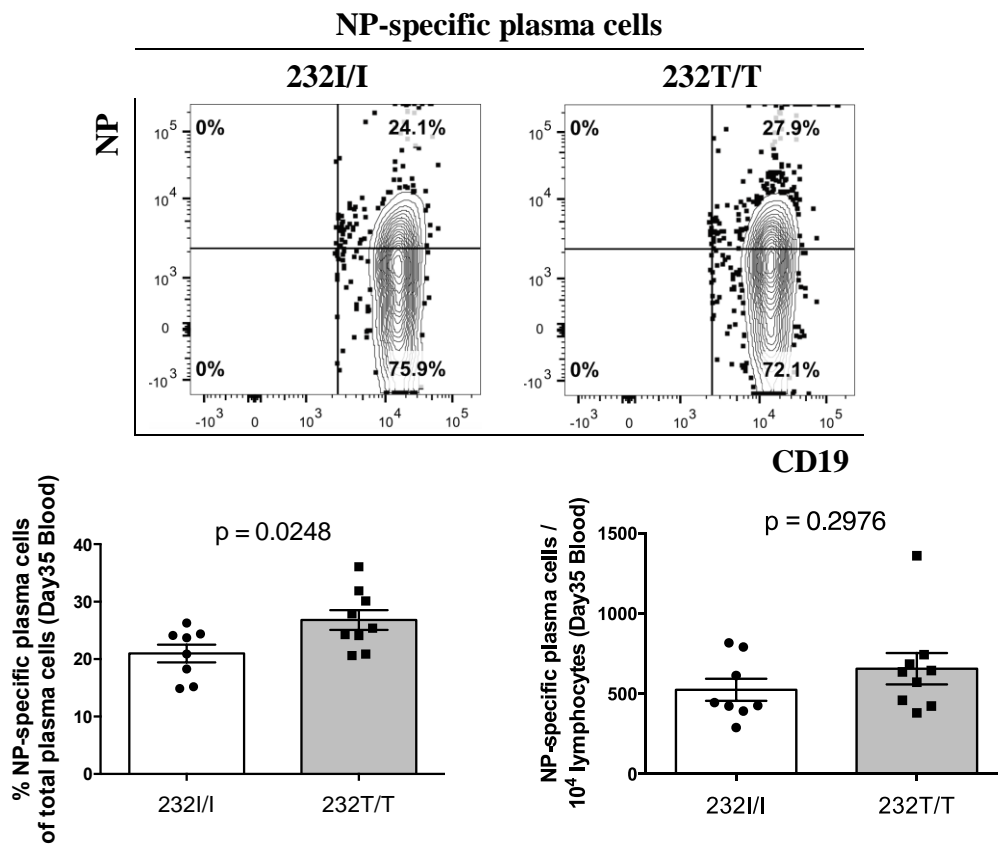**(B)**

(C)

Figure 3

(D)

(E)

80
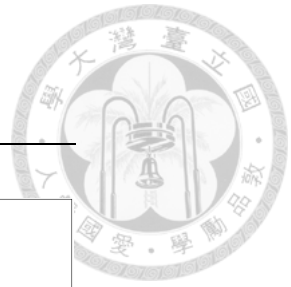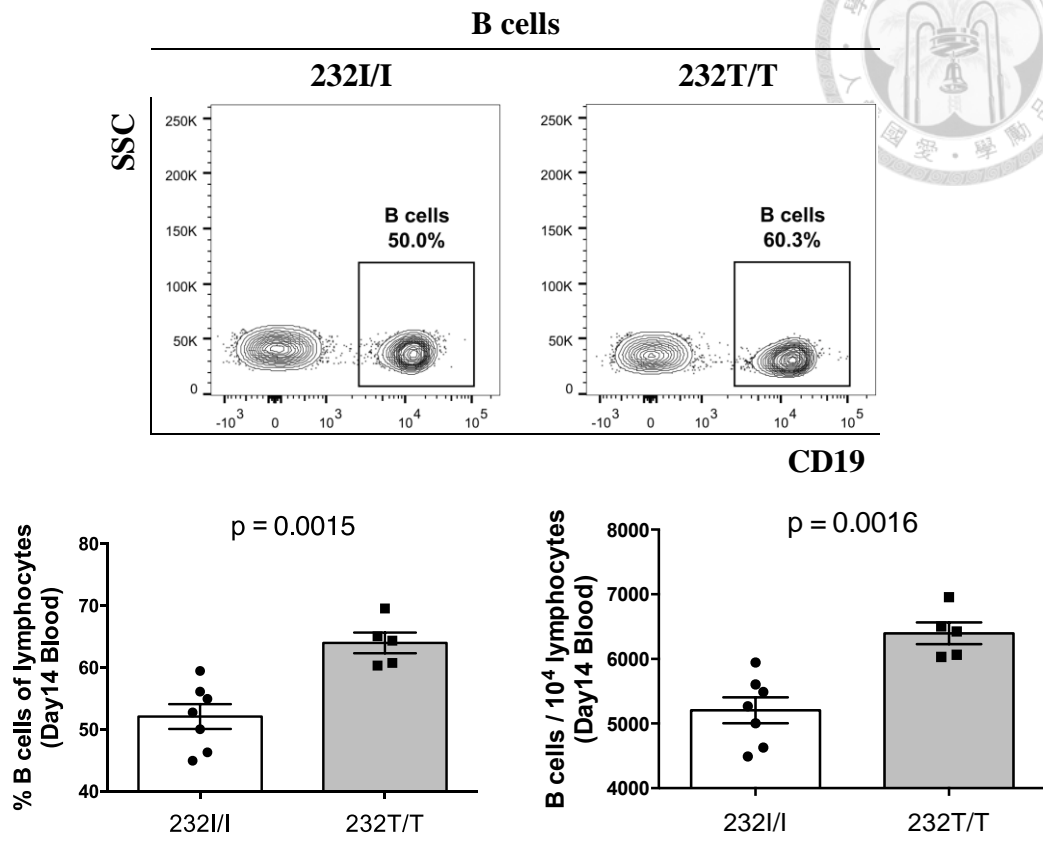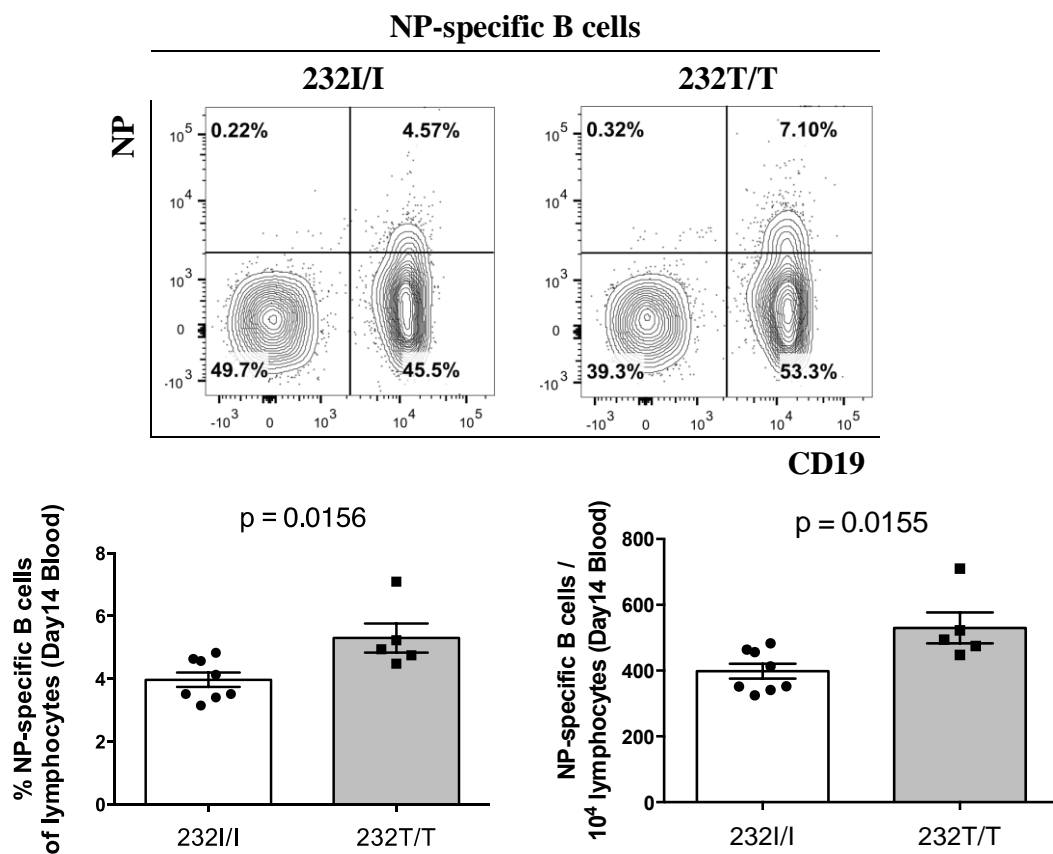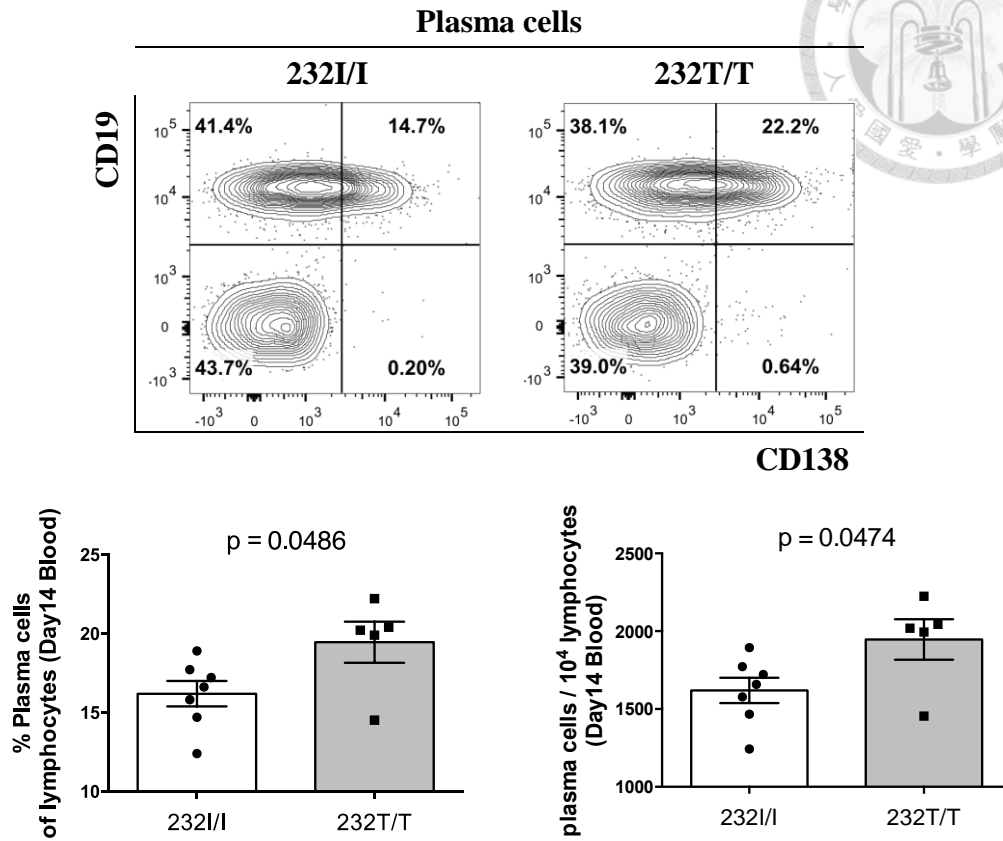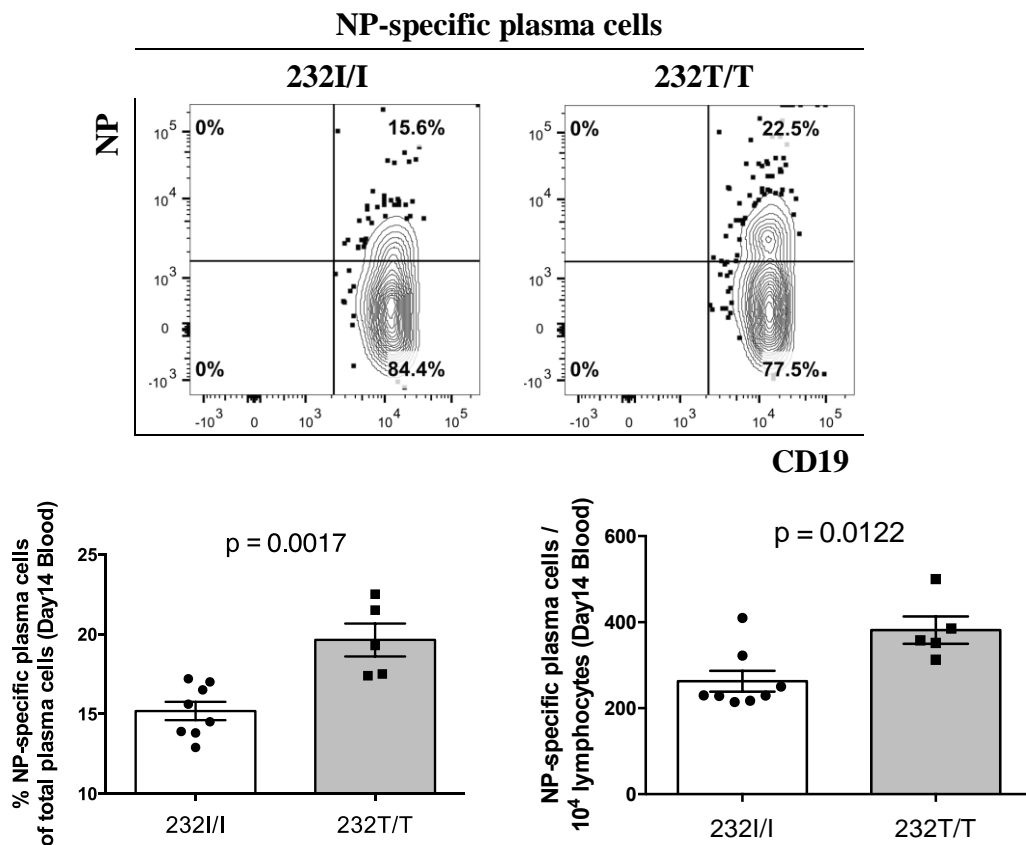
Figure 3. Analysis of cell subsets in the blood of FcγRIIB^{I232} and FcγRIIB^{T232} mice after primary immunization.

(**A**) The gating methods for flow cytometric analysis of blood samples collected after primary immunization. (**B-E**) As described in **Section 2.3.1** blood cells were isolated from FcγRIIB^{I232} (232I/I) or FcγRIIB^{T232} (232T/T) mice 14 days after primary immunization (Day 14) for phenotypic analysis by flow cytometry. A representative FACS plot (upper panel) showed frequencies (lower left panel) and cells number (lower right panel) of (**B**) B cells were gated by CD19$^+$/SSC from lymphocytes; (**C**) NP-specific B cells were defined as CD19$^+$NP$^+$ cells from lymphocyte gate; (**D**) plasma cells were CD138$^+$CD19$^+$; (**E**) NP-specific plasma cells were CD19$^+$NP$^+$ cells from CD138$^+$ plasma cells. The flow cytometric data were further analyzed by the two-tailed unpaired *t*-test and shown as histograms with mean ± SEM. N = 7 to 8 mice for the FcγRIIB$^{232I/I}$ and 5 mice for the FcγRIIB$^{232T/T}$, respectively. *P* value < 0.05 was considered as statistically significant.

Figure 4

(A)

Figure 4

(B)

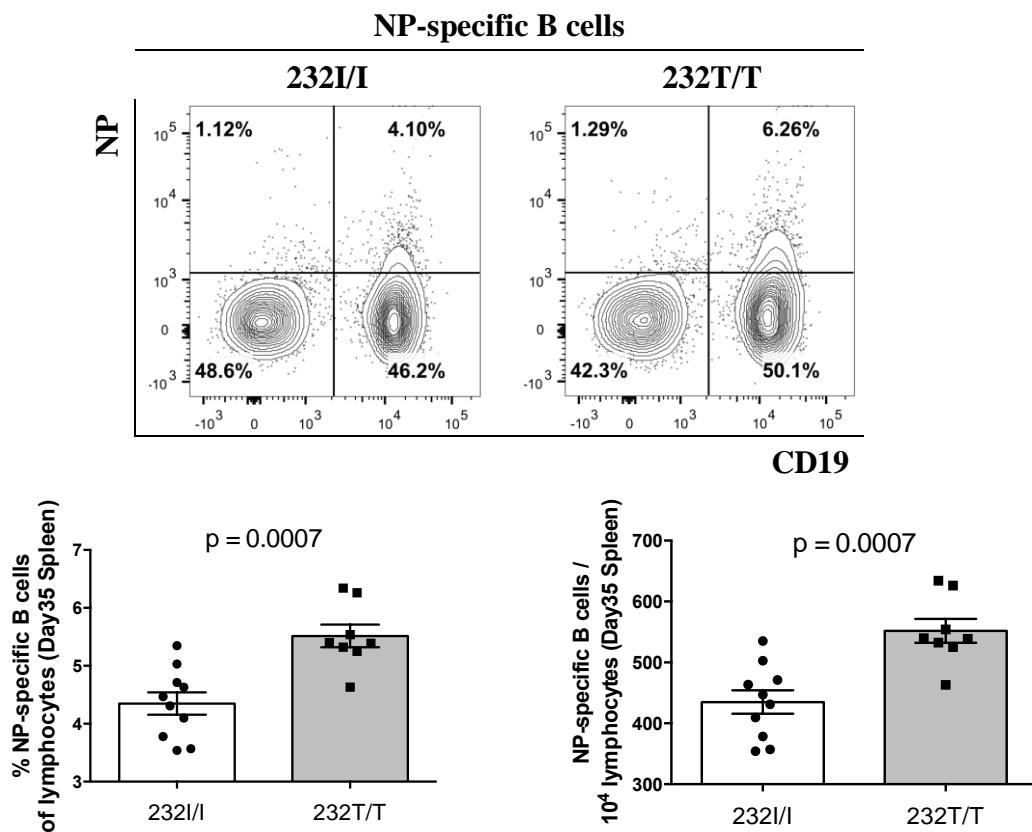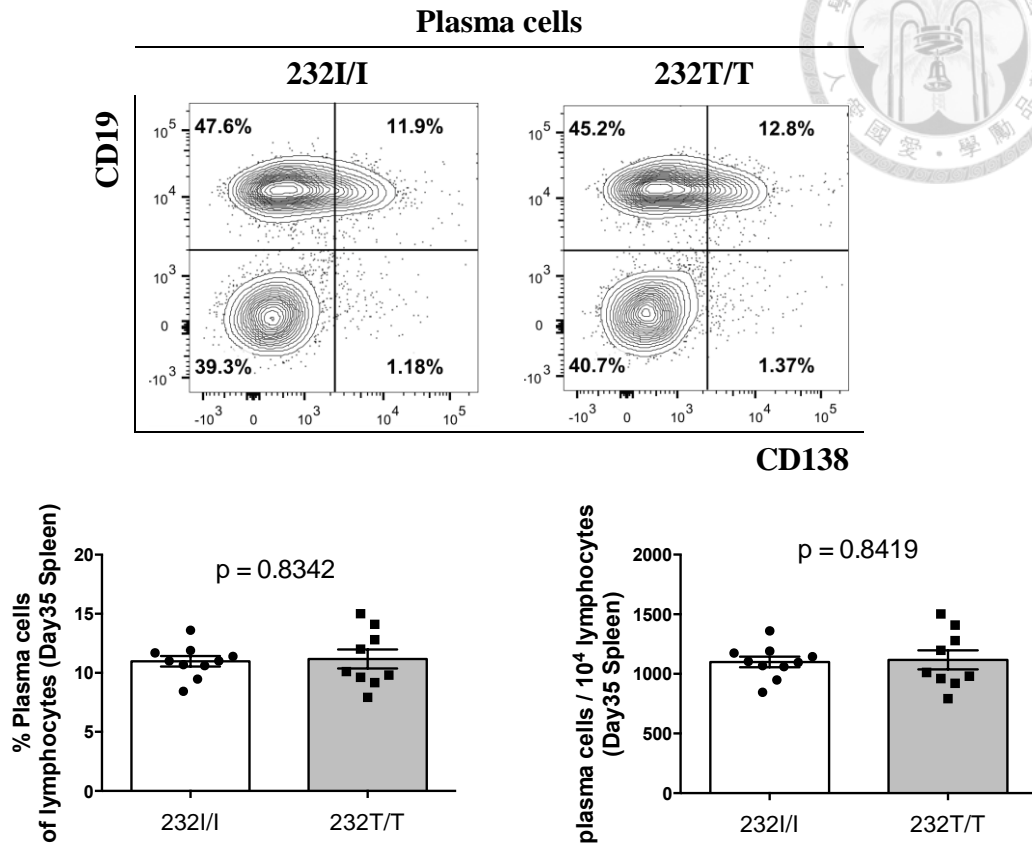**(C)**
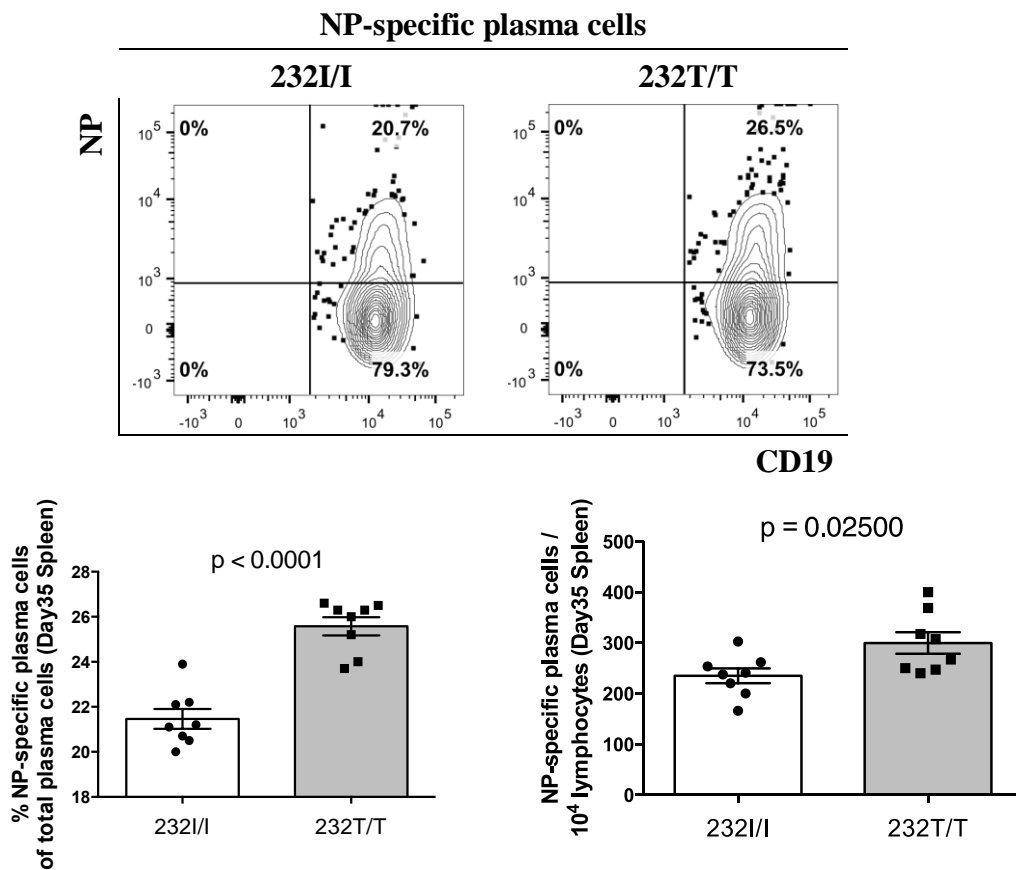

83
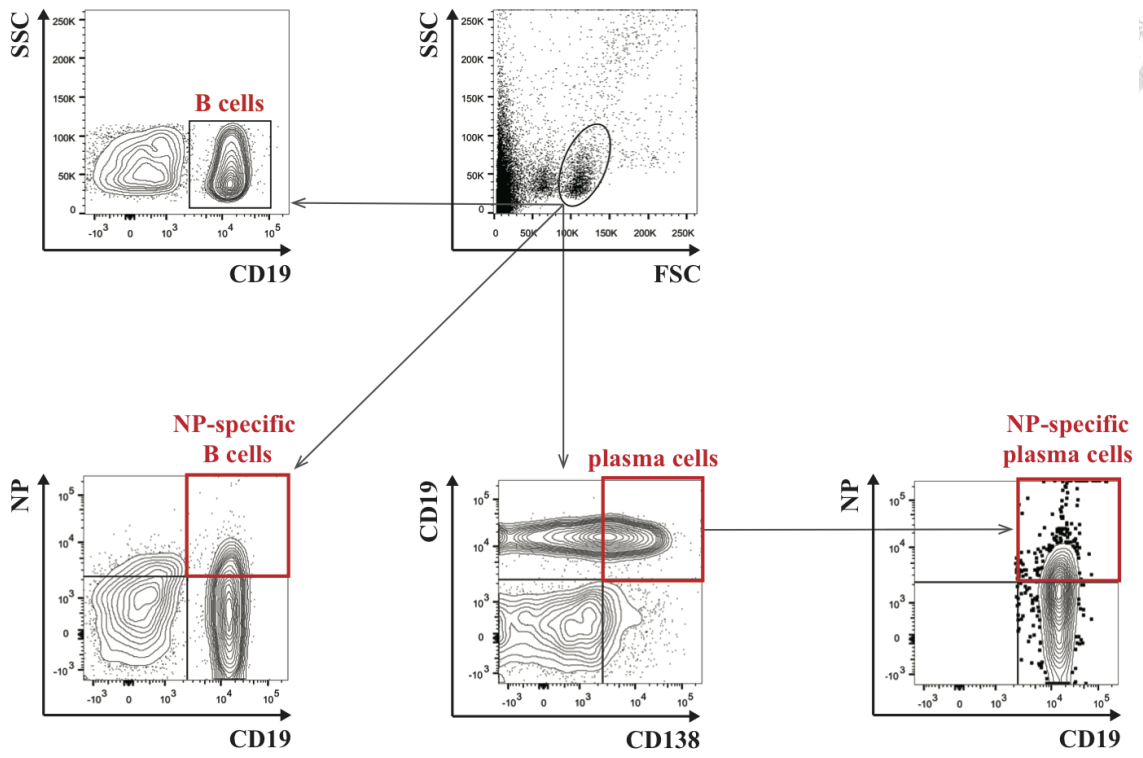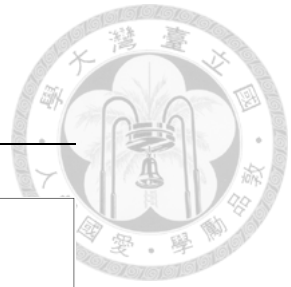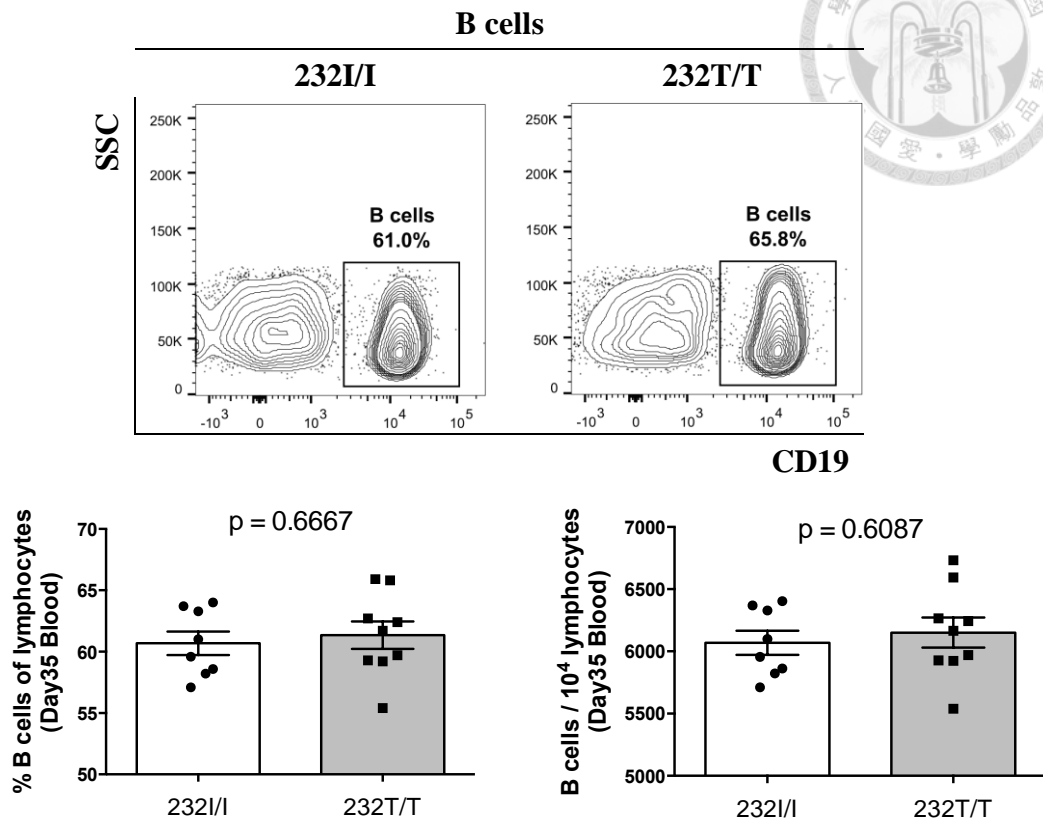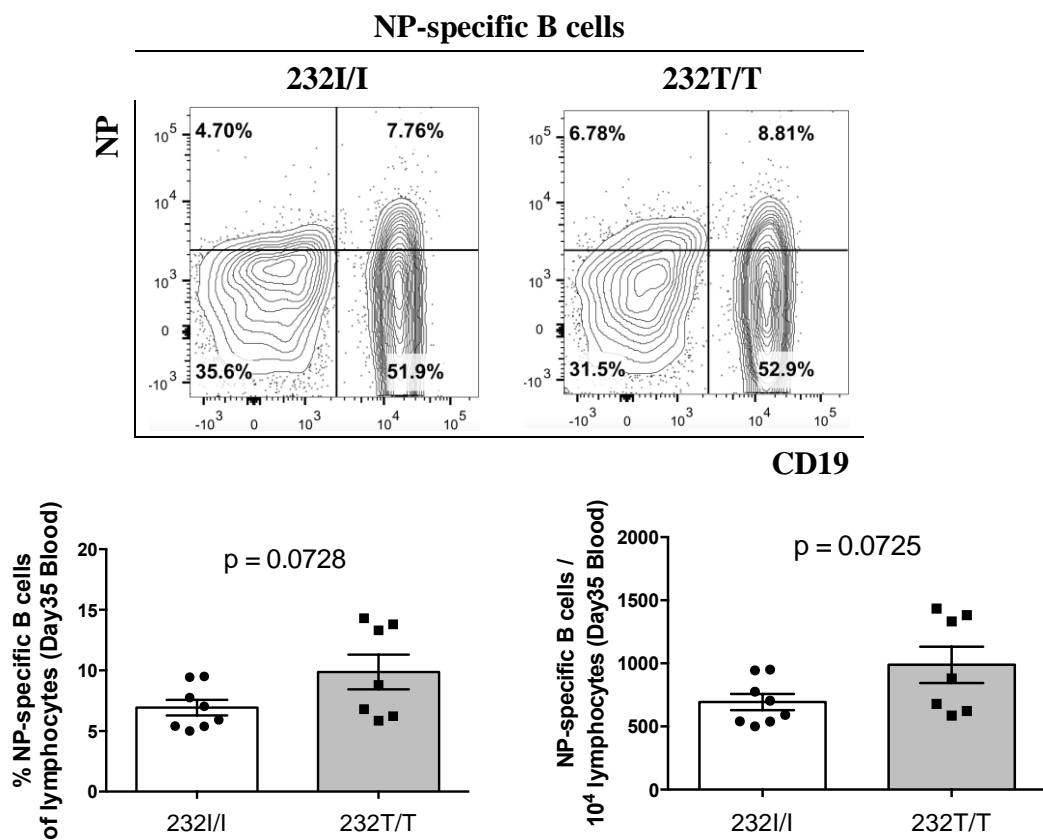
Figure 4

(D)
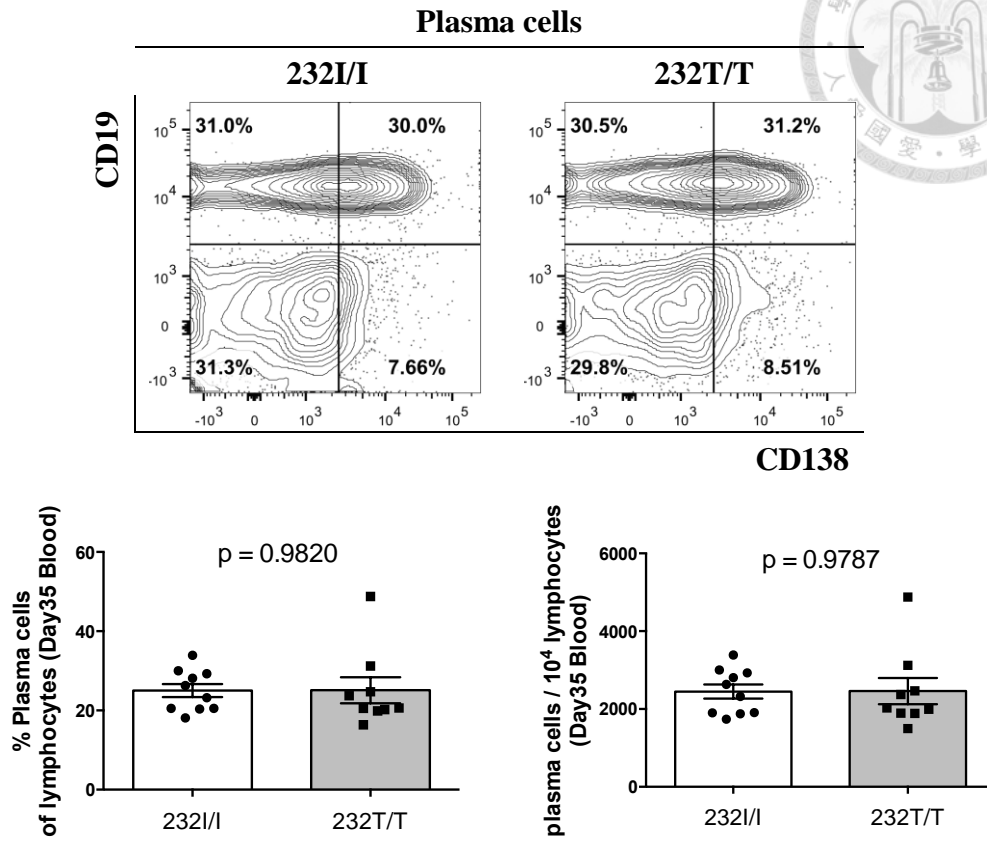
(E)

Figure 4. Analysis of cell subsets in the blood of FcγRIIB^{I232} and FcγRIIB^{T232} mice after secondary immunization.

(A) Gating strategies for cytometric analysis of blood samples collected after secondary immunization, **(B-E)** Blood cells were isolated from FcγRIIB^{I232} (232I/I) or FcγRIIB^{T232} (232T/T) mice as described in **Section 2.3.1** 7 days after secondary immunization (Day 35) and were analyzed by flow cytometry. A representative FACS plot (upper panel), illustrated subset frequencies (lower left panel), and cell numbers (lower right panel) of **(B)** B cells gated as CD19$^+$/SSC cells from lymphocytes; **(C)** NP-specific B cells gated as CD19$^+$NP$^+$ cells from lymphocytes; **(D)** plasma cells gated as CD138$^+$CD19$^+$ cells from lymphocytes, and **(E)** NP-specific plasma cells gated as CD19$^+$NP$^+$ cells from plasma cells. Results were analyzed using two-tailed unpaired *t*-test as **Figure 3**. N = 8 to 10 mice for the FcγRIIB$^{232I/I}$ and 7 to 9 mice for the FcγRIIB$^{232T/T}$, respectively.
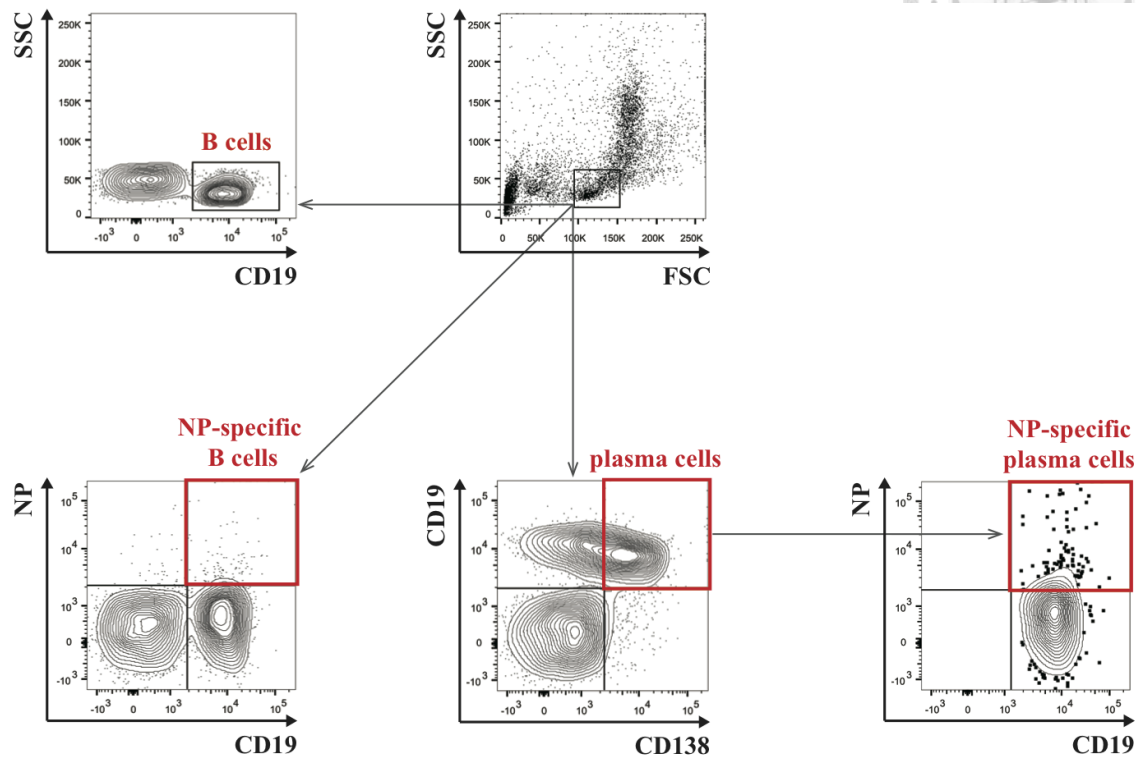
Figure 5

(A)
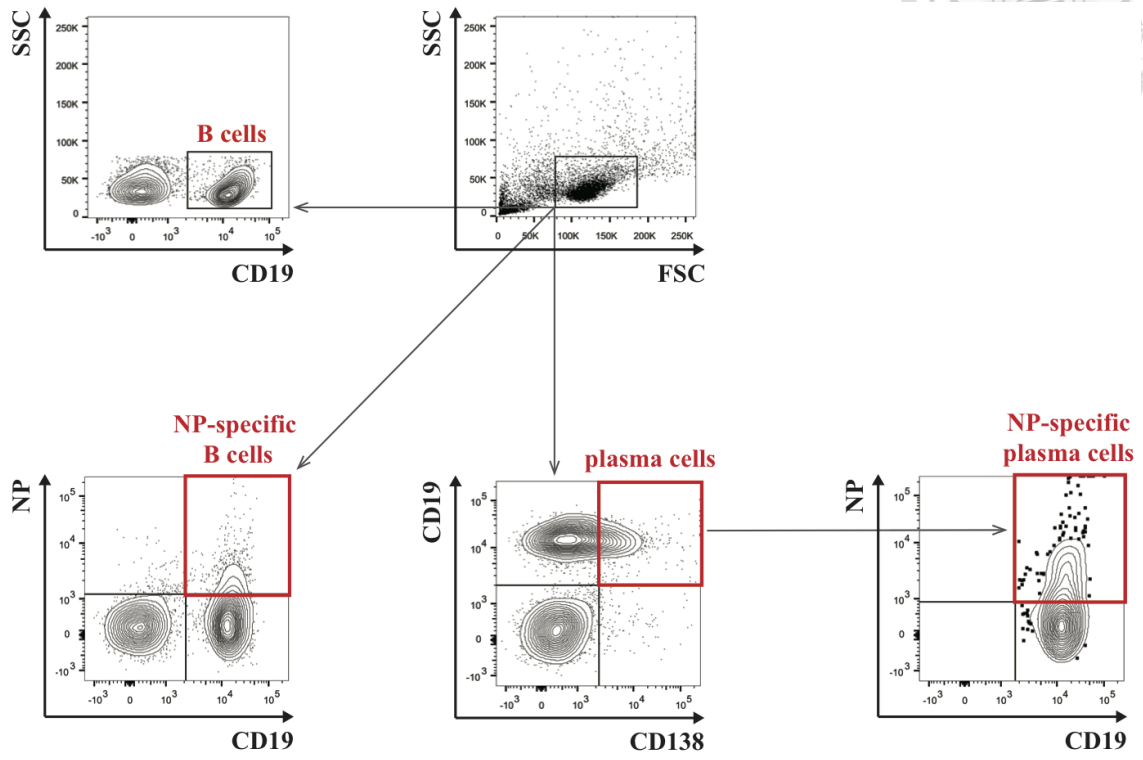
Figure 5

(B)

(C)

Figure 5

(D)

(E)

88
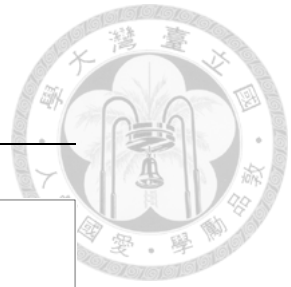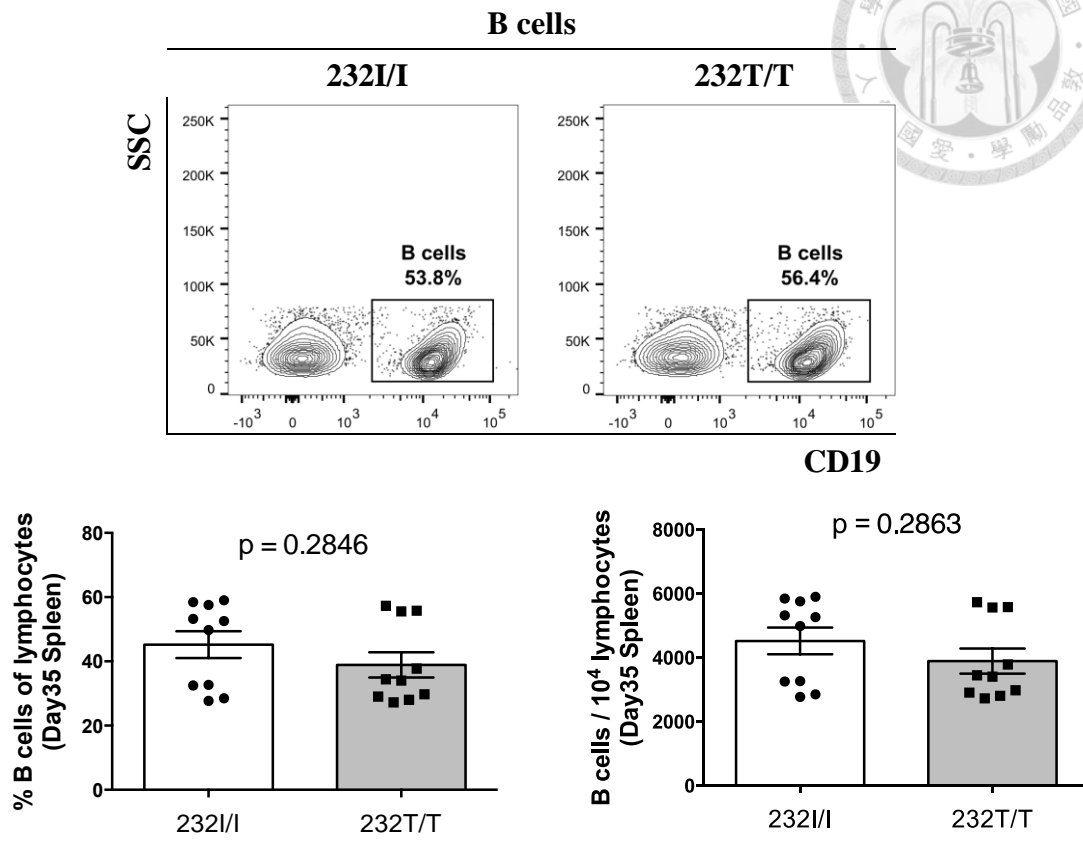
Figure 5. Analysis of cell subsets in the spleen of FcγRIIB^{I232} and FcγRIIB^{T232} mice after secondary immunization.

(A) Gating strategies for flow cytometric analysis of splenocytes isolated after secondary immunization, **(B-E)** Splenocytes from FcγRIIB^{I232} (232I/I) or FcγRIIB^{T232} (232T/T) mice were treated as described in **Section 2.3.2** seven days after secondary immunization (Day 35) and were analyzed by flow cytometry. A representative FACS plot (upper panel), illustrated subset frequencies (lower left panel), and cell numbers (lower right panel) of **(B)** B cells gated as CD19$^+$/SSC cells among lymphocytes; **(C)** NP-specific B cells gated as CD19$^+$NP$^+$ cells among lymphocytes; **(D)** plasma cells gated as CD138$^+$CD19$^+$ cells among lymphocytes, and **(E)** NP-specific plasma cells gated as CD19$^+$NP$^+$ cells among plasma cells. Results were analyzed using two-tailed unpaired *t*-test as described in **Figure 3**. N = 8 to 10 mice for the FcγRIIB$^{232I/I}$ and 8 to 10 mice for the FcγRIIB$^{232T/T}$, respectively.
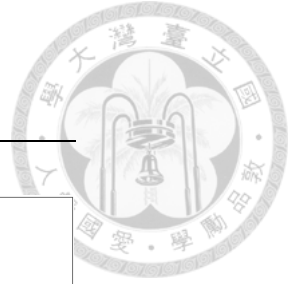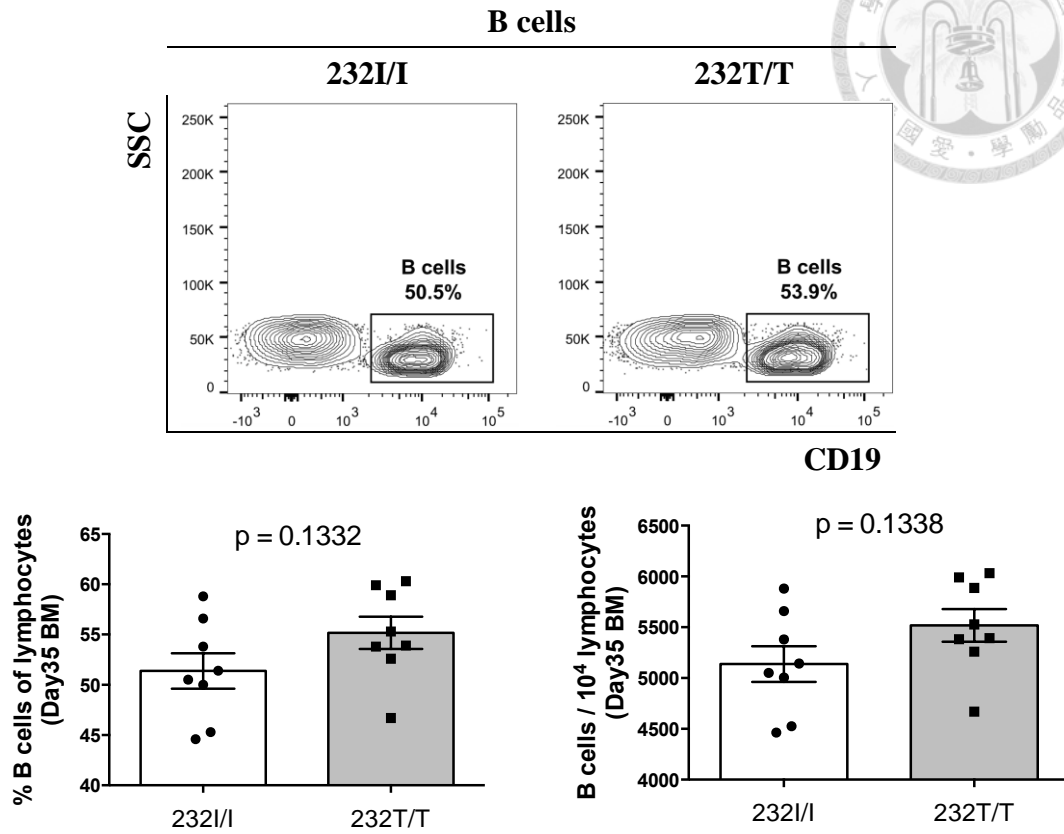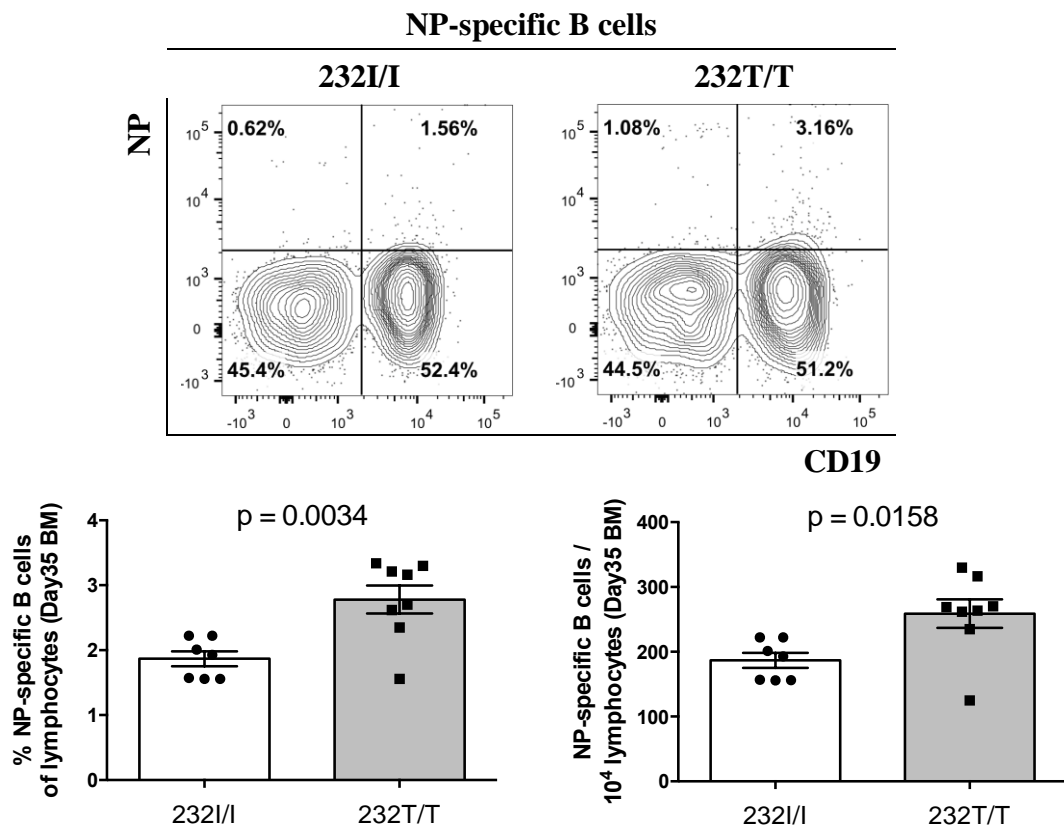
Figure 6

(A)

Figure 6

(B)

B cells

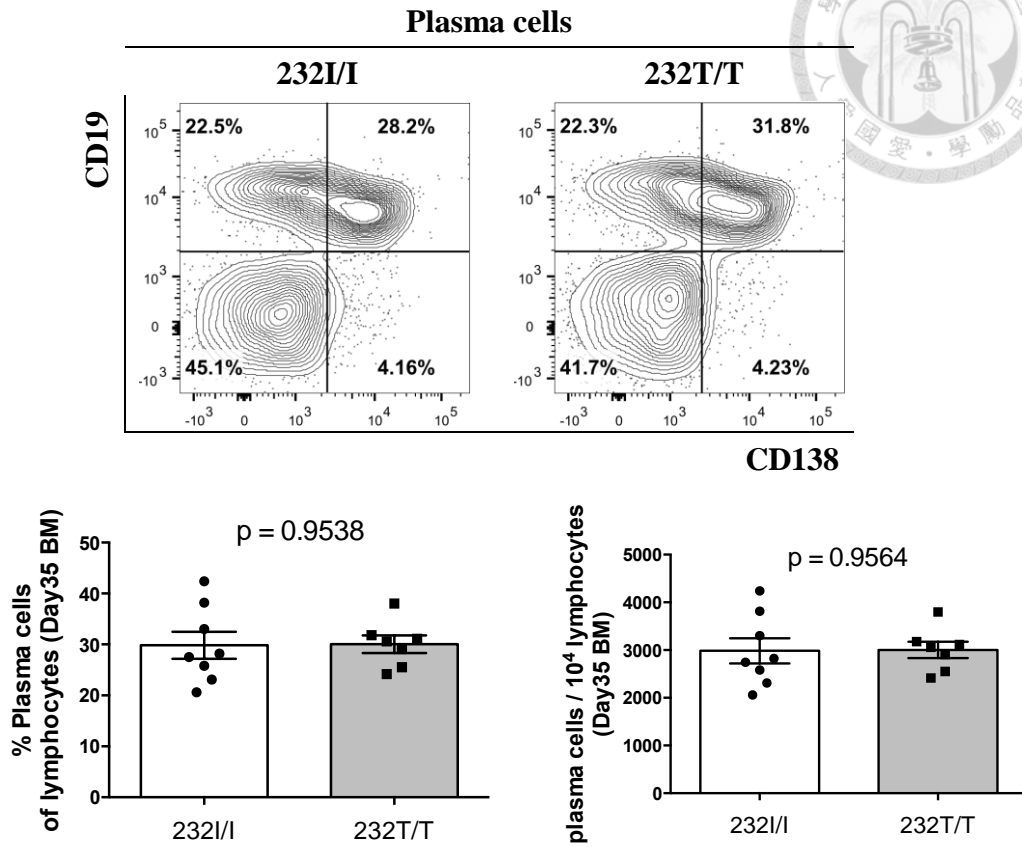
(C)

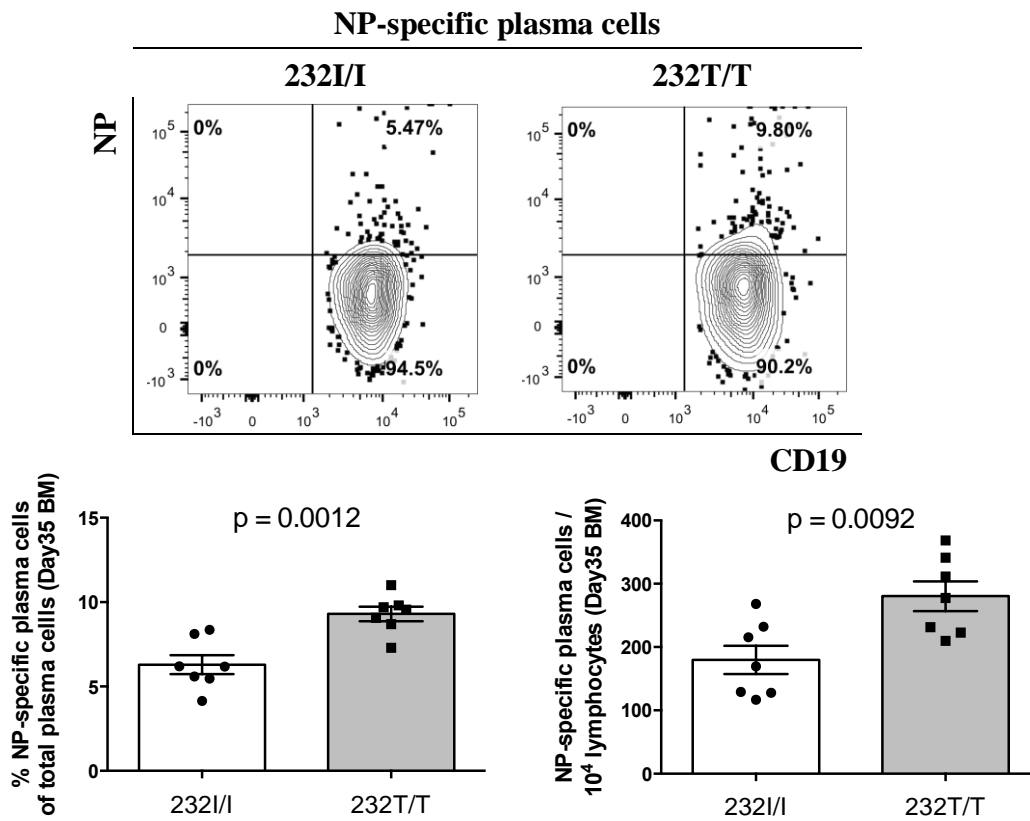**NP-specific B cells**

Figure 6

(D)

(E)

92

Figure 6. Analysis of cell subsets in the bone marrow of FcγRIIB^{I232} and FcγRIIB^{T232} mice after secondary immunization.

(A) Gating methods for flow cytometric analysis of the bone marrow sample after secondary immunization, **(B-E)** Bone marrow cells were isolated from FcγRIIB^{I232} (232I/I) or FcγRIIB^{T232} (232T/T) mice as described in **Section 2.3.3** on the 7th day after secondary immunization (Day 35) and were analyzed by flow cytometry. A representative FACS plot (upper panel), illustrated subset frequencies (lower left panel), and cell numbers (lower right panel) of **(B)** B cells gated as CD19$^+$/SSC cells among lymphocytes; **(C)** NP-specific B cells (CD19$^+$NP$^+$); **(D)** plasma cells (CD138$^+$CD19$^+$), and **(E)** NP-specific plasma cells (CD138$^+$CD19$^+$NP$^+$). Results were analyzed using two-tailed unpaired *t*-test as described in **Figure 3**. N = 7 or 8 mice for the FcγRIIB$^{232I/I}$ and 7 or 8 mice for the FcγRIIB$^{232T/T}$, respectively.
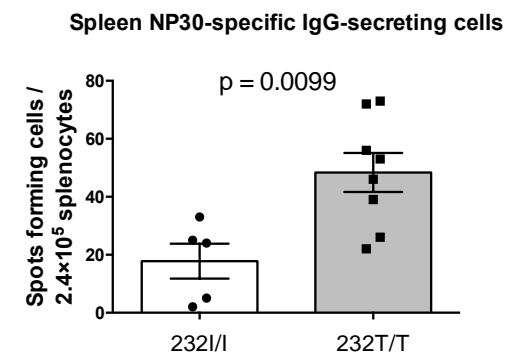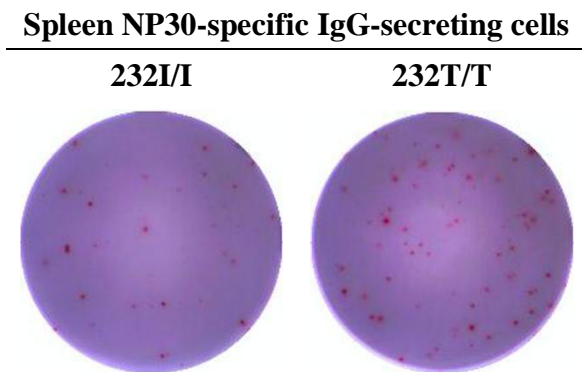
Figure 7
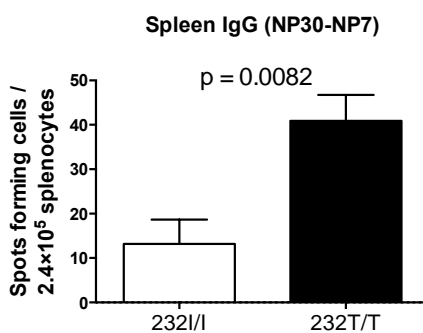
(A)
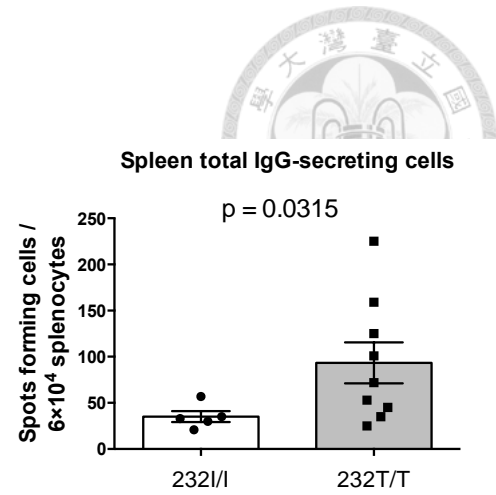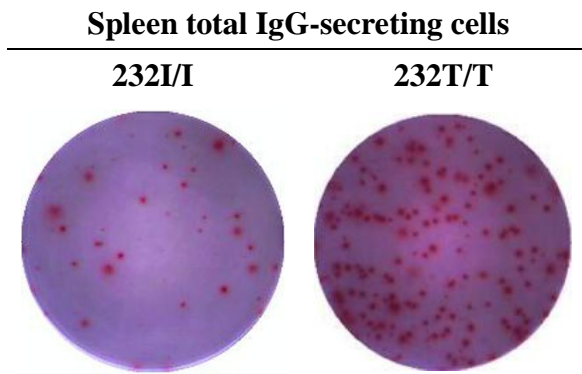
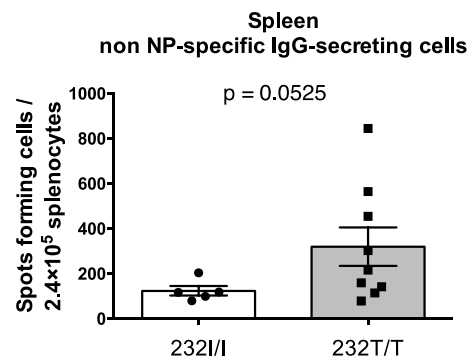**(B)**
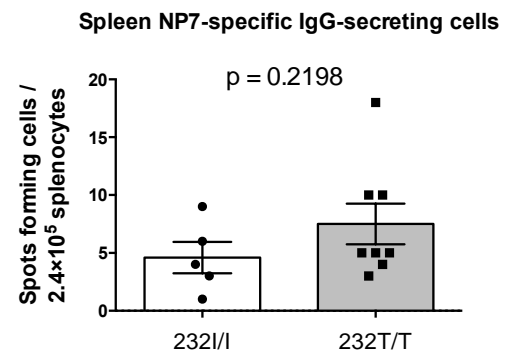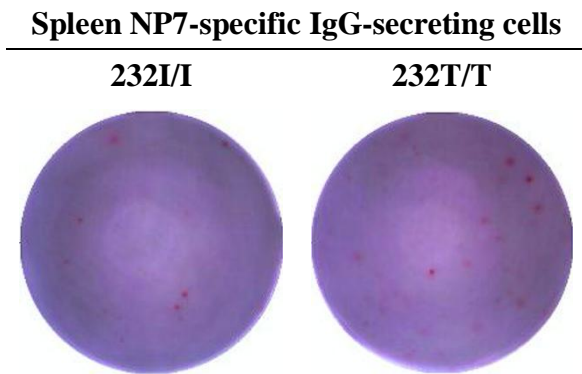
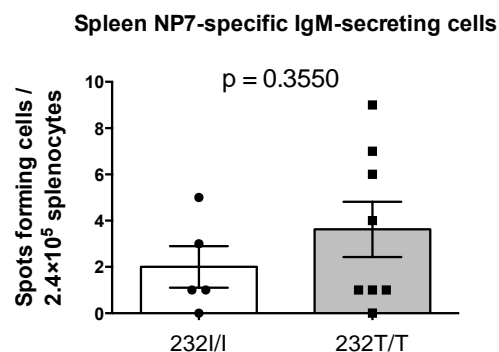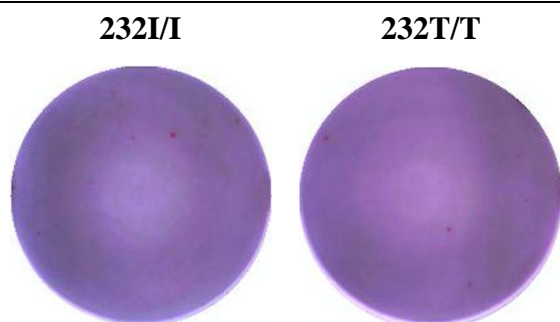**(C)**

(D)

(E)

Figure 7

(F)

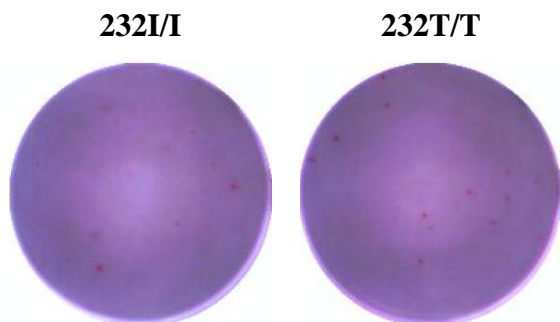**Spleen total IgM-secreting cells**
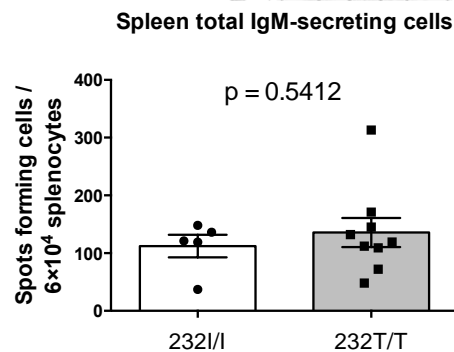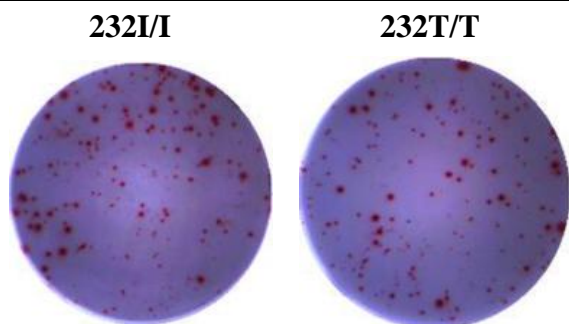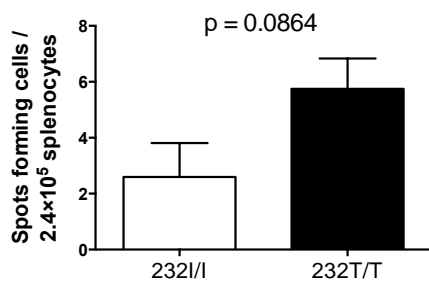

(G)

Spleen NP7-specific IgM-secreting cells

(H)

Spleen NP30-specific IgM-secreting cells
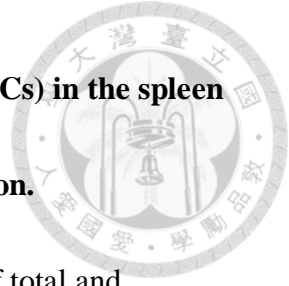

(I)

95
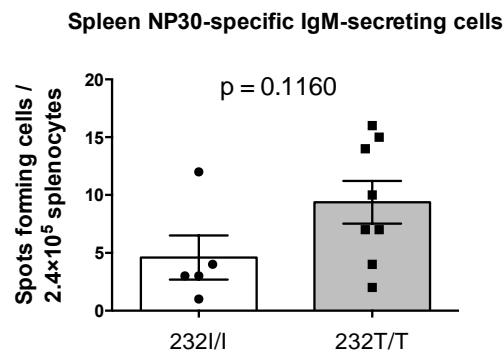
Figure 7. ELISPOT assay to analyze antibody-secreting cells (ASCs) in the spleen of FcγRIIB^{I232} and FcγRIIB^{T232} mice after secondary immunization.

(A-C) ELISPOT graph (left panel) and quantification (right panel) of total and NP-specific IgG-secreting cells in the spleen of FcγRIIB^{I232} (232I/I) or FcγRIIB^{T232} (232T/T) mice 7 days after secondary immunization (Day 35) were shown as follows: **(A)** total IgG-secreting cells, **(B)** NP7-specific IgG-secreting cells, and **(C)** NP30-specific IgG-secreting cells. **(D)** Low-affinity NP-specific ASCs (IgG) were assessed and quantified by subtracting the spot number of NP7-specific IgG-secreting cells from that of NP30-specific IgG-secreting cells. **(E)** Non-NP-specific ASCs (IgG) were assessed by subtracting the spot number of NP30-specific IgG-secreting cells from that of total IgG-secreting cells. **(F-H)** Spot graph (left panel) and quantification (right panel) of total and NP-specific IgM-secreting cells in the spleen of FcγRIIB^{I232} (232I/I) or FcγRIIB^{T232} (232T/T) mice 7 days after secondary immunization (Day 35) were illustrated, namely **(F)** total IgM-secreting cells, **(G)** NP7-specific IgM-secreting cells, and **(H)** NP30-specific IgM-secreting cells. **(I)** Low-affinity NP-specific ASCs (IgM) were assessed by subtracting the spot number of NP7-specific IgM-secreting cells from that of NP30-specific IgM-secreting cells. Splenocytes were seeded at a density of 6.0×10^4 cells **(A and F)** or 2.4×10^5 cells **(B-E and G-I)** per well and incubated for 16 hr at 37 $^{\circ}$C in a 5% CO_2 incubator. Results were analyzed using two-tailed unpaired *t*-test.

The *t*-test was modified by Welch's correction in the case of unequal variance.

Histograms of FcγRIIB$^{232I/I}$ mice (n=5) versus FcγRIIB$^{232T/T}$ (n=8 or 9) mice were

shown as mean ± SEM for comparison and statistical analysis.

Figure 8

(A)

Bone marrow total IgG-secreting cells

(B)

BM NP7-specific IgG-secreting cells

(C)

BM NP30-specific IgG-secreting cells
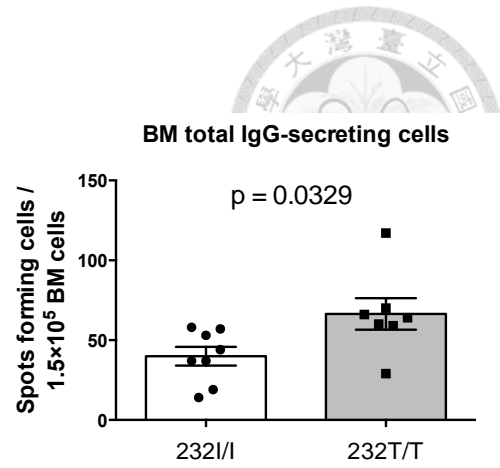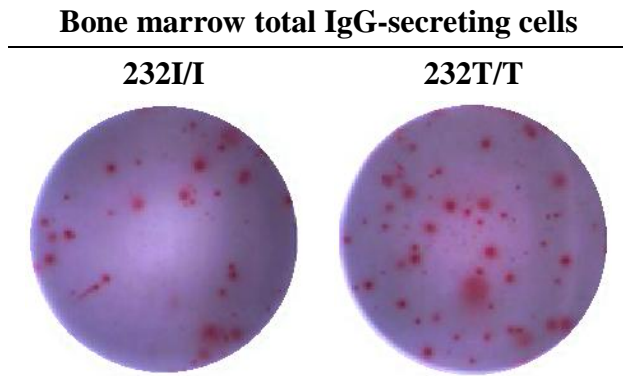
(D)
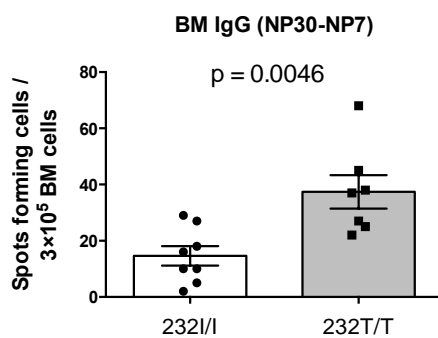
(E)
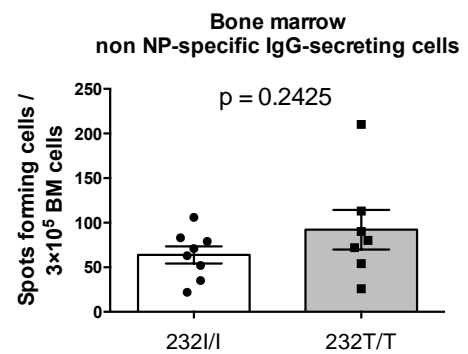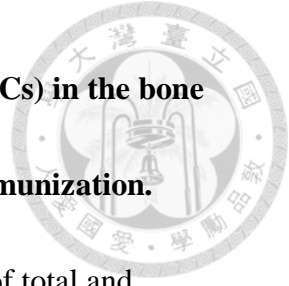
Figure 8. ELISPOT assay to analyze antibody-secreting cells (ASCs) in the bone marrow of FcγRIIB^{I232} and FcγRIIB^{T232} mice after secondary immunization.

(A-C) ELISPOT graphs (left panel) and quantification (right panel) of total and NP-specific IgG-secreting cells in the bone marrow of FcγRIIB^{I232} (232I/I) and FcγRIIB^{T232} (232T/T) mice, respectively, 7 days after secondary immunization (Day 35) were illustrated. **(A)** Total IgG-secreting cells. **(B)** NP7-specific IgG-secreting cells. **(C)** NP30-specific IgG-secreting cells. **(D)** Low-affinity NP-specific ASCs (IgG) were measured by subtracting the spot number of NP7-specific IgG-secreting cells from that of NP30-specific IgG-secreting cells. **(E)** Non-NP-specific ASCs (IgG) were measured by subtracting the spot number of NP30-specific IgG-secreting cells from that of total IgG-secreting cells. Bone marrow cells were seeded at a density of 1.5×10^5 cells **(A)** or 3.0×10^5 cells **(B-E)** per well and incubated for 16 hr at 37 ^{o}C in a 5% CO_2 incubator. Results were analyzed using two-tailed unpaired t-test. Histograms of FcγRIIB$^{232I/I}$ mice (n=8) versus FcγRIIB$^{232T/T}$ (n=7) mice were shown as mean ± SEM for comparison and statistical analysis.
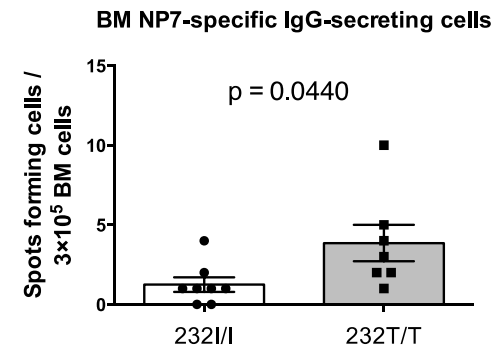
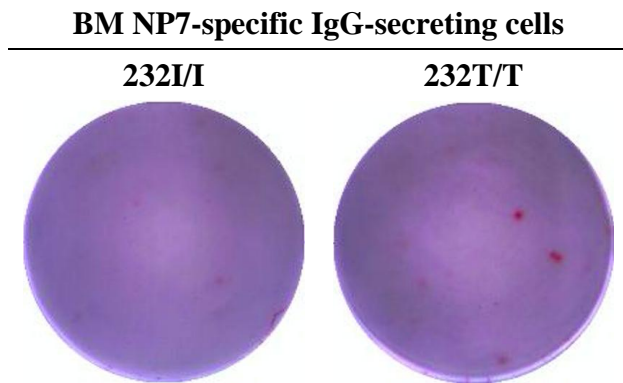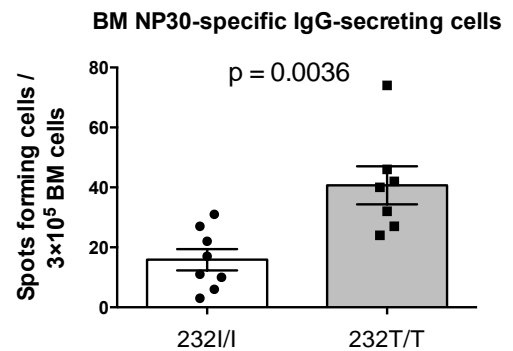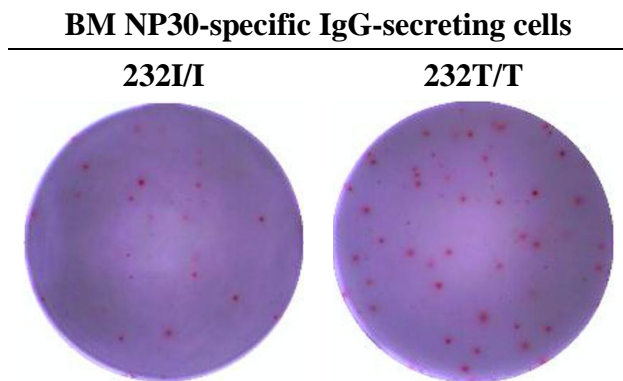# Figure 9

(A)
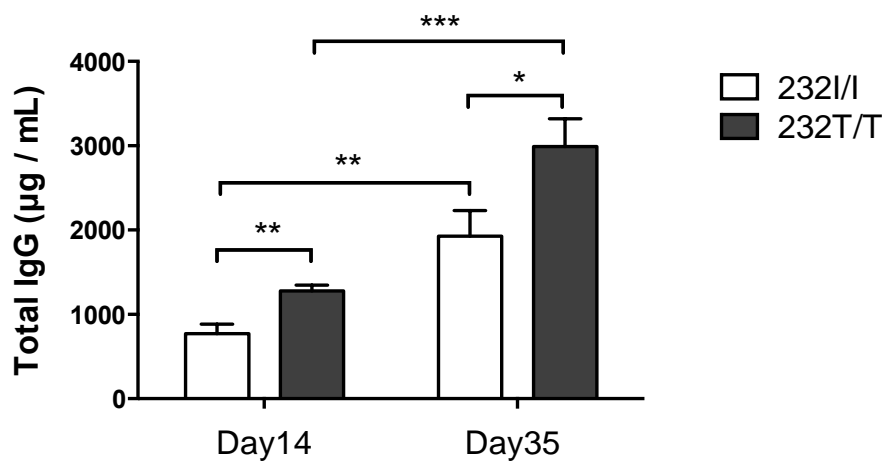
(B)
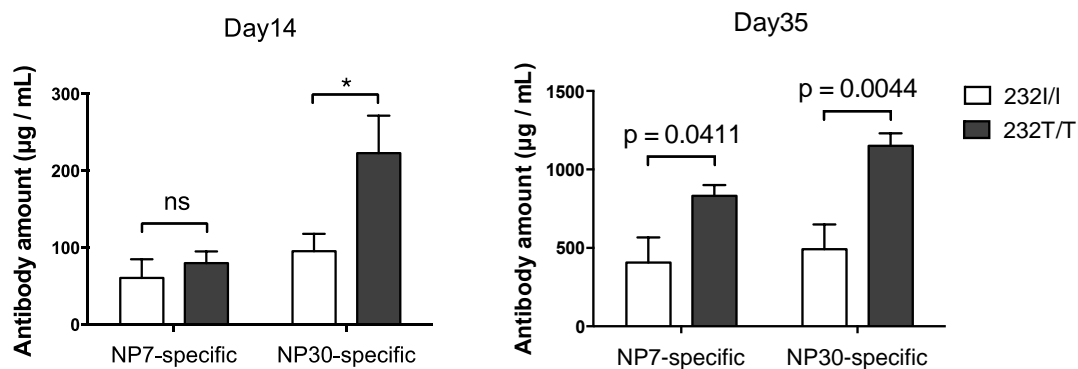
(C)
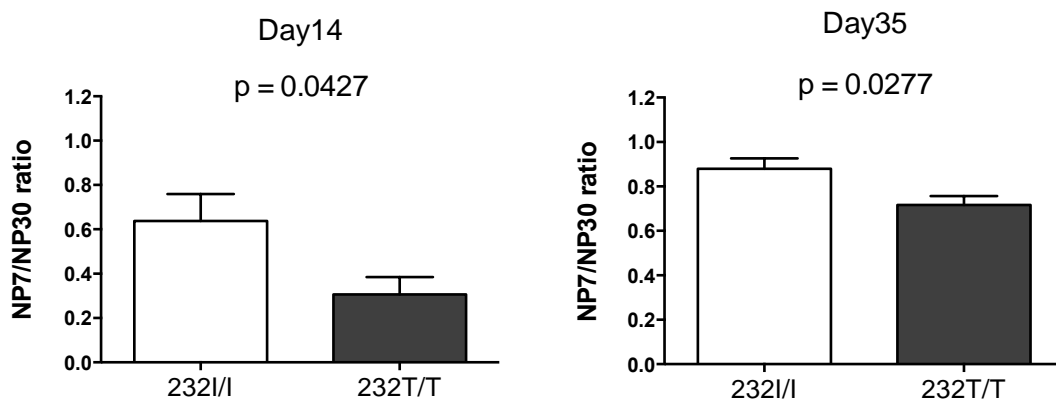
Figure 9. ELISA assay to detect the level of serum total IgG or antigen-specific IgG in FcγRIIB^{I232} and FcγRIIB^{T232} mice after primary and secondary immunization.
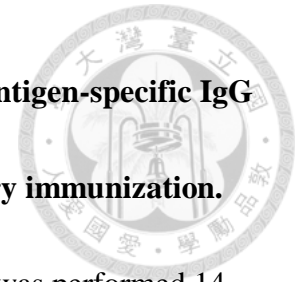
Detection of serum total IgG and NP7- or NP30-specific IgG levels was performed 14 days after primary immunization (Day 14) or 7 days after secondary immunization (Day 35). The difference of low- and high-affinity of the NP-specific IgG was determined by the ratio of NP7/NP30, of which NP7 represents the amount of high-affinity IgG whereas NP30 denotes the sum of low- and high-affinity IgG antibodies. Mouse sera were obtained from FcγRIIB^{I232} (232I/I) or FcγRIIB^{T232} (232T/T) mice as described in **Section 2.5.1** on Day 14 and Day 35, respectively. **(A)** Serum total IgG levels of FcγRIIB^{I232} (232I/I) or FcγRIIB^{T232} (232T/T) mice on Day 14 and Day 35, respectively were shown. Mouse sera were diluted 20,000 folds for Day 14 serum and 40,000 folds for Day 35 serum, respectively. **(B)** The NP7-specific and NP30-specific IgG levels of FcγRIIB^{I232} (232I/I) or FcγRIIB^{T232} (232T/T) mice on Day 14 and Day 35 were shown, respectively. Mouse sera were diluted 2,000 folds for Day 14 serum and 20,000 folds for Day 35 serum, respectively. **(C)** As described in **Section 2.5.2**, the affinity of serum NP-specific IgG was determined by the ratio of NP7/NP30 of OD$_{450}$ measurements from samples of Day 14 and Day 35, respectively. Results were analyzed using two-tailed unpaired *t*-test. Histograms of FcγRIIB$^{232I/I}$ mice (n=5 or 6) versus

FcγRIIB$^{232T/T}$ (n=6 to 8) mice were compared for statistical significance. *$P < 0.05$, **P

< 0.01, ***$P < 0.001$, ns denotes no significance.

Figure 10

(A)

(B)

Germinal center B cells

103
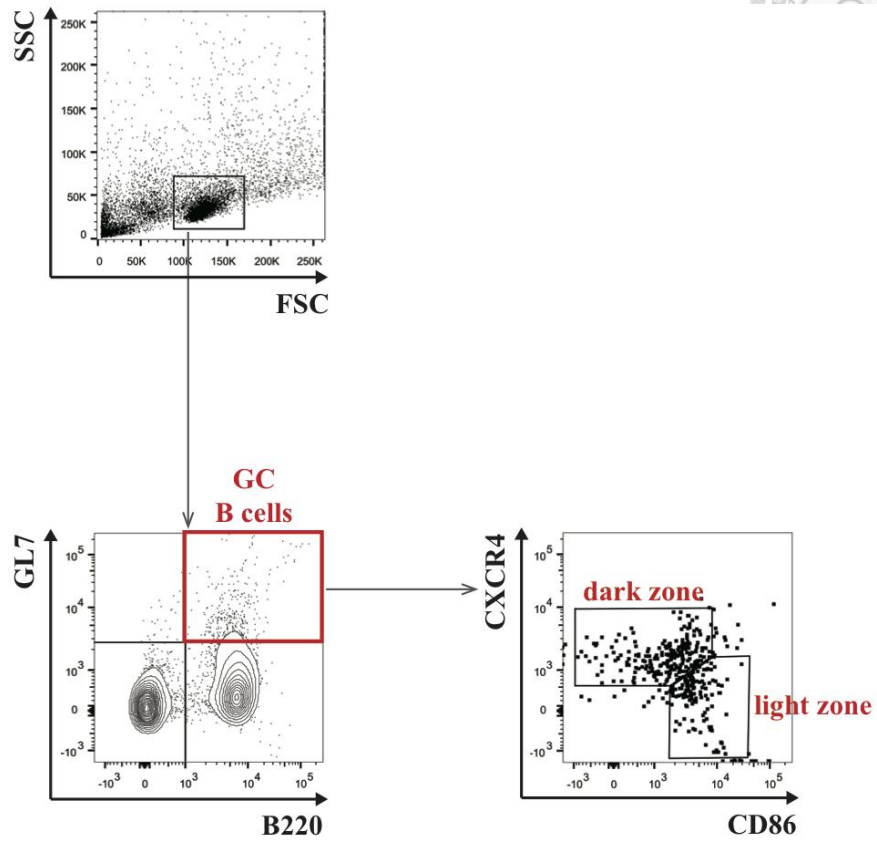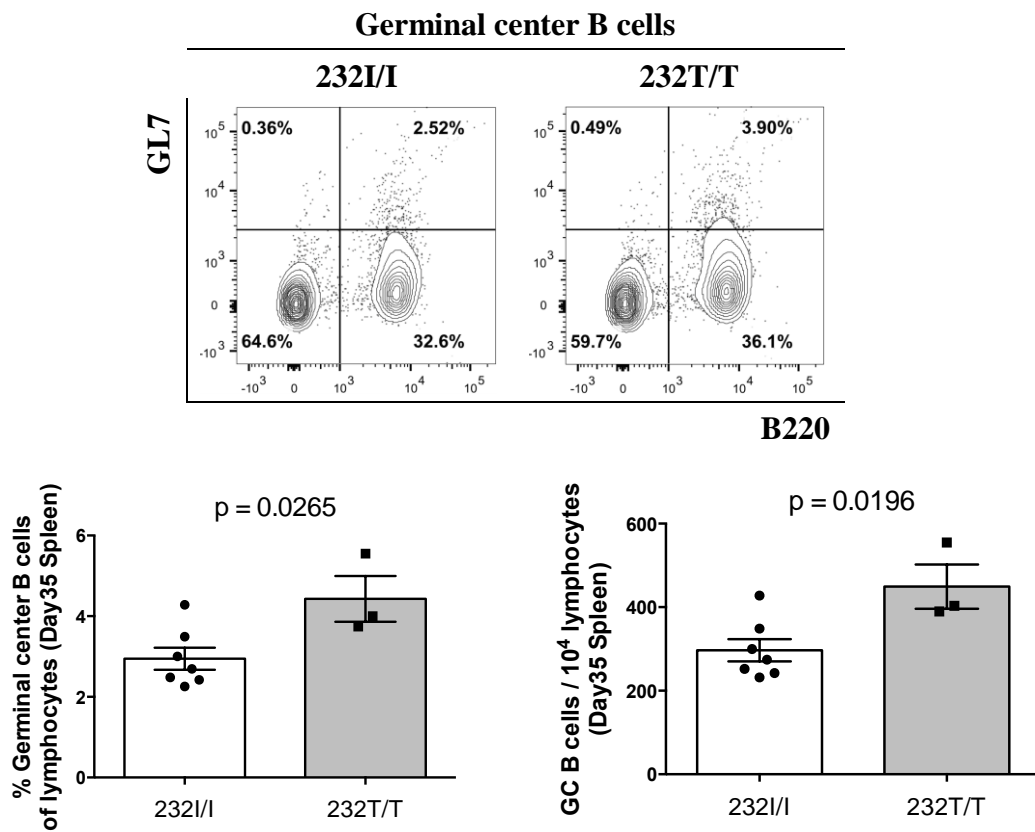
Figure 10

(C)
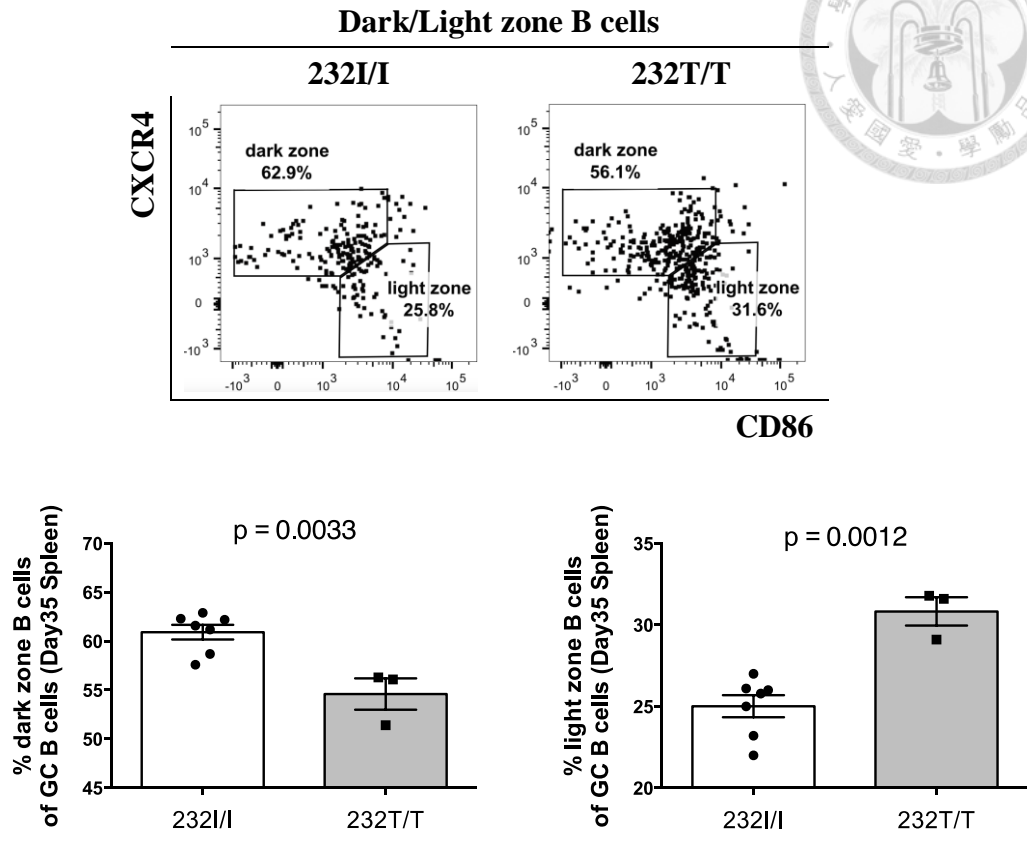
(D)
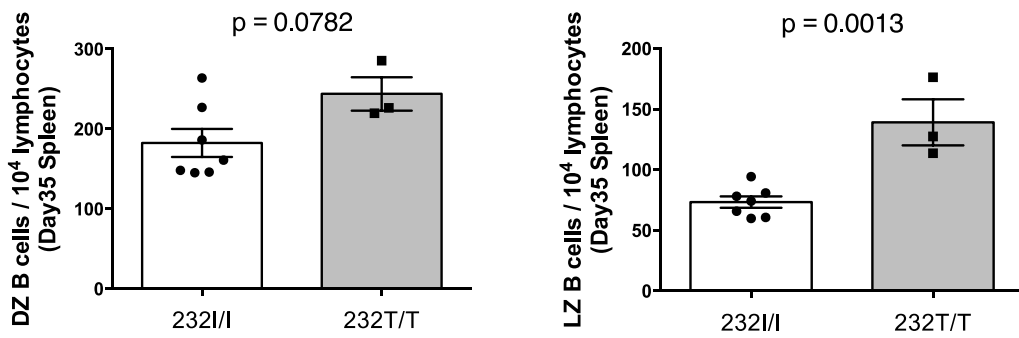
Figure 10. Flow cytometric analysis of the germinal center B cell subsets in the spleen of FcγRIIB^{I232} and FcγRIIB^{T232} mice after secondary immunization.

(A) Gating methods for flow cytometric analysis of GC B cells in the spleen after secondary immunization, **(B-D)** Splenocytes were isolated from FcγRIIB^{I232} (232I/I) or FcγRIIB^{T232} (232T/T) mice as described in **Section 2.3.2** seven days after secondary immunization (Day 35) and were analyzed by flow cytometry. **(B)** A representative FACS plot (upper panel) of the frequency (lower left panel) and cell number (lower right panel) of GC B cells (B220$^+$GL7$^+$) in lymphocytes. **(C)** (Upper panel) the dark zone (DZ) and light zone (LZ) B cells were distinguished according to surface expression of CD86 and CXCR4. DZ B cells were denoted as CD86^{low}CXCR4^{hi} cells while LZ B cells were characterized as CD86^{hi}CXCR4^{low} cells in GC B cells as in **(A)**. (Lower panel) Frequencies of DZ and LZ B cells in spleen samples of FcγRIIB^{I232} (232I/I) and FcγRIIB^{T232} (232T/T) mice were illustrated. **(D)** Cell numbers of DZ (left panel) and LZ (right panel) B cells of splenocytes. Results were analyzed using two-tailed unpaired t-test. Histograms of FcγRIIB$^{232I/I}$ mice (n=7) versus FcγRIIB$^{232T/T}$ (n=3) mice were compared for statistical significance. Abbreviations: GC, germinal center. DZ, dark zone. LZ, light zone.

Figure 11
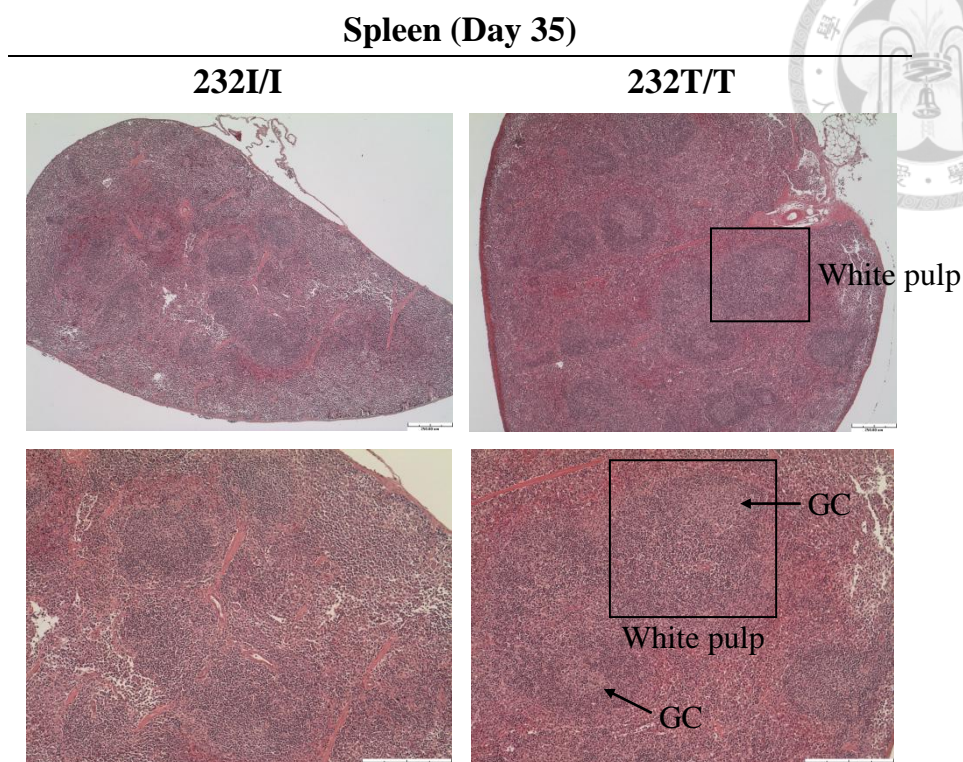
Figure 11. Morphological analysis of the germinal centers in spleens of FcγRIIB^{I232} and FcγRIIB^{T232} mice after secondary immunization.

H&E staining of spleen sections from FcγRIIB^{I232} (232I/I) and FcγRIIB^{T232} (232T/T) mice seven days after secondary immunization (Day 35) were shown. Square regions represented the white pulp, and arrows indicated the germinal center. The power of eyepiece was 10X. The visual magnification of 50X (upper panel) and 100X (lower panel) were used for acquiring images. Scale bar indicates 250 μm. Five mouse spleens of each group were analyzed and representative histological sections were depicted. GC stands for germinal center.

This Page Intentionally Left Blank

Figure 12

(A)
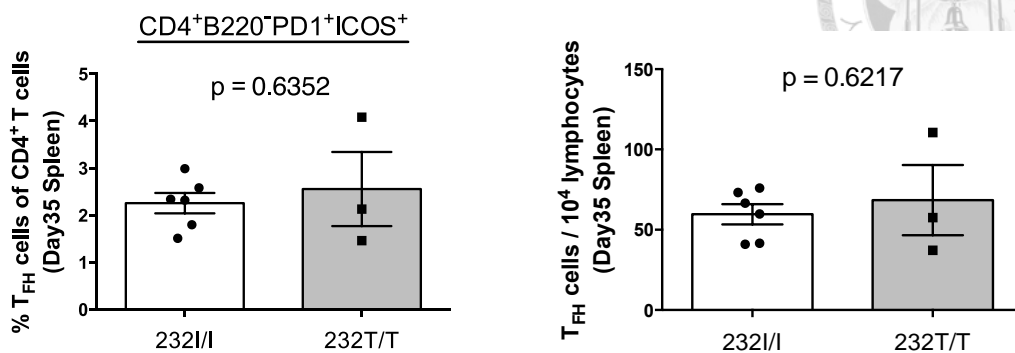
(B)
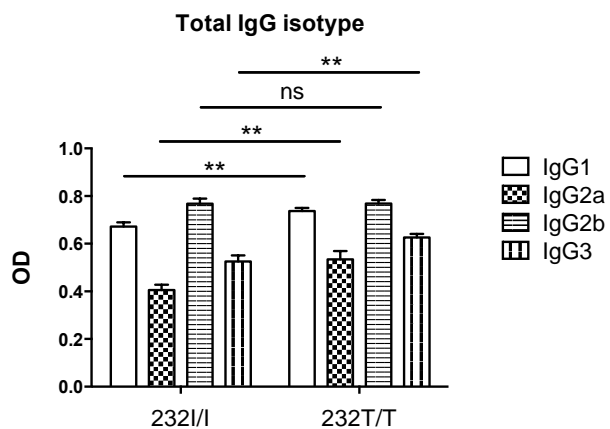
(C)
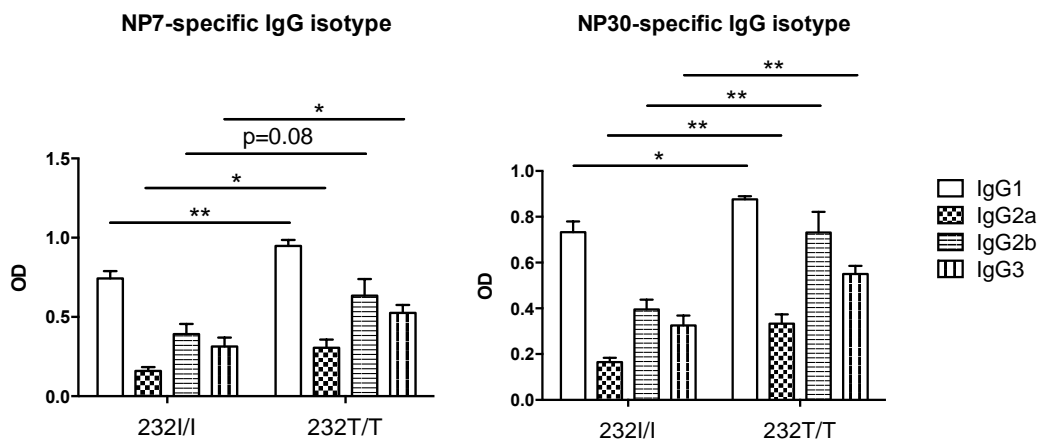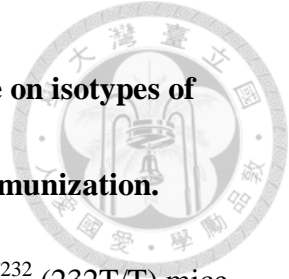
Figure 12. Analysis of the number of T_{FH} cells and their influence on isotypes of serum levels of total IgG and NP-specific IgG after secondary immunization.

(**A**) Splenocytes were isolated from FcγRIIB^{I232} (232I/I) or FcγRIIB^{T232} (232T/T) mice as described in **Section 2.3.2** seven days after secondary immunization (Day 35) and analyzed by flow cytometry. The frequencies (left panel) and cell numbers (right panel) of T follicular helper (T_{FH}) cells were gated as PD1$^+$ICOS$^+$ cells from CD4$^+$B220$^-$ T cells. Results were analyzed using two-tailed unpaired t-test. Histograms were shown as mean ± SEM. N=6 mice for FcγRIIB$^{232I/I}$ and n=3 mice for FcγRIIB$^{232T/T}$.

(**B-C**) Serum levels of total IgG isotypes as well as NP7- and NP30-specific IgG isotypes were performed using samples from 7 days after secondary immunization (Day 35). Mouse sera from FcγRIIB^{I232} (232I/I) or FcγRIIB^{T232} (232T/T) mice were collected on Day 35 as described in **Section 2.5.1**. (**B**) Serum levels of total IgG isotypes of FcγRIIB^{I232} and FcγRIIB^{T232} mice on Day 35 were shown, respectively. Mouse sera were diluted 20,000 folds for ELISA. (**C**) Serum levels of NP7- and NP30-specific IgG isotypes of FcγRIIB^{I232} or FcγRIIB^{T232} mice on Day 35. Mouse sera were diluted 15,000 folds for ELISA. Results were analyzed using two-tailed unpaired t-test for statistical significance. Histograms were shown as mean ± SEM with n=6 mice for each group of FcγRIIB^{I232} and FcγRIIB^{T232} mice, respectively. Abbreviations: OD, optical density; *P < 0.05; **P < 0.01; ns denotes no significance.

Figure 13

(A)

(B)

Immunohistochemical staining of active caspase-3 of spleen

232I/I	232T/T
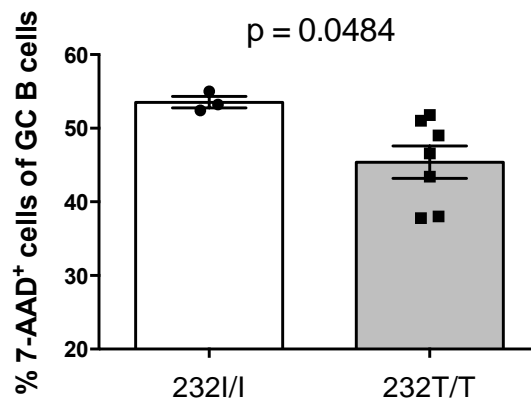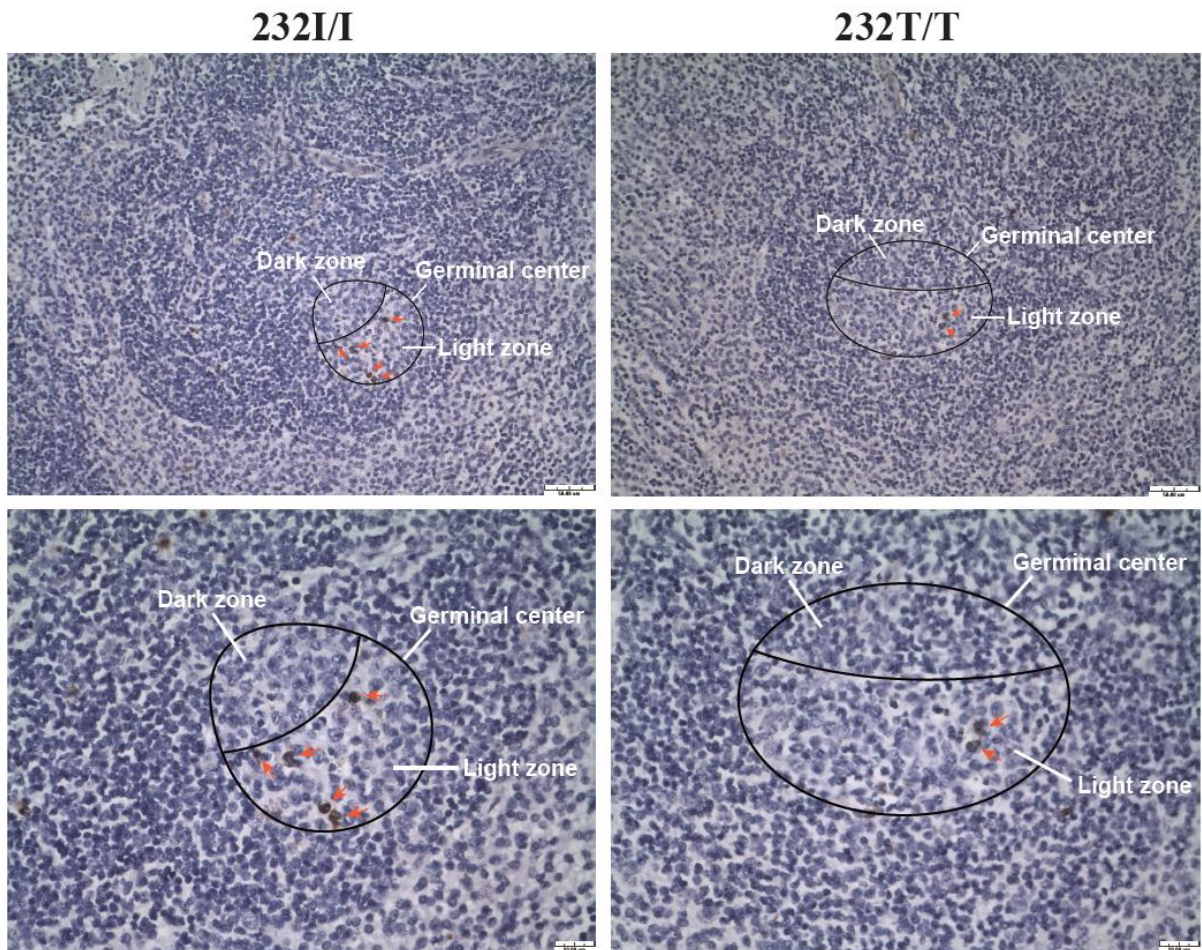
Figure 13. Analysis of the apoptosis of GC B cells using flow cytometry and immunohistochemistry.

(A) The frequency of 7-AAD$^+$ apoptotic CD19$^+$GL7$^+$ GC B cells was measured by flow cytometry. As described in **Section 2.3.2**, mouse splenocytes were isolated from FcγRIIB^{I232} (232I/I) and FcγRIIB^{T232} (232T/T) mice 7 days after secondary immunization (Day 35), respectively, and analyzed by flow cytometry. The data were analyzed for statistical significance using two-tailed unpaired *t*-test and illustrated as histograms (mean ± SEM). N=3 mice for the FcγRIIB$^{232I/I}$ and n=7 mice for the FcγRIIB$^{232T/T}$. GC stands for germinal center.

(B) Immunohistochemical staining of active caspase-3 of spleen sections from FcγRIIB^{I232} (232I/I) and FcγRIIB^{T232} (232T/T) mice at 7 days after secondary immunization (Day 35). Fields shown in upper panels represent 200x magnification and 50 μm scale bars. Images (lower panels) from upper panels were shown as 400x magnification with 20 μm scale bars. Arrows indicated active caspase-3 positive cells.

Figure 14

(A)
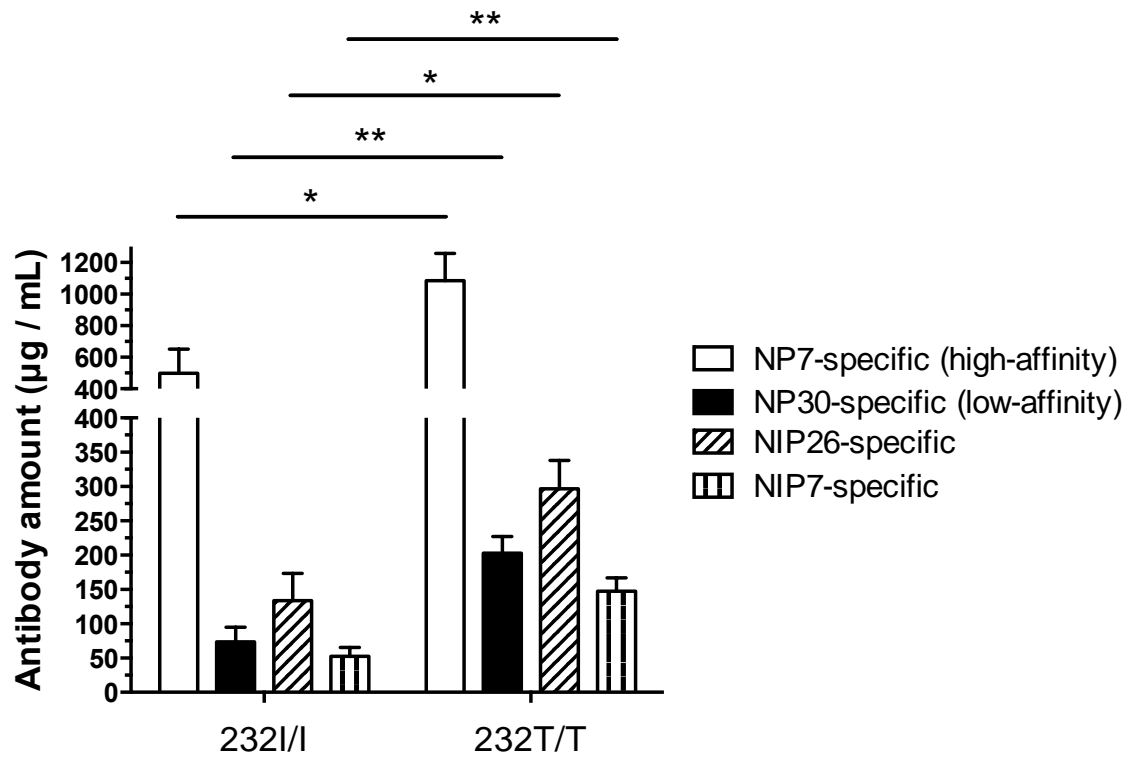
(B)
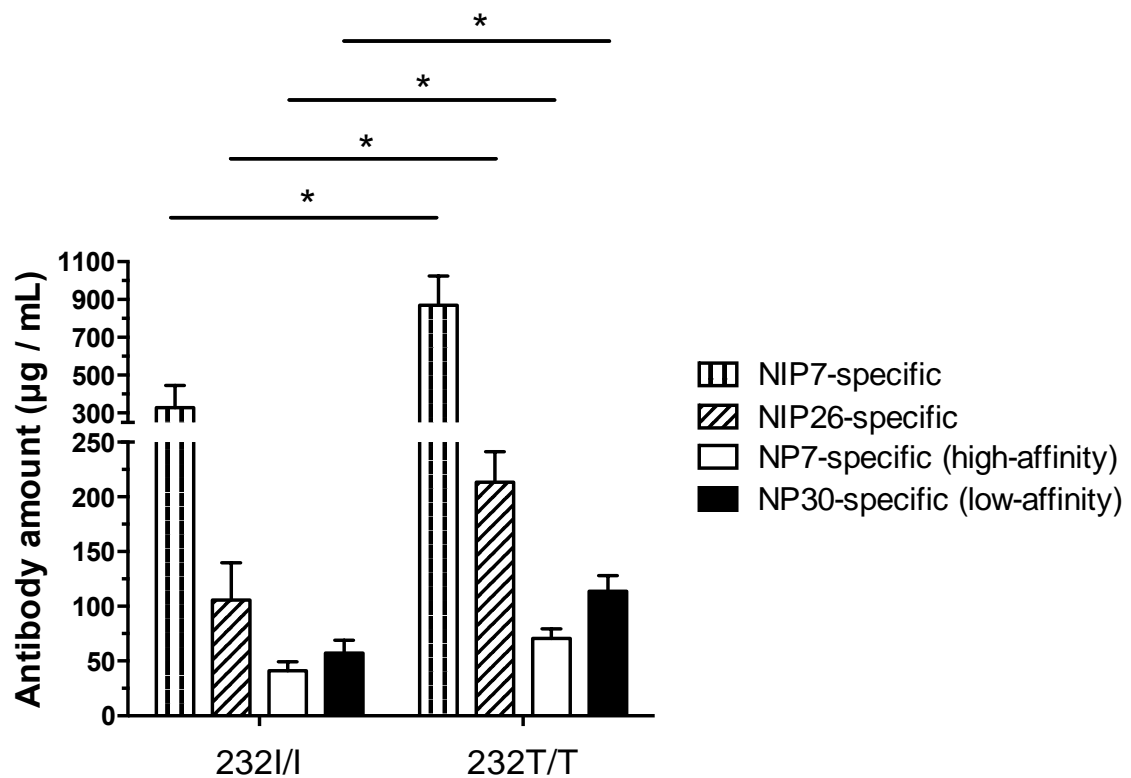
Figure 14. Sequential ELISA to detect cross-reactive antibodies in the serum of FcγRIIB^{I232} and FcγRIIB^{T232} mice after secondary immunization.

Mouse sera were collected from FcγRIIB^{I232} (232I/I) and FcγRIIB^{T232} (232T/T) mice 7 days after secondary immunization (Day 35), respectively as described in **Section 2.5.1**. **(A)** Mouse sera were diluted for 20,000-fold to pre-incubate in NP7-BSA coated plates for 12 hr at 4 $^{\circ}$C. After completion of incubation, sera were then transferred into the NP30-BSA, NIP26-BSA or NIP7-BSA coated wells, respectively for another incubation for 12 hr at 4 $^{\circ}$C. **(B)** Mouse sera were diluted as **(A)** and pre-incubated in NIP7-BSA coated plates for 12 hr at 4 $^{\circ}$C. After finish of incubation, sera were then transferred into the NIP26-BSA, NP7-BSA or NP30-BSA coated wells for second incubation for 12 hr at 4 $^{\circ}$C. The data were analyzed using two-tailed unpaired t-test and shown as histograms with mean ± SEM. N=6 mice for each group of FcγRIIB$^{232I/I}$ and FcγRIIB$^{232T/T}$, respectively. $*P < 0.05$ and $**P < 0.01$ indicate statistical significance.

Figure 15

(A)
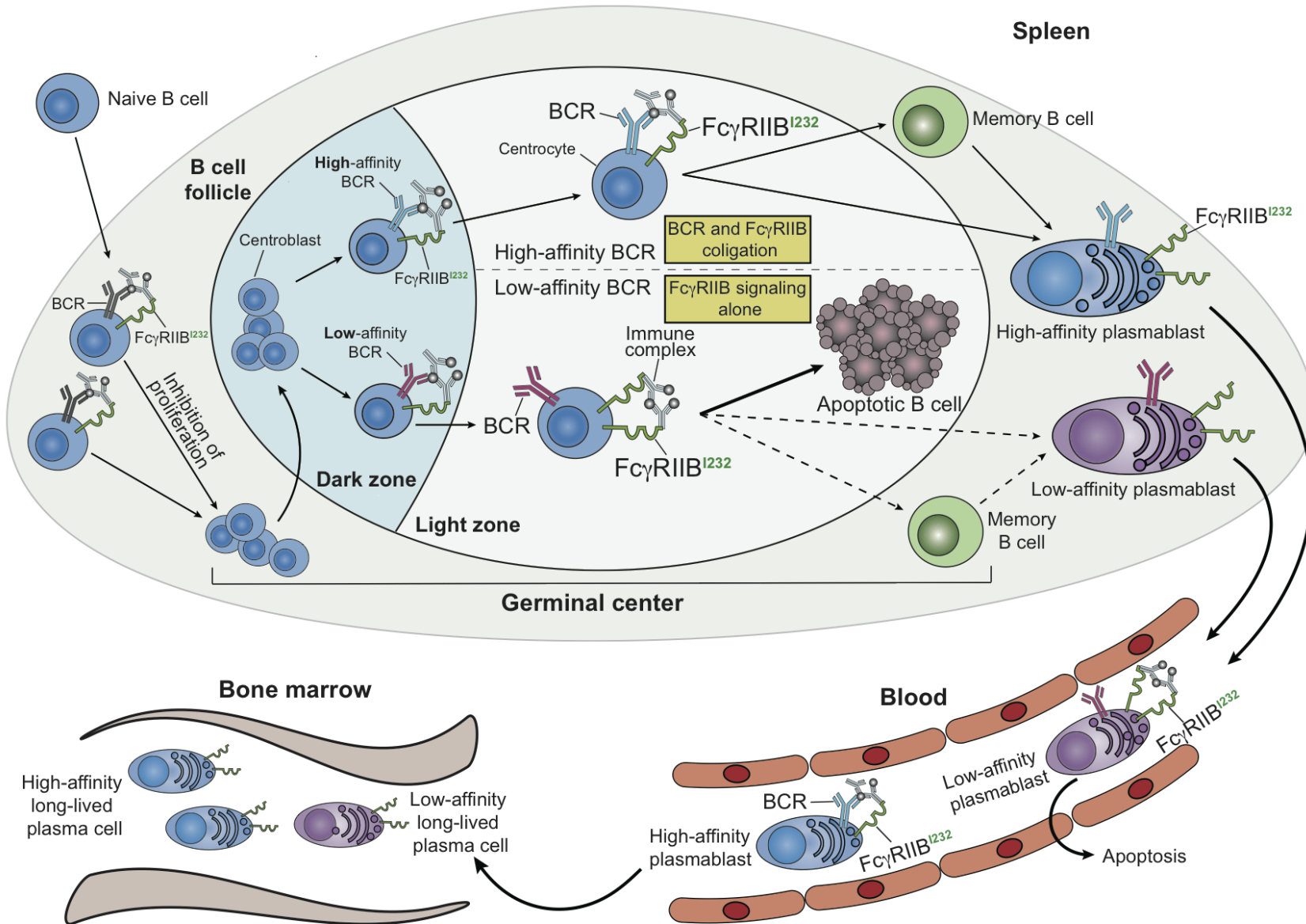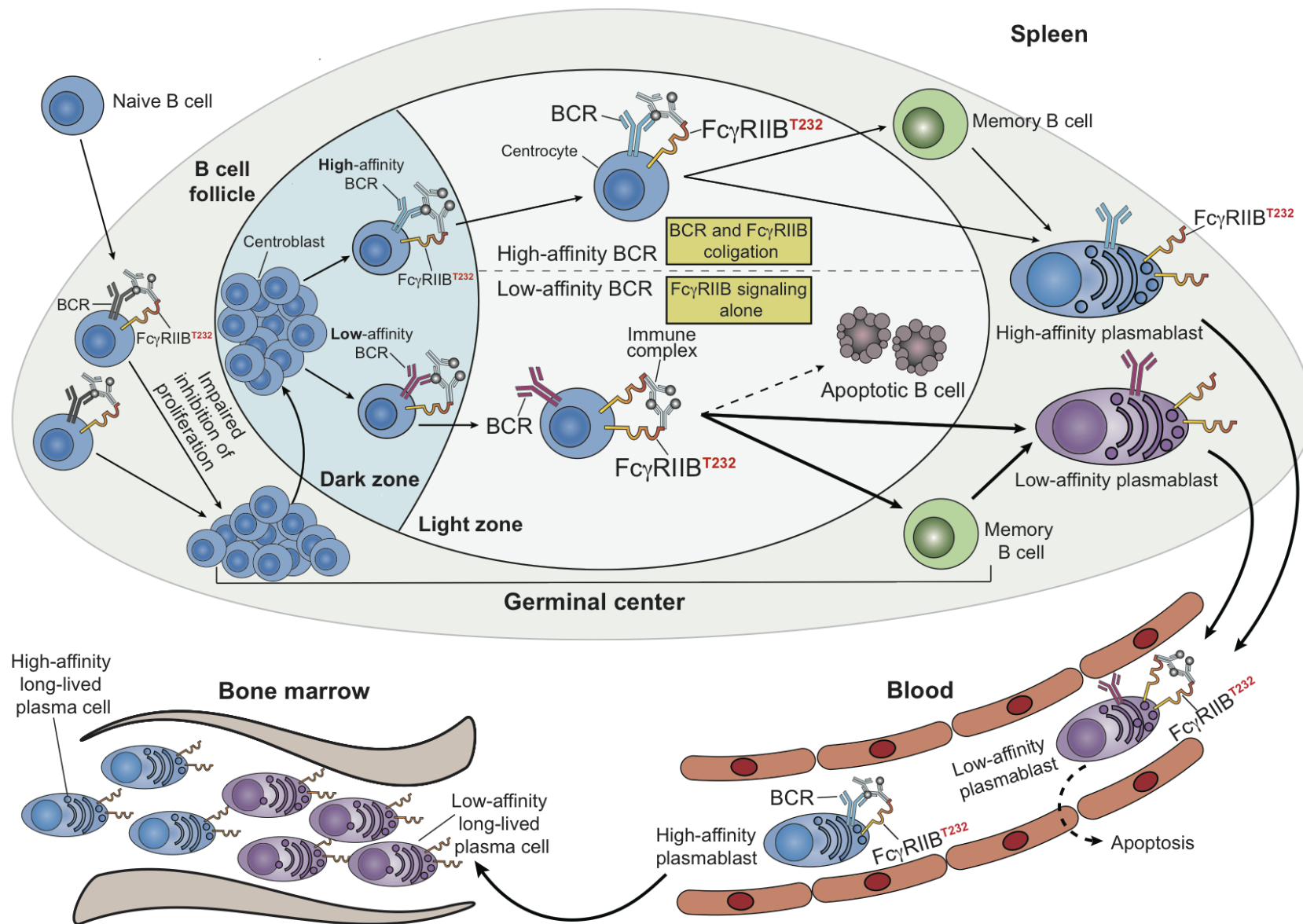
Figure 15. Illustrations to summarize of the proposed critical role of FcγRIIB in affinity selection and subsequent negative selection during the GC reaction.

(A) In FcγRIIB^{I232} (wild-type) mice, cognate IC-triggered co-ligation of BCR and FcγRIIB inhibits the proliferation of B cells in B-cell follicles, thereby maintaining a homeostatic control of normal input of B cells into the dark zone of GCs compared to that of FcγRIIB^{T232} mice. In the dark zone where somatic hypermutant B-cell clones with various affinities for Ag are produced, and subsequently these B cells enter the light zone for selection on the basis of their BCR (B-cell Ag receptor) to compete for Ag for survival. In other words, B cells with high-affinity BCR have advantages to capture Ags than those that have a low-affinity BCR. The selected high-affinity B cells then differentiate into memory B cells and plasmablasts and many of them interact with T$_{FH}$ cells before differentiation starts. In contrast, B cells with low-affinity BCR cannot bind Ags efficiently and are susceptible to cross-linking FcγRIIB^{I232} by itself. Therefore, we proposed the majority of low-affinity B-cell clones will be eliminated through apoptosis mediated by FcγRIIB while for some reason a small number of low-affinity B-cell clones were left to survive and able to differentiate into plasmablasts. Our data suggest the low-affinity Ag-specific B cells produce antibodies cross-reactive to homologous Ags and this is not yet appreciated in host immunity. After undergoing GC reaction,
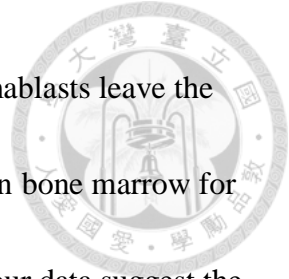
the low- and high-affinity Ag-specific memory B cells and plasmablasts leave the GC to enter circulation and a portion of plasmablasts will settle in bone marrow for terminal differentiation and permanent residence. In circulation our data suggest the existence of an additional negative selection through FcγRIIB to reduce the number of low-affinity plasmablasts since the low-affinity plasma cells in the bone marrow show a marked decrease in comparison to those in the spleen and blood.

(B) In FcγRIIB^{T232} (mutant) mice, cognate IC-triggered BCR and FcγRIIB co-ligation has an impaired function to inhibit the proliferation of B cells in B cell follicles, leading to an increase of the flux of B cells into the dark zone of GCs compared to that of wild-type FcγRIIB^{I232} mice. In the light zone, the low-affinity B-cell clones cannot bind Ags efficiently, rendering the non-cognate ICs to trigger clustering of FcγRIIB^{T232} itself. Since our data demonstrate a functional impairment of FcγRIIB^{T232} in the negative selection of low-affinity B cells, a defective apoptosis through FcγRIIB^{T232} of GC B cells supports this finding. Therefore, the majority of low-affinity B cells fail to be deleted, resulting in accumulation for further differentiate into plasmablasts. Once they leave GCs into blood vessels, it appears that low-affinity plasmablasts are also less sensitive to apoptosis upon aggregation of FcγRIIB^{T232} by non-cognate ICs, ultimately leading to more retention of low-affinity plasma cells in the bone marrow.

This Page Intentionally Left Blank

Tables
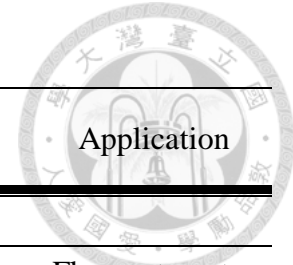
Table 1. Antibodies used for flow cytometry, ELISA, ELISPOT, and immunohistochemistry analysis.

Molecule/ Antigen	Host/Isotype	Reactivity	Fluorochrome	Clone	Manufacturer	Catalog	Application
Primary antibodies							
CD16/32	Rat/IgG2b, κ	Mouse	-	2.4G2	BD Biosciences	553142	Flow cytometry
CD16/32	Rat/IgG2b, κ	Mouse	FITC	2.4G2	BD Biosciences	553144	Flow cytometry
CD138	Rat/IgG2a, κ	Mouse	BV421	281-2	BD Biosciences	562610	Flow cytometry
CD19	Rat/IgG2a, κ	Mouse	PE-Cy7	1D3	eBioscience	25-0193-82	Flow cytometry
NP	-	-	PE	-	Biosearch Technologies	N-5070	Flow cytometry
CD11b	Rat/IgG2b, κ	Mouse	PerCP-Cy5.5	M1/70	BD Biosciences	550993	Flow cytometry
CD11c	Armenian hamster/IgG1, λ2	Mouse	AlexaFluor700	HL3	BD Biosciences	560583	Flow cytometry
GL7	Rat/IgM, κ	Mouse	AlexaFluor647	GL7	BD Biosciences	561529	Flow cytometry
B220	Rat/IgG2a, κ	Mouse	APC-Cy7	RA3-6B2	BD Biosciences	552094	Flow cytometry
CD86	Rat/IgG2a, κ	Mouse	BV605	GL1	BD Biosciences	563055	Flow cytometry

Table 1. Antibodies used for flow cytometry, ELISA, ELISPOT, and immunohistochemistry analysis (continued).

Molecule/ Antigen	Host/Isotype	Reactivity	Fluorochrome	Clone	Manufacturer	Catalog	Application
Primary antibodies							
CXCR4	Rat/IgG2b, κ	Mouse	BV421	2B11	BD Biosciences	562738	Flow cytometry
CD4	Rat/IgG2a, κ	Mouse	AlexaFluor647	RM4-5	BD Biosciences	557681	Flow cytometry
PD-1	Armenian hamster/IgG2, κ	Mouse	BV421	J43	BD Biosciences	562584	Flow cytometry
CXCR5	Rat/IgG2a, κ	Mouse	PE	2G8	BD Biosciences	561988	Flow cytometry
ICOS	Rat/IgG2b, κ	Mouse	FITC	7E.17G9	eBioscience	11-9942-80	Flow cytometry
IgG, F(ab')$_2$ fragment specific	Goat/F(ab')$_2$ fragment	Mouse	-	Polyclonal	Jackson ImmunoResearch	115-006-072	ELISPOT/ELISA
IgM, μ chain specific	Goat/IgG	Mouse	-	Polyclonal	Jackson ImmunoResearch	115-005-020	ELISPOT/ELISA
Caspase-3	Rabbit	Human, Mouse, Rat, Monkey	-	Polyclonal	Cell Signaling	9661	Immunohistochemistry

Table 1. Antibodies used for flow cytometry, ELISA, ELISPOT, and immunohistochemistry analysis (continued).

Molecule/ Antigen	Host/Isotype	Reactivity	Fluorochrome	Clone	Manufacturer	Catalog	Application
Secondary antibodies (HRP-conjugated)							
IgG, Fcγ fragment specific	Rabbit/IgG	Mouse	-	Polyclonal	Jackson ImmunoResearch	315-035-046	ELISPOT/ELISA
IgM, μ chain specific	Goat/IgG	Mouse	-	Polyclonal	Jackson ImmunoResearch	115-035-075	ELISPOT/ELISA

Table 2. Primers used for genotyping of FcγRIIB-I232T mice.

Primers	Sequence
Cu	5'-CACATGGAGATCTAGGAGTG-3'
FD	5'-CCCAGCGATTGAACTAAGAT-3'
Neo3'	5'-CATTGTCTGAGTAGGTGTCATTC-3'
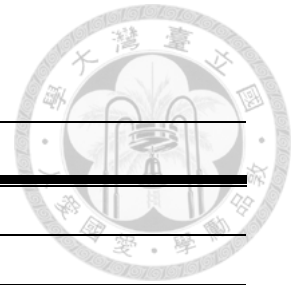
This Page Intentionally Left Blank

References

Abbas AK, Urioste S, Collins TL, Boom WH. Heterogeneity of helper/inducer T lymphocytes. IV. Stimulation of resting and activated B cells by Th1 and Th2 clones. *J. Immunol.* 1990, **144**(6): 2031-2037.
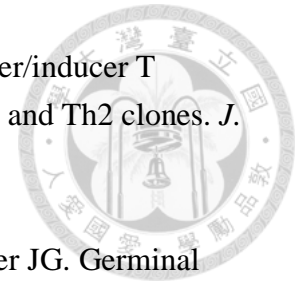
Allen CD, Ansel KM, Low C, Lesley R, Tamamura H, Fujii N, Cyster JG. Germinal center dark and light zone organization is mediated by CXCR4 and CXCR5. *Nat. Immunol.* 2004, **5**(9): 943-952.

Allen CD, Cyster JG. Follicular dendritic cell networks of primary follicles and germinal centers: phenotype and function. *Semin. Immunol.* 2008, **20**(1): 14-25.

Amezcua Vesely MC, Schwartz M, Bermejo DA, Montes CL, Cautivo KM, Kalergis AM, Rawlings DJ, Acosta-Rodriguez EV, Gruppi A. FcγRIIB and BAFF differentially regulate peritoneal B1 cell survival. *J. Immunol.* 2012, **188**(10): 4792-4800.

Baerenwaldt A, Lux A, Danzer H, Spriewald BM, Ullrich E, Heidkamp G, Dudziak D, Nimmerjahn F. Fcγ receptor IIB (FcγRIIB) maintains humoral tolerance in the human immune system in vivo. *Proc. Natl. Acad. Sci. USA* 2011, **108**(46): 18772-18777.

Bannard O, Horton RM, Allen CD, An J, Nagasawa T, Cyster JG. Germinal center centroblasts transition to a centrocyte phenotype according to a timed program and depend on the dark zone for effective selection. *Immunity* 2013, **39**(5): 912-924.

Baumgarth N, Tung JW, Herzenberg LA. Inherent specificities in natural antibodies: a key to immune defense against pathogen invasion. *Springer Semin. Immunopathol.* 2005, **26**(4): 347-362.

Blank MC, Stefanescu RN, Masuda E, Marti F, King PD, Redecha PB, Wurzburger RJ, Peterson MG, Tanaka S, Pricop L. Decreased transcription of the human *FCGR2B* gene mediated by the -343 G/C promoter polymorphism and association with systemic lupus erythematosus. *Hum. Genet.* 2005, **117**(2-3): 220-227.

Bolland S, Ravetch JV. Inhibitory pathways triggered by ITIM-containing receptors. *Adv. Immunol.* 1999, **72**: 149-177.

Bolland S, Ravetch JV. Spontaneous autoimmune disease in FcγRIIB-deficient mice results from strain-specific epistasis. *Immunity* 2000, **13**(2): 277-285.

Boulianne B, Rojas OL, Haddad D, Zaheen A, Kapelnikov A, Nguyen T, Li C, Hakem R, Gommerman JL, Martin A. AID and caspase 8 shape the germinal center response through apoptosis. *J. Immunol.* 2013, **191**(12): 5840-5847.
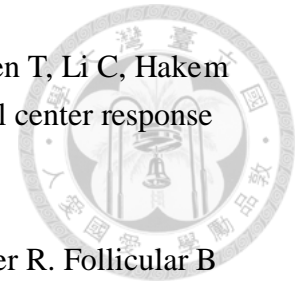
Breitfeld D, Ohl L, Kremmer E, Ellwart J, Sallusto F, Lipp M, Forster R. Follicular B helper T cells express CXC chemokine receptor 5, localize to B cell follicles, and support immunoglobulin production. *J. Exp. Med.* 2000, **192**(11): 1545-1552.

Brooks DG, Qiu WQ, Luster AD, Ravetch JV. Structure and expression of human IgG FcRII(CD32). Functional heterogeneity is encoded by the alternatively spliced products of multiple genes. *J. Exp. Med.* 1989, **170**(4): 1369-1385.

Brownlie RJ, Lawlor KE, Niederer HA, Cutler AJ, Xiang Z, Clatworthy MR, Floto RA, Greaves DR, Lyons PA, Smith KG. Distinct cell-specific control of autoimmunity and infection by FcγRIIb. *J. Exp. Med.* 2008, **205**(4): 883-895.

Chang YK, Yang W, Zhao M, Mok CC, Chan TM, Wong RW, Lee KW, Mok MY, Wong SN, Ng IO, Lee TL, Ho MH, Lee PP, Wong WH, Lau CS, Sham PC, Lau YL. Association of *BANK1* and *TNFSF4* with systemic lupus erythematosus in Hong Kong Chinese. *Genes. Immun.* 2009, **10**(5): 414-420.

Chen JY, Wang CM, Ma CC, Luo SF, Edberg JC, Kimberly RP, Wu J. Association of a transmembrane polymorphism of Fcγ receptor IIb (*FCGR2B*) with systemic lupus erythematosus in Taiwanese patients. *Arthritis Rheum.* 2006, **54**(12): 3908-3917.

Clatworthy MR, Smith KG. FcγRIIb balances efficient pathogen clearance and the cytokine-mediated consequences of sepsis. *J. Exp. Med.* 2004, **199**(5): 717-723.

Clatworthy MR, Willcocks L, Urban B, Langhorne J, Williams TN, Peshu N, Watkins NA, Floto RA, Smith KG. Systemic lupus erythematosus-associated defects in the inhibitory receptor FcγRIIb reduce susceptibility to malaria. *Proc. Natl. Acad. Sci. USA* 2007, **104**(17): 7169-7174.

Clynes R, Maizes JS, Guinamard R, Ono M, Takai T, Ravetch JV. Modulation of immune complex-induced inflammation in vivo by the coordinate expression of activation and inhibitory Fc receptors. *J. Exp. Med.* 1999, **189**(1): 179-185.

Daeron M, Malbec O, Latour S, Arock M, Fridman WH. Regulation of high-affinity IgE

receptor-mediated mast cell activation by murine low-affinity IgG receptors. *J. Clin. Invest.* 1995, **95**(2): 577-585.

Dal Porto JM. Very low affinity B cells form germinal centers, become memory B cells, and participate in secondary immune responses when higher affinity competition is reduced. *J. Exp. Med.* 2002, **195**(9): 1215-1221.

Dauphinee M, Tovar Z, Talal N. B cells expressing CD5 are increased in Sjögren's syndrome. *Arthritis Rheum.* 1988, **31**(5): 642-647.

Davidson A, Shefner R, Livneh A, Diamond B. The role of somatic mutation of immunoglobulin genes in autoimmunity. *Annu. Rev. Immunol.* 1987, **5**: 85-108.

De Silva NS, Klein U. Dynamics of B cells in germinal centres. *Nat. Rev. Immunol.* 2015, **15**(3): 137-148.

Dhodapkar KM, Banerjee D, Connolly J, Kukreja A, Matayeva E, Veri MC, Ravetch JV, Steinman RM, Dhodapkar MV. Selective blockade of the inhibitory Fcγ receptor (FcγRIIB) in human dendritic cells and monocytes induces a type I interferon response program. *J. Exp. Med.* 2007, **204**(6): 1359-1369.

Dhodapkar KM, Kaufman JL, Ehlers M, Banerjee DK, Bonvini E, Koenig S, Steinman RM, Ravetch JV, Dhodapkar MV. Selective blockade of inhibitory Fcγ receptor enables human dendritic cell maturation with IL-12p70 production and immunity to antibody-coated tumor cells. *Proc. Natl. Acad. Sci. USA* 2005, **102**(8): 2910-2915.

Dijstelbloem HM, van de Winkel JG, Kallenberg CG. Inflammation in autoimmunity: receptors for IgG revisited. *Trends Immunol.* 2001, **22**(9): 510-516.

Ferguson SE, Han SH, Kelsoe G, Thompson CB. CD28 is required for germinal center formation. *J. Immunol.* 1996, **156**(12): 4576-4581.

Floto RA, Clatworthy MR, Heilbronn KR, Rosner DR, MacAry PA, Rankin A, Lehner PJ, Ouwehand WH, Allen JM, Watkins NA, Smith KG. Loss of function of a lupus-associated FcγRIIb polymorphism through exclusion from lipid rafts. *Nat. Med.* 2005, **11**(10): 1056-1058.

Futterer A, Mink K, Luz A, Kosco-Vilbois MH, Pfeffer K. The lymphotoxin β receptor

controls organogenesis and affinity maturation in peripheral lymphoid tissues. *Immunity* 1998, **9**(1): 59-70.
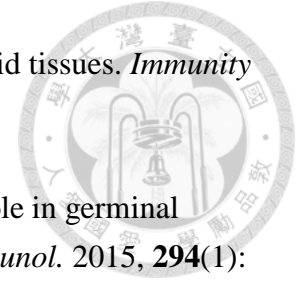
Gao F, Yang Y, Wang Z, Gao X, Zheng B. BRAD4 plays a critical role in germinal center response by regulating Bcl-6 and NF-κB activation. *Cell Immunol.* 2015, **294**(1): 1-8.

Gitlin AD, Shulman Z, Nussenzweig MC. Clonal selection in the germinal centre by regulated proliferation and hypermutation. *Nature* 2014, **509**(7502): 637-640.

Guo L, Deshmukh H, Lu R, Vidal GS, Kelly JA, Kaufman KM, Dominguez N, Klein W, Kim-Howard X, Bruner GR, Scofield RH, Moser KL, Gaffney PM, Dozmorov IM, Gilkeson GS, Wakeland EK, Li QZ, Langefeld CD, Marion MC, Williams AH, Divers J, Alarcon GS, Brown EE, Kimberly RP, Edberg JC, Ramsey-Goldman R, Reveille JD, McGwin G, Jr., Vila LM, Petri MA, Vyse TJ, Merrill JT, James JA, Nath SK, Harley JB, Guthridge JM. Replication of the *BANK1* genetic association with systemic lupus erythematosus in a European-derived population. *Genes Immun.* 2009, **10**(5): 531-538.

Haberman AM, Shlomchik MJ. Reassessing the function of immune-complex retention by follicular dendritic cells. *Nat. Rev. Immunol.* 2003, **3**(9): 757-764.

Hannum LG, Haberman AM, Anderson SM, Shlomchik MJ. Germinal center initiation, variable gene region hypermutation, and mutant B cell selection without detectable immune complexes on follicular dendritic cells. *J. Exp. Med.* 2000, **192**(7): 931-942.

Hayakawa K, Hardy RR, Parks DR, Herzenberg LA. The "Ly-1 B" cell subpopulation in normal immunodefective, and autoimmune mice. *J. Exp. Med.* 1983, **157**(1): 202-218.

Hibbs ML, Hogarth PM, McKenzie IF. The mouse *Ly-17* locus identifies a polymorphism of the Fc receptor. *Immunogenetics* 1985, **22**(4): 335-348.

Hogarth PM, Witort E, Hulett MD, Bonnerot C, Even J, Fridman WH, McKenzie IF. Structure of the mouse *β*Fcγ receptor II gene. *J. Immunol.* 1991, **146**(1): 369-376.

Holmdahl R. Estrogen exaggerates lupus but suppresses T-cell-dependent autoimmune-disease. *J. Autoimmun.* 1989, **2**(5): 651-656.

Hom G, Graham RR, Modrek B, Taylor KE, Ortmann W, Garnier S, Lee AT, Chung SA,

Ferreira RC, Pant PV, Ballinger DG, Kosoy R, Demirci FY, Kamboh MI, Kao AH, Tian C, Gunnarsson I, Bengtsson AA, Rantapaa-Dahlqvist S, Petri M, Manzi S, Seldin MF, Ronnblom L, Syvanen AC, Criswell LA, Gregersen PK, Behrens TW. Association of systemic lupus erythematosus with *C8orf13-BLK* and *ITGAM-ITGAX*. *N. Engl. J. Med.* 2008, **358**(9): 900-909.

Imanishi T, Makela O. Strain differences in the fine specificity of mouse anti-hapten antibodies. *Eur. J. Immunol.* 1973, **3**(6): 323-330.

Iruretagoyena MI, Riedel CA, Leiva ED, Gutierrez MA, Jacobelli SH, Kalergis AM. Activating and inhibitory Fcγ receptors can differentially modulate T cell-mediated autoimmunity. *Eur. J. Immunol.* 2008, **38**(8): 2241-2250.

Ito I, Kawasaki A, Ito S, Hayashi T, Goto D, Matsumoto I, Tsutsumi A, Hom G, Graham RR, Takasaki Y, Hashimoto H, Ohashi J, Behrens TW, Sumida T, Tsuchiya N. Replication of the association between the *C8orf13-BLK* region and systemic lupus erythematosus in a Japanese population. *Arthritis Rheum.* 2009, **60**(2): 553-558.

Jacob J, Kelsoe G, Rajewsky K, Weiss U. Intraclonal generation of antibody mutants in germinal centres. *Nature* 1991, **354**(6352): 389-392.

Jiang Y, Hirose S, Abe M, Sanokawa-Akakura R, Ohtsuji M, Mi X, Li N, Xiu Y, Zhang D, Shirai J, Hamano Y, Fujii H, Shirai T. Polymorphisms in IgG Fc receptor IIB regulatory regions associated with autoimmune susceptibility. *Immunogenetics* 2000, **51**(6): 429-435.

Jiang Y, Hirose S, Sanokawa-Akakura R, Abe M, Mi X, Li N, Miura Y, Shirai J, Zhang D, Hamano Y, Shirai T. Genetically determined aberrant down-regulation of FcγRIIB$_1$ in germinal center B cells associated with hyper-IgG and IgG autoantibodies in murine systemic lupus erythematosus. *Int. Immunol.* 1999, **11**(10): 1685-1691.

Johnston RJ, Poholek AC, DiToro D, Yusuf I, Eto D, Barnett B, Dent AL, Craft J, Crotty S. Bcl6 and Blimp-1 are reciprocal and antagonistic regulators of T follicular helper cell differentiation. *Science* 2009, **325**(5943): 1006-1010.

Joshi T, Ganesan LP, Cao X, Tridandapani S. Molecular analysis of expression and function of hFcγRIIb1 and b2 isoforms in myeloid cells. *Mol. Immunol.* 2006, **43**(7): 839-850.

Jungers P, Dougados M, Pelissier C, Kuttenn F, Tron F, Lesavre P, Bach JF. Influence of oral-contraceptive therapy on the activity of systemic lupus-erythematosus. *Arthritis Rheum.* 1982, **25**(6): 618-623.

Kalergis AM, Ravetch JV. Inducing tumor immunity through the selective engagement of activating Fcγ receptors on dendritic cells. *J. Exp. Med.* 2002, **195**(12): 1653-1659.

Kepley CL, Cambier JC, Morel PA, Lujan D, Ortega E, Wilson BS, Oliver JM. Negative regulation of FcεRI signaling by FcγRII costimulation in human blood basophils. *J. Allergy Clin. Immunol.* 2000, **106**(2): 337-348.

Kim CH, Rott LS, Clark-Lewis I, Campbell DJ, Wu L, Butcher EC. Subspecialization of CXCR5^{+} T cells: B helper activity is focused in a germinal center-localized subset of CXCR5^{+} T cells. *J. Exp. Med.* 2001, **193**(12): 1373-1381.

Kitabatake M, Toda T, Kuwahara K, Igarashi H, Ohtsuji M, Tsurui H, Hirose S, Sakaguchi N. Transgenic overexpression of G5PR that is normally augmented in centrocytes impairs the enrichment of high-affinity antigen-specific B cells, increases peritoneal B-1a cells, and induces autoimmunity in aged female mice. *J. Immunol.* 2012, **189**(3): 1193-1201.

Kono H, Kyogoku C, Suzuki T, Tsuchiya N, Honda H, Yamamoto K, Tokunaga K, Honda Z. FcγRIIB Ile232Thr transmembrane polymorphism associated with human systemic lupus erythematosus decreases affinity to lipid rafts and attenuates inhibitory effects on B cell receptor signaling. *Hum. Mol. Genet.* 2005, **14**(19): 2881-2892.

Kosco-Vilbois MH. Are follicular dendritic cells really good for nothing? *Nat. Rev. Immunol.* 2003, **3**(9): 764-769.

Kozyrev SV, Abelson AK, Wojcik J, Zaghlool A, Linga Reddy MV, Sanchez E, Gunnarsson I, Svenungsson E, Sturfelt G, Jonsen A, Truedsson L, Pons-Estel BA, Witte T, D'Alfonso S, Barizzone N, Danieli MG, Gutierrez C, Suarez A, Junker P, Laustrup H, Gonzalez-Escribano MF, Martin J, Abderrahim H, Alarcon-Riquelme ME. Functional variants in the B-cell gene *BANK1* are associated with systemic lupus erythematosus. *Nat. Genet.* 2008, **40**(2): 211-216.

Kyogoku C, Dijstelbloem HM, Tsuchiya N, Hatta Y, Kato H, Yamaguchi A, Fukazawa T,
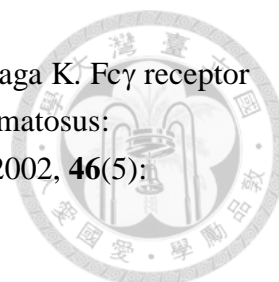
Jansen MD, Hashimoto H, van de Winkel JG, Kallenberg CG, Tokunaga K. Fcγ receptor gene polymorphisms in Japanese patients with systemic lupus erythematosus: Contribution of *FCGR2B* to genetic susceptibility. *Arthritis Rheum.* 2002, **46**(5): 1242-1254.

Lanzavecchia A. Antigen-specific interaction between T and B cells. *Nature* 1985, **314**(6011): 537-539.

Leung WH, Tarasenko T, Biesova Z, Kole H, Walsh ER, Bolland S. Aberrant antibody affinity selection in SHIP-deficient B cells. *Eur. J. Immunol.* 2013, **43**(2): 371-381.

Linterman MA, Beaton L, Yu D, Ramiscal RR, Srivastava M, Hogan JJ, Verma NK, Smyth MJ, Rigby RJ, Vinuesa CG. IL-21 acts directly on B cells to regulate Bcl-6 expression and germinal center responses. *J. Exp. Med.* 2010, **207**(2): 353-363.

Lu R, Vidal GS, Kelly JA, Delgado-Vega AM, Howard XK, Macwana SR, Dominguez N, Klein W, Burrell C, Harley IT, Kaufman KM, Bruner GR, Moser KL, Gaffney PM, Gilkeson GS, Wakeland EK, Li QZ, Langefeld CD, Marion MC, Divers J, Alarcon GS, Brown EE, Kimberly RP, Edberg JC, Ramsey-Goldman R, Reveille JD, McGwin G, Jr., Vila LM, Petri MA, Bae SC, Cho SK, Bang SY, Kim I, Choi CB, Martin J, Vyse TJ, Merrill JT, Harley JB, Alarcon-Riquelme ME, Biolupus, Collaborations GM, Nath SK, James JA, Guthridge JM. Genetic associations of *LYN* with systemic lupus erythematosus. *Genes Immun.* 2009, **10**(5): 397-403.

Mackay M, Stanevsky A, Wang T, Aranow C, Li M, Koenig S, Ravetch JV, Diamond B. Selective dysregulation of the FcγIIB receptor on memory B cells in SLE. *J. Exp. Med.* 2006, **203**(9): 2157-2164.

MacLennan IC. Germinal Centers. *Annu. Rev. Immunol.* 1994, **12**: 117-139.

Malbec O, Fong DC, Turner M, Tybulewicz VL, Cambier JC, Fridman WH, Daeron M. Fcε receptor I-associated *lyn*-dependent phosphorylation of Fcγ receptor IIB during negative regulation of mast cell activation. *J. Immunol.* 1998, **160**(4): 1647-1658.

Mandel TE, Phipps RP, Abbot A, Tew JG. The follicular dendritic cell: long term antigen retention during immunity. *Immunol. Rev.* 1980, **53**(1): 29-59.

McGaha TL, Karlsson MC, Ravetch JV. FcγRIIB deficiency leads to autoimmunity and

a defective response to apoptosis in Mrl-MpJ mice. *J. Immunol.* 2008, **180**(8): 5670-5679.

McGaha TL, Sorrentino B, Ravetch JV. Restoration of tolerance in lupus by targeted inhibitory receptor expression. *Science* 2005, **307**(5709): 590-593.

Mercolino TJ, Arnold LW, Hawkins LA, Haughton G. Normal mouse peritoneum contains a large population of Ly-1^{+} (CD5) B cells that recognize phosphatidyl choline. Relationship to cells that secrete hemolytic antibody specific for autologous erythrocytes. *J. Exp. Med.* 1988, **168**(2): 687-698.

Meyer-Hermann M, Mohr E, Pelletier N, Zhang Y, Victora GD, Toellner KM. A theory of germinal center B cell selection, division, and exit. *Cell Rep.* 2012, **2**(1): 162-174.

Miettinen HM, Matter K, Hunziker W, Rose JK, Mellman I. Fc receptor endocytosis is controlled by a cytoplasmic domain determinant that actively prevents coated pit localization. *J. Cell Biol.* 1992, **116**(4): 875-888.

Mohan C, Putterman C. Genetics and pathogenesis of systemic lupus erythematosus and lupus nephritis. *Nat. Rev. Nephrol.* 2015, **11**(6): 329-341.

Moll T, Nitschke L, Carroll M, Ravetch JV, Izui S. A critical role for FcγRIIB in the induction of rheumatoid factors. *J. Immunol.* 2004, **173**(7): 4724-4728.

Murakami M, Honjo T. Involvement of B-1 cells in mucosal immunity and autoimmunity. *Immunol. Today* 1995, **16**(11): 534-539.

Nimmerjahn F, Bruhns P, Horiuchi K, Ravetch JV. FcγRIV: a novel FcR with distinct IgG subclass specificity. *Immunity* 2005, **23**(1): 41-51.

Nimmerjahn F, Ravetch JV. Fcγ receptors as regulators of immune responses. *Nat. Rev. Immunol.* 2008, **8**(1): 34-47.

Nurieva RI, Chung Y, Martinez GJ, Yang XO, Tanaka S, Matskevitch TD, Wang YH, Dong C. Bcl6 mediates the development of T follicular helper cells. *Science* 2009, **325**(5943): 1001-1005.

Ono M, Bolland S, Tempst P, Ravetch JV. Role of the inositol phosphatase SHIP in

negative regulation of the immune system by the receptor FcγRIIB. *Nature* 1996, **383**(6597): 263-266.

Ono M, Okada H, Bolland S, Yanagi S, Kurosaki T, Ravetch JV. Deletion of SHIP or SHP-1 reveals two distinct pathways for inhibitory signaling. *Cell* 1997, **90**(2): 293-301.

Paul E, Nelde A, Verschoor A, Carroll MC. Follicular exclusion of autoreactive B cells requires FcγRIIb. *Int. Immunol.* 2007, **19**(4): 365-373.

Pearse RN, Kawabe T, Bolland S, Guinamard R, Kurosaki T, Ravetch JV. SHIP recruitment attenuates FcγRIIB-induced B cell apoptosis. *Immunity* 1999, **10**(6): 753-760.

Pisitkun P, Deane JA, Difilippantonio MJ, Tarasenko T, Satterthwaite AB, Bolland S. Autoreactive B cell responses to RNA-related antigens due to *TLR7* gene duplication. *Science* 2006, **312**(5780): 1669-1672.

Pritchard NR, Cutler AJ, Uribe S, Chadban SJ, Morley BJ, Smith KGC. Autoimmune-prone mice share a promoter haplotype associated with reduced expression and function of the Fc receptor FcγRII. *Curr. Biol.* 2000, **10**(4): 227-230.

Pulendran B, Kannourakis G, Nouri S, Smith KGC, Nossal GJV. Soluble antigen can cause enhanced apoptosis of germinal-centre B cells. *Nature* 1995, **375**(6529): 331-334.

Qin D, Wu J, Vora KA, Ravetch JV, Szakal AK, Manser T, Tew JG. Fcγ receptor IIB on follicular dendritic cells regulates the B cell recall response. *J. Immunol.* 2000, **164**(12): 6268-6275.

Rajewsky K. Clonal selection and learning in the antibody system. *Nature* 1996, **381**(6585): 751-758.

Ravetch JV, Kinet JP. Fc receptors. *Annu. Rev. Immunol.* 1991, **9**: 457-492.

Ravetch JV, Luster AD, Weinshank R, Kochan J, Pavlovec A, Portnoy DA, Hulmes J, Pan YC, Unkeless JC. Structural heterogeneity and functional domains of murine immunoglobulin G Fc receptors. *Science* 1986, **234**(4777): 718-725.

Roubinian JR, Talal N, Greenspan JS, Goodman JR, Siiteri PK. Effect of castration and sex hormone treatment on survival, anti-nucleic acid antibodies, and glomerulonephritis in NZB/NZW F1 Mice. *J. Exp. Med.* 1978, **147**(6): 1568-1583.
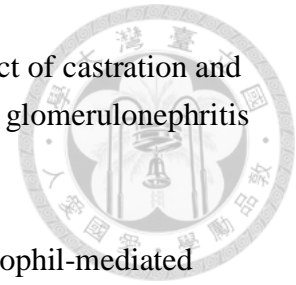
Rubin RL. Autoantibody specificity in drug-induced lupus and neutrophil-mediated metabolism of lupus-inducing drugs. *Clin. Biochem.* 1992, **25**(3): 223-234.

Schaerli P, Willimann K, Lang AB, Lipp M, Loetscher P, Moser B. CXC chemokine receptor 5 expression defines follicular homing T cells with B cell helper function. *J. Exp. Med.* 2000, **192**(11): 1553-1562.

Schwickert TA, Victora GD, Fooksman DR, Kamphorst AO, Mugnier MR, Gitlin AD, Dustin ML, Nussenzweig MC. A dynamic T cell-limited checkpoint regulates affinity-dependent B cell entry into the germinal center. *J. Exp. Med.* 2011, **208**(6): 1243-1252.

Shih TA, Meffre E, Roederer M, Nussenzweig MC. Role of BCR affinity in T cell dependent antibody responses in vivo. *Nat. Immunol.* 2002, **3**(6): 570-575.

Shokat KM, Goodnow CC. Antigen-induced B-cell death and elimination during germinal-centre immune responses. *Nature* 1995, **375**(6529): 334-338.

Siriboonrit U, Tsuchiya N, Sirikong M, Kyogoku C, Bejrachandra S, Suthipinittharm P, Luangtrakool K, Srinak D, Thongpradit R, Fujiwara K, Chandanayingyong D, Tokunaga K. Association of Fcγ receptor IIb and IIIb polymorphisms with susceptibility to systemic lupus erythematosus in Thais. *Tissue Antigens* 2003, **61**(5): 374-383.

Smith KG, Clatworthy MR. FcγRIIB in autoimmunity and infection: evolutionary and therapeutic implications. *Nat. Rev. Immunol.* 2010, **10**(5): 328-343.

Stall AM, Wells SM, Lam KP. B-1 cells: unique origins and functions. *Semin. Immunol.* 1996, **8**(1): 45-59.

Stuart SG, Simister NE, Clarkson SB, Kacinski BM, Shapiro M, Mellman I. Human IgG Fc receptor (hFcRII; CD32) exists as multiple isoforms in macrophages, lymphocytes and IgG-transporting placental epithelium. *EMBO J.* 1989, **8**(12): 3657-3666.

Su K, Li X, Edberg JC, Wu J, Ferguson P, Kimberly RP. A promoter haplotype of the immunoreceptor tyrosine-based inhibitory motif-bearing FcγRIIb alters receptor expression and associates with autoimmunity. II. Differential binding of GATA4 and Yin-Yang1 transcription factors and correlated receptor expression and function. *J. Immunol.* 2004a, **172**(11): 7192-7199.

Su K, Wu J, Edberg JC, Li X, Ferguson P, Cooper GS, Langefeld CD, Kimberly RP. A promoter haplotype of the immunoreceptor tyrosine-based inhibitory motif-bearing FcγRIIb alters receptor expression and associates with autoimmunity. I. Regulatory *FCGR2B* polymorphisms and their association with systemic lupus erythematosus. *J. Immunol.* 2004b, **172**(11): 7186-7191.

Takahashi Y, Cerasoli DM, Dal Porto JM, Shimoda M, Freund R, Fang W, Telander DG, Malvey EN, Mueller DL, Behrens TW, Kelsoe G. Relaxed negative selection in germinal centers and impaired affinity maturation in Bcl-xL transgenic mice. *J. Exp. Med.* 1999, **190**(3): 399-410.

Takahashi Y, Dutta PR, Cerasoli DM, Kelsoe G. In situ studies of the primary immune response to (4-hydroxy-3-nitrophenyl)acetyl. V. Affinity maturation develops in two stages of clonal selection. *J. Exp. Med.* 1998, **187**(6): 885-895.

Takai T, Ono M, Hikida M, Ohmori H, Ravetch JV. Augmented humoral and anaphylactic responses in FcγRII-deficient mice. *Nature* 1996, **379**(6563): 346-349.

Tartour E, de la Salle H, de la Salle C, Teillaud C, Camoin L, Galinha A, Latour S, Hanau D, Fridman WH, Sautes C. Identification, in mouse macrophages and in serum, of a soluble receptor for the Fc portion of IgG (FcγR) encoded by an alternatively spliced transcript of the *FcγRII* gene. *Int. Immunol.* 1993, **5**(8): 859-868.

Tchorbanov AI, Voynova EN, Mihaylova NM, Todorov TA, Nikolova M, Yomtova VM, Chiang BL, Vassilev TL. Selective silencing of DNA-specific B lymphocytes delays lupus activity in MRL/lpr mice. *Eur. J. Immunol.* 2007, **37**(12): 3587-3596.

Tew JG, Phipps RP, Mandel TE. The maintenance and regulation of the humoral immune response: persisting antigen and the role of follicular antigen-binding dendritic cells as accessory cells. *Immunol. Rev.* 1980, **53**(1): 175-201.

Tiller T, Kofer J, Kreschel C, Busse CE, Riebel S, Wickert S, Oden F, Mertes MM,

Ehlers M, Wardemann H. Development of self-reactive germinal center B cells and plasma cells in autoimmune FcγRIIB-deficient mice. *J. Exp. Med.* 2010, **207**(12): 2767-2778.
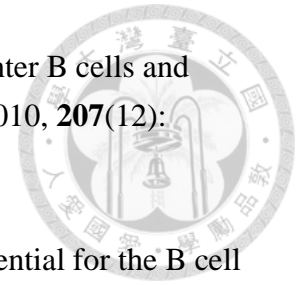
Todo K, Koga O, Nishikawa M, Hikida M. Modulation of Igβ is essential for the B cell selection in germinal center. *Sci. Rep.* 2015, **5**: 10303.

Tzeng SJ, Bolland S, Inabe K, Kurosaki T, Pierce SK. The B cell inhibitory Fc receptor triggers apoptosis by a novel c-Abl family kinase-dependent pathway. *J. Biol. Chem.* 2005, **280**(42): 35247-35254.

Vaughn SE, Kottyan LC, Munroe ME, Harley JB. Genetic susceptibility to lupus: the biological basis of genetic risk found in B cell signaling pathways. *J. Leukoc. Biol.* 2012, **92**(3): 577-591.

Victora GD. Snapshot: the germinal center reaction. *Cell* 2014, **159**(3): 700-700 e701.

Victora GD, Nussenzweig MC. Germinal centers. *Annu. Rev. Immunol.* 2012, **30**: 429-457.

Victora GD, Schwickert TA, Fooksman DR, Kamphorst AO, Meyer-Hermann M, Dustin ML, Nussenzweig MC. Germinal center dynamics revealed by multiphoton microscopy with a photoactivatable fluorescent reporter. *Cell* 2010, **143**(4): 592-605.

Wensveen FM, Derks IA, van Gisbergen KP, de Bruin AM, Meijers JC, Yigittop H, Nolte MA, Eldering E, van Lier RA. BH3-only protein Noxa regulates apoptosis in activated B cells and controls high-affinity antibody formation. *Blood* 2012, **119**(6): 1440-1449.

Wu YY, Georg I, Diaz-Barreiro A, Varela N, Lauwerys B, Kumar R, Bagavant H, Castillo-Martin M, El Salem F, Maranon C, Alarcon-Riquelme ME. Concordance of increased B1 cell subset and lupus phenotypes in mice and humans is dependent on BLK expression levels. *J. Immunol.* 2015, **194**(12): 5692-5702.

Xiang Z, Cutler AJ, Brownlie RJ, Fairfax K, Lawlor KE, Severinson E, Walker EU, Manz RA, Tarlinton DM, Smith KG. FcγRIIb controls bone marrow plasma cell persistence and apoptosis. *Nat. Immunol.* 2007, **8**(4): 419-429.

Xing Y, Igarashi H, Wang X, Sakaguchi N. Protein phosphatase subunit G5PR is needed for inhibition of B cell receptor-induced apoptosis. *J. Exp. Med.* 2005, **202**(5): 707-719.

Xiu Y, Nakamura K, Abe M, Li N, Wen XS, Jiang Y, Zhang D, Tsurui H, Matsuoka S, Hamano Y, Fujii H, Ono M, Takai T, Shimokawa T, Ra C, Shirai T, Hirose S. Transcriptional regulation of *Fcgr2b* gene by polymorphic promoter region and its contribution to humoral immune responses. *J. Immunol.* 2002, **169**(8): 4340-4346.

Yang W, Ng P, Zhao M, Hirankarn N, Lau CS, Mok CC, Chan TM, Wong RW, Lee KW, Mok MY, Wong SN, Avihingsanon Y, Lee TL, Ho MH, Lee PP, Wong WH, Lau YL. Population differences in SLE susceptibility genes: *STAT4* and *BLK*, but not *PXK*, are associated with systemic lupus erythematosus in Hong Kong Chinese. *Genes Immun.* 2009, **10**(3): 219-226.

Youinou P, Mackenzie L, Katsikis P, Merdrignac G, Isenberg DA, Tuaillon N, Lamour A, Le Goff P, Jouquan J, Drogou A, et al. The relationship between CD5-expressing B lymphocytes and serologic abnormalities in rheumatoid arthritis patients and their relatives. *Arthritis Rheum.* 1990, **33**(3): 339-348.

Yu D, Rao S, Tsai LM, Lee SK, He Y, Sutcliffe EL, Srivastava M, Linterman M, Zheng L, Simpson N, Ellyard JI, Parish IA, Ma CS, Li QJ, Parish CR, Mackay CR, Vinuesa CG. The transcriptional repressor Bcl-6 directs T follicular helper cell lineage commitment. *Immunity* 2009, **31**(3): 457-468.

Yuasa T, Kubo S, Yoshino T, Ujike A, Matsumura K, Ono M, Ravetch JV, Takai T. Deletion of Fcγ receptor IIB renders H-2^b mice susceptible to collagen-induced arthritis. *J. Exp. Med.* 1999, **189**(1): 187-194.

Zhang Y, Liu S, Liu J, Zhang T, Shen Q, Yu Y, Cao X. Immune complex/Ig negatively regulate TLR4-triggered inflammatory response in macrophages through FcγRIIb-dependent PGE_2 production. *J. Immunol.* 2009, **182**(1): 554-562.

Zotos D, Coquet JM, Zhang Y, Light A, D'Costa K, Kallies A, Corcoran LM, Godfrey DI, Toellner KM, Smyth MJ, Nutt SL, Tarlinton DM. IL-21 regulates germinal center B cell differentiation and proliferation through a B cell-intrinsic mechanism. *J. Exp. Med.* 2010, **207**(2): 365-378.
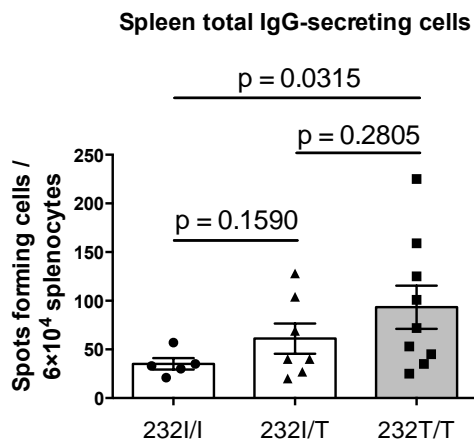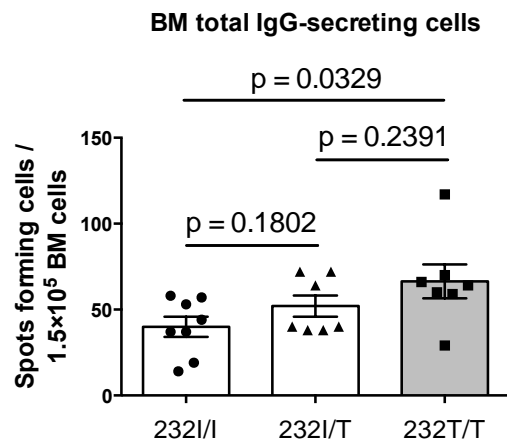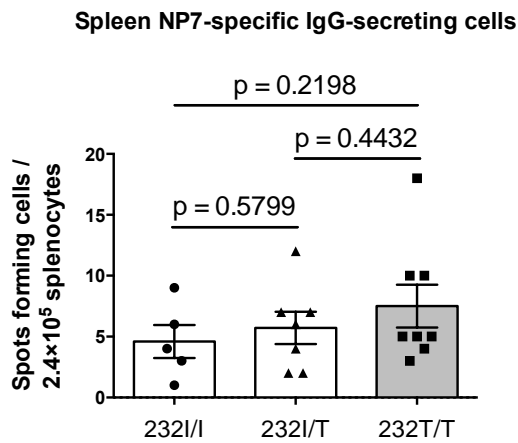
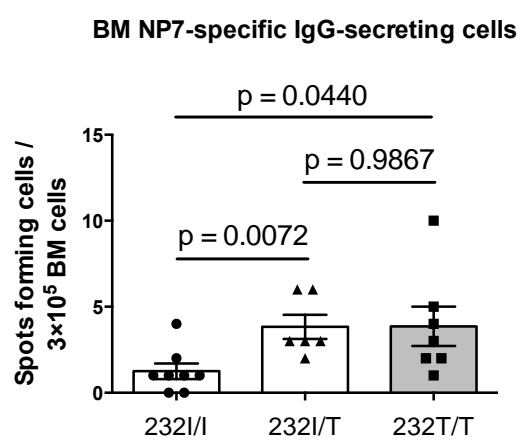# Supplementary Figures

Supplementary Figure 1

(A)

Spleen total IgG-secreting cells

p = 0.0315

p = 0.2805

p = 0.1590

Spots forming cells / $6×10^4$ splenocytes

232I/I   232I/T   232T/T

(D)

BM total IgG-secreting cells

p = 0.0329

p = 0.2391

p = 0.1802

Spots forming cells / $1.5×10^5$ BM cells

232I/I   232I/T   232T/T

(B)

Spleen NP7-specific IgG-secreting cells

p = 0.2198

p = 0.4432

p = 0.5799

Spots forming cells / $2.4×10^5$ splenocytes

232I/I   232I/T   232T/T

(E)

BM NP7-specific IgG-secreting cells

p = 0.0440

p = 0.9867

p = 0.0072

Spots forming cells / $3×10^5$ BM cells

232I/I   232I/T   232T/T

(C)

Spleen NP30-specific IgG-secreting cells

p = 0.0099

p = 0.0747

p = 0.0649

Spots forming cells / $2.4×10^5$ splenocytes

232I/I   232I/T   232T/T

(F)

BM NP30-specific IgG-secreting cells

p = 0.0036

p = 0.5894

p = 0.0040

Spots forming cells / $3×10^5$ BM cells

232I/I   232I/T   232T/T

(G)

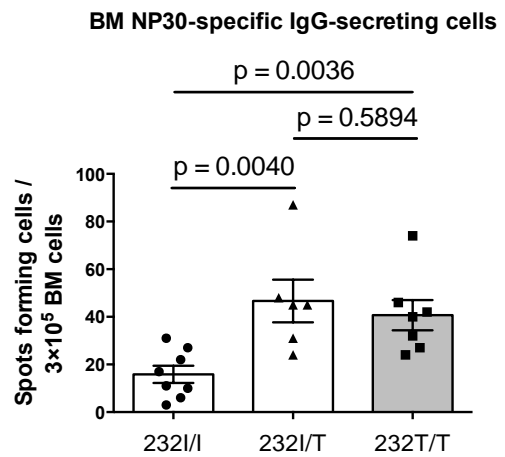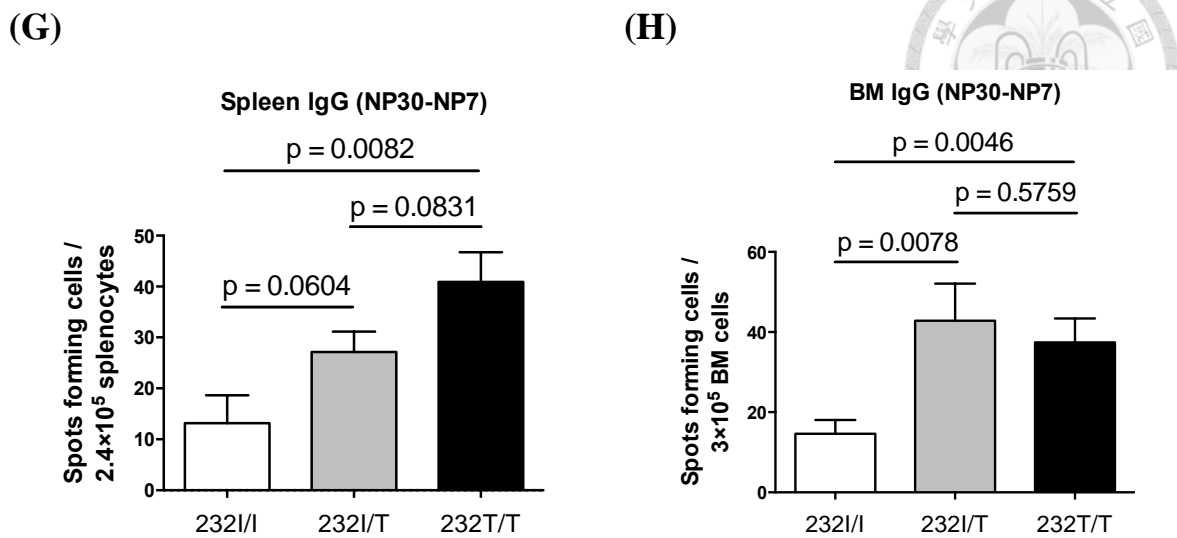**(H)**

Supplementary Figure 1. ELISPOT assay to analyze antibody-secreting cells
(ASCs) in the spleen and bone marrow of FcγRIIB-232I/I, -232I/T, and -232T/T
mice after secondary immunization.

(A-C) Quantification of total and NP-specific IgG-secreting cells in the spleen of

FcγRIIB-232I/I (232I/I), -232I/T (232I/T), or -232T/T (232T/T) mice at 7 days after

secondary immunization (Day 35). (A) Total IgG-secreting cells. (B) NP7-specific

IgG-secreting cells. (C) NP30-specific IgG-secreting cells. (D-F) Quantification of total

and NP-specific IgG-secreting cells in the bone marrow of FcγRIIB-232I/I (232I/I),

-232I/T (232I/T), or -232T/T (232T/T) mice at 7 days after secondary immunization

(Day 35). (D) Total IgG-secreting cells. (E) NP7-specific IgG-secreting cells. (F)

NP30-specific IgG-secreting cells. (G-H) Low-affinity NP-specific ASCs (IgG) were

assessed and quantified by subtracting the spot number of NP7-specific IgG-secreting cells from that of NP30-specific IgG-secreting cells in **(G)** spleen and **(H)** bone marrow. Splenocytes were seeded at 6.0×10^4 cells in **(A)** or 2.4×10^5 cells in **(B, C and G)** per well. Bone marrow cells were seeded at 1.5×10^5 cells in **(D)** or 3.0×10^5 cells in **(E, F and H)** per well. Cells were incubated for 16 hr at 37 ^{o}C in a 5% CO_2 incubator. Results were analyzed using two-tailed unpaired *t*-test. The *t*-test was modified by Welch's correction in case of unequal variance. Graphs show mean ± SEM. n = 5 mice for the 232I/I, 6~7 mice for the 232I/T, and 7-9 mice for the 232T/T.